A Rapid Liquid Chromatography / Tandem Mass Spectrometry Assay for *In Vivo* Monitoring of Extracellular Monoamine Neurotransmitters and their Metabolites

Vasiliki Bablekis

A Thesis

in

The Department

of

Chemistry

Presented in Partial Fulfilment of the Requirements
for the Degree of Master of Science (Chemistry) at
Concordia University
Montreal, Quebec, Canada

March 2004

Your file Votre référence
ISBN: 0-612-90998-0
Our file Notre référence
ISBN: 0-612-90998-0

ABSTRACT

A Rapid Liquid Chromatography / Tandem Mass Spectrometry Assay for *In Vivo* Monitoring of Extracellular Monoamine Neurotransmitters and their Metabolites

Vasiliki Bablekis

In this study, a rapid and selective method using microdialysis liquid chromatography / tandem mass spectrometry was developed for the *in vivo* analysis of the catecholamine dopamine, and its metabolites DOPAC and HVA, and the indolamine serotonin, and its metabolite 5-HIAA.

Sampling of the extracellular fluid by microdialysis enables continuous monitoring of intercellular chemical concentrations, which allows for the study of neuronal communications. Liquid chromatography using a Fluophase PFP column (1.0x50 mm, 5 μm), packed with a fluorinated phase, provided sufficient retention and separation of both monoamine neurotransmitters and their respective acid metabolites. This analytical column allowed for online desalting, which was critical for successful detection, by combining hydrophilic interaction chromatography (HILIC) and reverse phase chromatography. Mass spectrometric detection was performed using electrospray ionization coupled to an AB/MDS Sciex API3000 triple quadrupole mass spectrometer operating in both negative and positive ion modes.

Performance and reliability of the method were assessed by monitoring the neurochemical response of rats to amphetamine, pargyline, and fluoxetine - three drugs having well-known effects on dopamine, serotonin and their metabolites.

Basal levels for all neurotransmitters in 2 μL rat microdialysis samples were above the limit of quantitation. For dopamine and serotonin, a linear dynamic range was observed from 0.5 pg to 50 pg on column. Limit of detection was estimated at 60 fg on column for DA and 5-HT and 6 pg on column for DOPAC, HVA and 5-HIAA. Total run time was 3.0 min. This assay offers the advantage of high temporal and anatomical resolution and, accordingly, the potential to assess the dynamics of dopamine and serotonin function in the nucleus accumbens of the male rat.

ACKNOWLEDGEMENTS

I would like to thank my supervisor, Dr. Jim Pfaus, for his direction, knowledge and guidance throughout the conductance of my research project.

I would like to express my gratitude towards Themis Flarakos and Dr. Mark Reimer for providing me with the opportunity and tools to perform my research in such a stimulating learning environment. This collaboration allowed me to discover and gain knowledge otherwise unattainable. In particular, personal attention given to me by Themis was indispensable, as well as his advice and mentorship.

A sincere thank you to Dr. Cameron Skinner, my second examiner, for his guidance, advice, valuable implication in this project, editing of this thesis and for encouraging me to purse graduate studies.

I would also like to thank Dr. Paul Joyce for taking interest in my work by accepting to be part of my thesis committee.

A special thank you to my husband Mino for his tremendous ability to motivate and encourage me through his unconditional love, understanding and patience. Without him this would not be possible.

I want to acknowledge my parents and brother for providing me with the support system to be able to achieve everything that I have.

I am grateful to my best friends Maya and Mirna for their endless words of encouragement throughout this entire research, for their countless hours of editing of this thesis and for being a continuous source of inspiration.

Last but not least, I want to acknowledge my friends from the lab, Amelie, Michaela and Veronica, for their support and for their willingness to help and teach me various surgical and testing techniques.

TABLE OF CONTENTS

TABLE OF FIGURES

TABLE OF TABLES

ABBREVIATIONS

αCSF	Artificial cerebrospinal fluid
CE	Capillary electrophoresis
CID	Collisional induced dissociation
ESI	Electrospray Ionization
HILIC	Hydrophilic interaction chromatography
HPLC	High pressure liquid chromatography
IS	Internal standard
LC	Liquid chromatography
MAO	Monoamine oxidase
m/z	Mass-to-charge ratio
MS	Mass spectrometry
MS/MS	Tandem mass spectrometry
NAcc	Nucleus accumbens
PCA	Post column addition
S/B	Signal-to-baseline ratio
SRM	Selected reaction monitoring
SSRI	Selective serotonin reuptake inhibitor
TIC	Total ion chromatogram
ZDV	Zero dead volume

OVERVIEW OF THE THESIS

The primary goal of this research was to develop a versatile analytical technique that would allow for the analysis of neurotransmitters, and their metabolites, with high temporal and anatomical resolution. In the present work neurotransmitters are being examined, but the general methods developed are suitable for a wider variety of analytes. Accurate measurement of monoamine neurotransmitters, such as catecholamines and indolamines, in biological matrices is a difficult problem due to the low concentrations and the presence of many concomitant species. However, their importance in clinical diagnosis, pathological studies and neurological research demands the development of a robust analytical method of analysis.

To quantitate these monoamine neurotransmitters and their metabolites at basal levels in the rat brain, a rapid and selective method using microdialysis sampling and liquid chromatographic separation coupled with tandem mass spectrometry (LC/MS/MS) was developed. Specifically, the method was developed for the *in vivo* analysis of the catecholamine dopamine, and its metabolites DOPAC and HVA, and the indolamine serotonin, and its metabolite 5-HIAA.

Microdialysis combined with LC/MS detection is gaining momentum as an important tool in biochemical and pharmaceutical research. Microdialysis perfusion techniques are widely used to monitor the extracellular levels of various neurochemicals and their metabolites *in vivo*. This method allows for the direct investigation of the mechanisms of drug actions in a very specific area of a living body.

Once microdialysis samples are collected, it is important to establish a chromatographic method that provides adequate retention of all analytes of interest on an

analytical column. The diverse nature of the analytes and complex sample matrix necessitate the use of sophisticated on-column desalting combining two modes of separation. The first is a newer type of separation based on a normal phase mechanism in aqueous mobile phases termed hydrophilic interaction chromatography (HILIC) and, the second is reverse phase chromatography.

Mass spectrometry is a powerful technique for detecting analytes with very high sensitivity and, more importantly, very high selectivity. The extremely low detection limits of this instrument permit basal neurotransmitter levels to be measured. The high degree of specificity is necessary to insure that other concomitant molecules in the sample are not interfering with, or contributing to, the signal produced by the molecule of interest.

This study will demonstrate that the analytical method described is capable of monitoring basal extracellular monoamine levels in male rats. Additionally, the application of this method in monitoring the responses of these neurotransmitters to the psychostimulant amphetamine, and the antidepressants pargyline and fluoxetine, will demonstrate that the combination of microdialysis and LC-MS/MS is a useful tool for monitoring rapid changes in brain biochemistry.

1. INTRODUCTION

1.1 Monoamine Neurotransmitters

Neurotransmitters are the basic chemical molecules that modulate our mobility, memory, emotions, perceptions, and attitudes. Neuroscientists have estimated that there are over 200 different types of neurotransmitters that play a variety of roles throughout the body. Neurotransmitters are small molecules that are liberated by presynaptic neurons into the synaptic cleft and bind to specific sites on the post-synaptic membrane, causing a change in the postsynaptic membrane potential. The four major groups of small molecule neurotransmitters are acetylcholine, monoamines, soluble gases and amino acids. There are four monoamine neurotransmitters, that are divided into two subsets on the basis of their chemical structure: the catecholamines, that include dopamine, norepinephrine, and epinephrine, and indolamines, that include serotonin.[1,2,3] The present study focused on one neurotransmitter from each group, namely dopamine and serotonin. In addition, two internal standards, dopamine-d_4 and homovanillic acid-d_2, were used to ensure reliability of the assay. The molecular structure of the analytes and internal standards are shown in Figure 1.

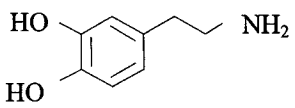

Dopamine (DA)
3-hydroxytyramine
$C_8H_{11}NO_2$
M.W. = 153.18

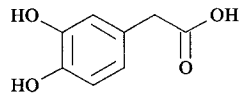

3,4-dihydroxyphenylacetic acid (DOPAC)
$C_8H_8O_4$
M.W. = 168.1

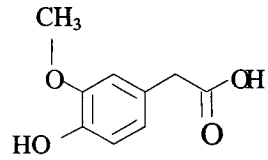

Homovanillic acid (HVA)
4-hydroxy-3-methoxyphenylacetic acid
$C_9H_{10}O_4$
M.W. = 182.2

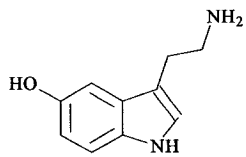

Serotonin (5-HT)
5-hydroxytryptamine
$C_{10}H_{12}N_2O$
M.W. = 176.2

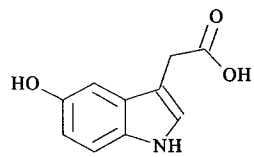

5-hydroxyindolacetic acid (5-HIAA)
$C_{10}H_9NO_3$
M.W. = 191.2

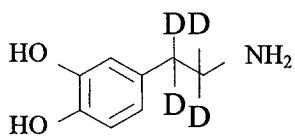

DA-d_4
Internal Standard
$C_8H_{11}D_4NO_2$
M.W. = 157.18

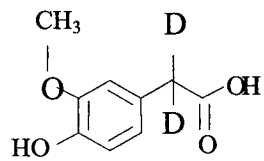

HVA-d_2
Internal Standard
$C_9H_{10}D_2O_4$
M.W. = 184.2

Figure 1 Structures of monoamine neurotransmitters, their metabolites and the internal standards (IS) selected for study.

Pathways of Dopamine Synthesis and Metabolism

The catecholamines are synthesized from the amino acid tyrosine, as shown in Figure 2. The initial, and rate-limiting step, of catecholamine synthesis is the conversion of tyrosine to 3,4-dihydroxyphenylalanine (L-DOPA) by the enzyme tyrosine hydroxylase. L-DOPA is then converted to dopamine by an L-aromatic amino acid, L-DOPA decarboxylase. Dopamine is then translocated into storage vesicles by the vesicular monoamine transporter.

Neurons that release norepinephrine have an extra enzyme, dopamine β-hydroxylase, located inside the amine storage vesicles. This enzyme catalyzes the conversion of dopamine to norepinephrine. The additional action of phenylethanolamine N-methyltransferase (PNMT), an enzyme mainly localized in chromaffin cells of the adrenal medulla, leads to conversion of norepinephrine to epinephrine.[3,4,5,6]

The maintenance of appropriate synaptic levels of dopamine is critical to the proper functioning of the nervous system. While reuptake of dopamine into the presynaptic nerve terminal plays an important role in ensuring this equilibrium, metabolism of the neurotransmitter also contributes significantly to the termination of catecholamine neurotransmission.

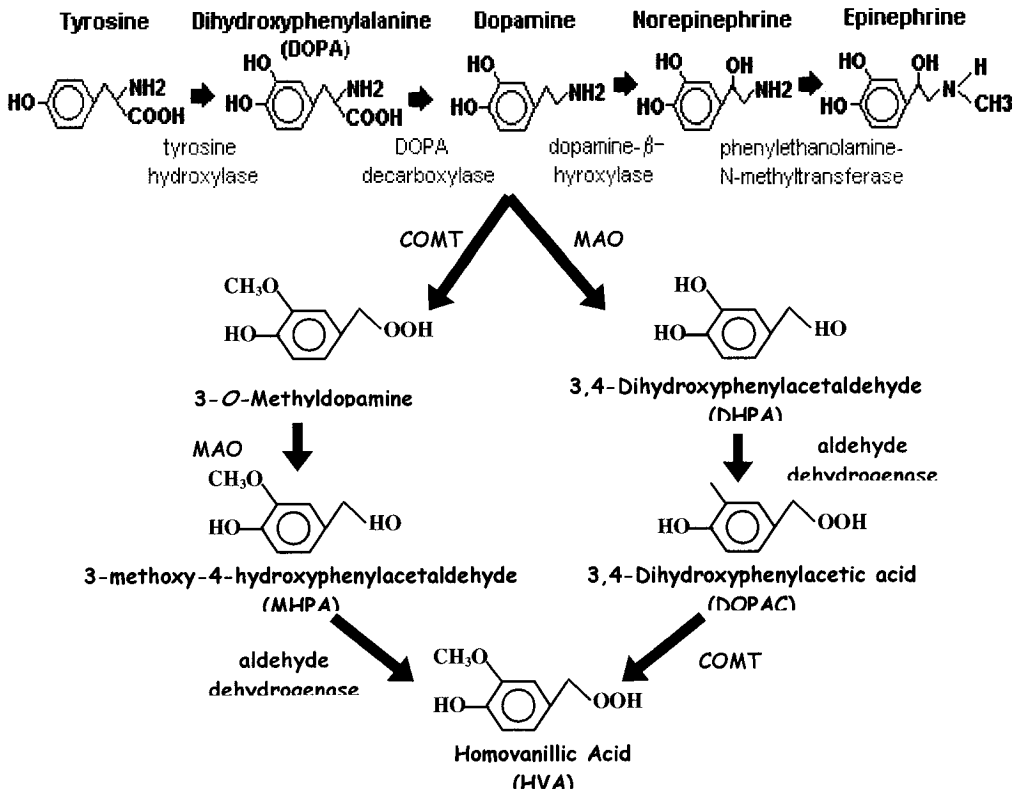

Figure 2 Synthesis and metabolism of dopamine.

There are two primary pathways of dopamine metabolism. Either monoamine oxidase (MAO) or catechol-O-methyltransferase (COMT) can catalyze the first step in catecholamine catabolism. MAO is located on the outer membranes of mitochondria thus, in the brain, is present primarily in nerve terminals and glia. There are two different isoforms of MAO (type A and B), that can be distinguished by substrate specificity and sensitivity to selective inhibitors. In the brain, MAO-A is most often located in dopaminergic and noradrenergic neurons, while MAO-B appears to be the major form present in serotonergic neurons and glia.[7] Deamination by MAO represents the more important of the two primary pathways of dopamine metabolism. The potentially toxic aldehyde intermediate, 3,4-dihydroxyphenylacetaldehyde (DHPA), generated in the

MAO reaction is rapidly oxidized to an acid, 3,4 dihydroxyphenylacetic acid (DOPAC), by aldehyde dehydrogenase. As such, DOPAC is the principal product formed by deamination of dopamine. DOPAC can then be metabolized to the end product, homovanillic acid (HVA), by membrane-bound COMT.[8]

The second primary pathway of dopamine metabolism involves catalysis by COMT and results in methoxytyramine production. HVA is obtained as the end product of this pathway as well, in this case as a result of MAO deamination followed by reaction with aldehyde dehydrogenase.[3,9]

Pathways of Serotonin Synthesis and Metabolism

In contrast to the other monoamines, serotonin (5-hydroxytryptamine or 5-HT) is synthesized from the amino acid tryptophan, as shown in Figure 3. The biochemical pathway for serotonin synthesis is initiated by the conversion of L-tryptophan to 5-hydroxytryptophan (5-HTP) by the enzyme L-tryptophan hydroxylase. The subsequent metabolic step involves the decarboxylation of 5-HTP by the enzyme L-aromatic amino acid decarboxylase.

Metabolism of serotonin is carried out primarily by the enzyme monoamine oxidase, which converts serotonin to 5-hydroxyindoleacetaldehyde (5-HIA).[10,11] This product is, in turn, readily metabolized by aldehyde dehydrogenase to produce 5-hydroxyindoleacetic acid (5-HIAA), which is the major excreted metabolite of serotonin.[12,13]

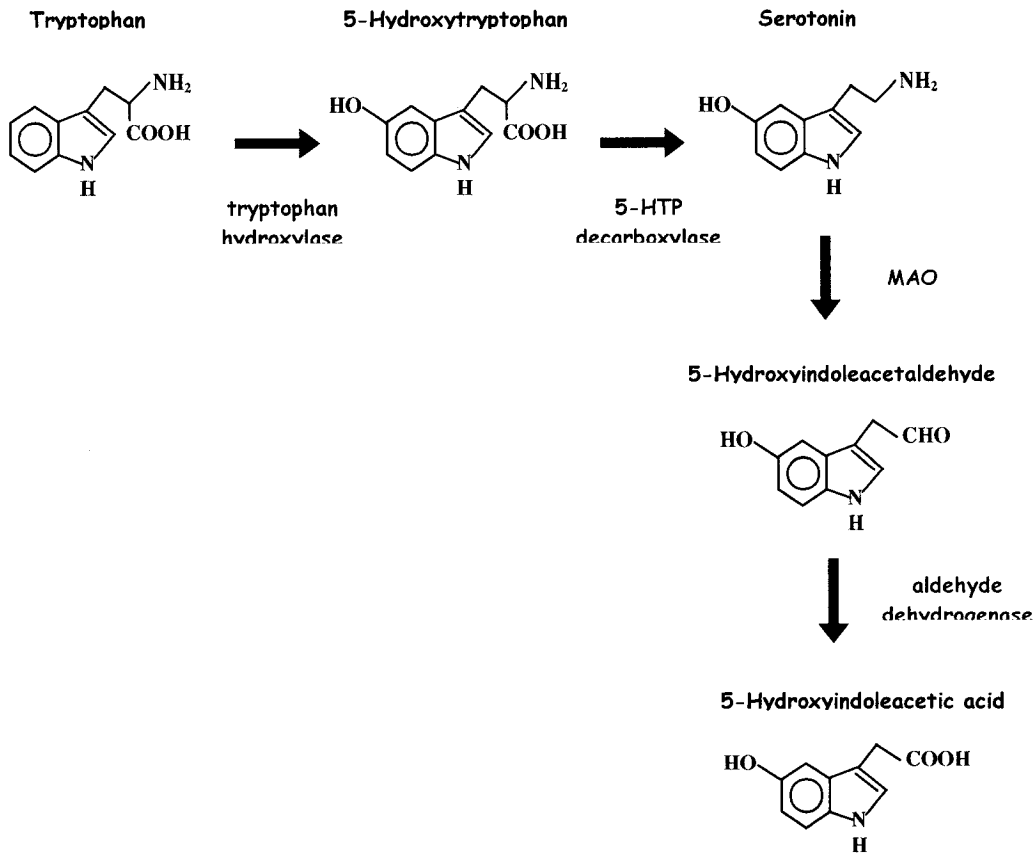

Figure 3 Synthesis and metabolism of serotonin.

1.2 Clinical Implications

Accurate and selective measurement of monoamine neurotransmitters and their metabolites in biological matrices is important in clinical diagnosis, pathological studies and neurological research. The specific functions of dopamine are not all known, and complete mechanisms of action have not yet been elucidated, but it is thought to play a crucial role in learning, memory, emotion, arousal, and regulation of cardiovascular and nervous system activity.

One dopamine function relates to its action in the basal ganglia, where it plays a critical role in the way the brain controls movements. Thus shortage of dopamine, specifically the death of dopamine neurons in the nigrostriatal pathway, is a cause of Parkinson's disease, in which a person loses the ability to execute smooth, controlled movements. In the frontal lobes, dopamine plays a role in controlling the flow of information arriving from other areas of the brain. Dopamine disorders in the frontal lobes can cause a decline in those neurocognitive functions whose central control resides in the frontal lobes, namely memory, attention and problem solving.

Disruption to the dopamine system has also been strongly linked to psychosis and schizophrenia.[14,15] In addition, the release of dopamine in the limbic system causes pleasure. Although meant to reward vital activities such as eating and sex, this same mechanism is responsible for the craving connected with addiction to drugs, such as cocaine.[16]

Additionally, dopamine can act as a hormone. Dopamine release by the hypothalamus acts as the direct signal to the anterior pituitary gland that inhibits the secretion of prolactin. Prolactin is the hormone that controls milk synthesis in the mammary gland.[17,18]

The serotonin system, however, is the most expansive of all the neurotransmitter systems within the central nervous system (CNS). The diversity of receptors and transduction pathways that underlie the varied actions of 5-HT, together with the differential expression of these receptors in different neuronal populations, provides adequate explanation as to how one neurotransmitter can be associated with such a large array of behaviours, clinical conditions, and drug actions.

Serotonin is released in response to emotional stimuli arising in the limbic system.[19,20] Disorders of the serotonergic system have been implicated in affective disorders such as depression, anxiety states, schizophrenia, suicide, aggression, obsessive compulsive disorder, eating disorders such as bulimia, migraine, and sleep disorders.[21,22] In many instances, medications that alter the metabolism and reuptake of 5-HT are known to produce beneficial therapeutic effects even in diseases with no known serotonergic system deficiencies.[23,24]

There are numerous origins of depression, many of which are unknown, and the associated neuronal circuits are complex. The development of monoamine oxidase inhibitors, and their effectiveness in the treatment of depression, provided the initial evidence of the importance of 5-HT in these disorders. More recently, there has been increasing interest in serotonin and its involvement in schizophrenia. The new approach to treating this disease has shifted to prescribing a combination of antipsychotic drugs including 5-HT and DA receptor antagonists.[25] Also, another line of research suggests that increased serotonin activity in the brain may be responsible for anorexic behaviour, while decreased serotonin activity is associated with enhanced appetite, and may be responsible for bulimic behaviour.[26,27]

A variety of drugs have been developed with the aim of improving or alleviating the symptoms of certain psychiatric disorders. Drugs of abuse also have strong effects on the limbic system. These drugs function via several distinct pathways but are responsible for the modulation of neurotransmitter levels in the brain.

Amphetamines, also known as speed, are stimulants of the central nervous system and of the sympathetic division of the peripheral nervous system. The amphetamine

reward system includes dopaminergic neurons located in the ventral tegmental area (VTA). The reinforcing and psychomotor stimulant effects of amphetamines have been attributed mainly to activation of dopaminergic transmission in the nucleus accumbens.[28,29] Physiologically, amphetamine causes elevated blood pressure, heart rate, body temperature, respiration rate, agitation and energy metabolism. Despite these and other side effects, amphetamine is used therapeutically in the treatment of narcolepsy, attention deficit hyperactivity disorder (ADHD) and certain types of mental depression.[30,31]

Amphetamine has a wider assortment of cellular effects than cocaine, increasing the activity of monoamines in several important ways. Amphetamine stimulates the release of dopamine and norepinephrine from catecholamine nerve terminals, increasing the amount of these neurotransmitters in the synapse. Like cocaine, amphetamine also inhibits reuptake of the catecholamines, increasing their ability to activate receptors. In addition, amphetamine inhibits monoamine oxidase, the enzyme responsible for the metabolism of monoamine neurotransmitters, further increasing the availability of these neurotransmitters. Finally, there is some evidence that amphetamine may directly activate catecholamine receptors, further contributing to monoaminergic activity.[32,33]

Traditional tricyclic antidepressants (TCAs) made a positive contribution to improving quality of life for depressed patients when they were introduced more than a generation ago, but they have many limitations. The TCAs produce a wide range of pharmacological actions affecting a variety of neurotransmitters. This lack of specificity results in a decreased therapeutic efficiency and is the source of a number of serious, and potentially life-threatening, side effects. The impetus for the development of the highly

selective serotonin reuptake inhibitors (SSRIs) was the perceived need for antidepressants with an improved therapeutic profile.

TCAs and SSRIs bind to the serotonin transporter (SERT), noradrenaline transporter (NET) and/or dopamine transporters (DAT), to inhibit transport of monoamines into the cytoplasm, thereby increasing monoamine levels within the synaptic cleft. Compounds that inhibit the action of MAO have been shown to have beneficial effects in the treatment of clinical depression, even when tricyclic antidepressants are ineffective. Monoamine oxidase (MAO) causes the oxidative deamination of dopamine and serotonin. By preventing the metabolism of dopamine and serotonin with monoamine oxidase inhibitors, it increases the availability of these monoamine neurotransmitters.

Although some of the serotonin released into the synaptic cleft is metabolized by MAO, most of it is typically removed by the pre-synaptic neuron via a reuptake mechanism. This latter pathway is inhibited by tricyclic antidepressants and the newer and more selective serotonin reuptake inhibitors (SSRIs).

In recent years, SSRIs have been increasingly prescribed for depression. These drugs possess the dual advantages of increased selectivity for the serotonin receptor and an improved therapeutic profile. Fluoxetine (Prozac) is the most famous drug in this class. These drugs act by terminating the reuptake of neurotransmitter by the presynaptic cell, resulting in prolonged serotonin presence in the synaptic cleft. Although highly effective, the mode of action of these antidepressant drugs on their direct target, the serotonin transport protein, and possible regulatory mechanisms with respect to long-term alleviation of depression, are not completely understood.[34]

Several classes of psychotropic drugs increase the overflow of dopamine and serotonin. Three of these, each with a different mechanism of action, were chosen to stimulate the release of extracellular levels of monoamines in the nucleus accumbens of the male rat. More specifically, the psychostimulant amphetamine was selected due to its ability to acutely increase extracellular dopamine levels. This action is thought to mediate increased locomotor and stereotype behaviors produced by psychostimulant drugs. Pargyline, known to increase monoamine concentration by inhibiting monoamine oxidase, was the second drug used. Finally, the antidepressant drug fluoxetine, an SSRI, was chosen in order to monitor a change in extracellular serotonin levels.

1.3 Nucleus Accumbens

The effects of acute administration of psychotropic drugs on extracellular dopamine and serotonin concentrations were examined in the nucleus accumbens (NAcc). The NAcc was chosen because it is both an area rich in dopaminergic and serotonergic neurons, and due to its widespread involvement in a variety of neuronal functions. The NAcc has been ascribed several functional roles, including the regulation of motivational and emotional processes, reward function, and drug addiction.[35,36]

The NAcc is located in the basal forebrain, and receives dopamine terminals from cells in the ventral tegmental area. The NAcc is typically divided into two major subdivisions, the ventromedial shell and the dorsolateral core. The core receives major projections from the dorsal prefrontal cortex, the rostral division of the basolateral amygdala, and the dorsal subiculum of the hippocampal formation. It projects to the dorsolateral ventral pallidum, that projects to the subthalamic nucleus and substantia nigra. The shell, on the other hand, projects to the ventromedial ventral pallidum, that in

turn projects to the ventral tegmental area (VTA), the origin of midbrain DA neurons innervating both mesolimbic and mesocortical areas. These synaptic inputs are, in turn, regulated by a number of neurochemical signalling agents that can ultimately influence information processing in the NAcc.[37,38,39]

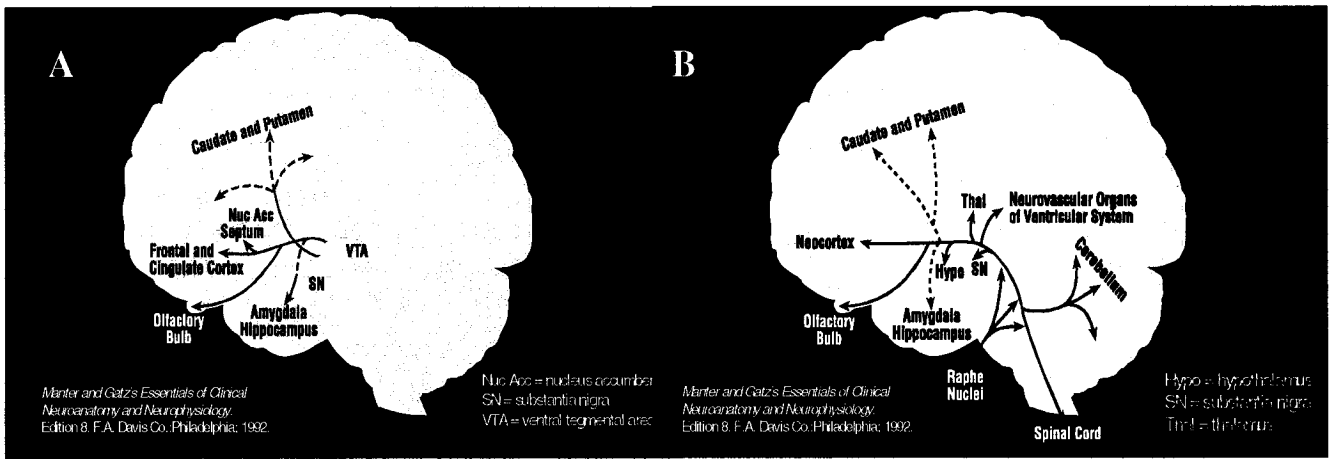

Figure 4 Diagram displaying the A) dopaminergic and B) serotonergic intricate pathways. Projections to and from the nucleus accumbens are illustrated.[40]

1.4 Microdialysis

Determination of drug levels in bodily fluids (cerebrospinal fluid, blood, urine) is performed via routine clinical procedures in order to correlate observed clinical effects of pharmacological agents with the objective biochemical changes that occur. To monitor biochemical changes in the brain requires greater finesse since invasive sampling methods (by syringe) are not suitable. An alternative technique is to sacrifice the animal and immediately remove the brain and select specific brain areas for *in vitro* analysis. However, these *in vitro* methods disrupt the integrity of brain nuclei, thus resulting in misleading measures of neurotransmitter activity. In addition, only one data point can be obtained per animal.

Using microdialysis, one can obtain a complete response curve, including control levels, from a single animal. This advantage is conferred on this technique because microdialysis is an *in vivo* technique that permits near instantaneous monitoring of local concentrations of drugs and metabolites at specific sites in the body over an extended time course. The only method that offers time resolution results comparable to microdialysis is *in vivo* voltammetry. *In vivo* voltammetry has become a valuable tool for monitoring neurochemicals present in extracellular fluid, with high temporal resolution, by implanting electrodes into the brain of a live animal. The drawbacks of voltammetry, however, such as the limited measurements of DA, DOPAC and to some extent 5-HIAA, and the impossibility of exact calibration make it a rather exclusive and laborious procedure. Moreover, another limitation of *in vivo* voltammetry resides in its limited capacity to identify the substances to be detected.[41]

Microdialysis involves the insertion of a microdialysis probe into a selected tissue or fluid. The probe consists of a small semipermeable hollow cellulose fibre membrane, connected to a small diameter inlet and outlet tubing.[42] The membrane acts as a barrier preventing the perfusion solution from directly contacting the tissue while allowing analytes to be sampled. Therefore, continuous sampling can be performed while minimizing infection and disruption of the physiological system. In the brain, the probe is continuously perfused with artificial cerebrospinal fluid that has an ionic composition and pH similar to the extracellular fluid. Small molecules present in the extracellular fluid diffuse across the membrane, down their concentration gradient into the perfusion medium, and are collected in small vials at the end of the tubing for analysis. Membranes

with different molecular weight cut-offs can be used to select the upper molecular weight sampled.

The recovery of substances depends on numerous factors, namely the effective surface area of the membrane, the flow rate of artificial CSF, temperature, molecular weight and charge of the substance, binding to the membrane and tubing, pH of the medium and degradation of the substance.

Perfusion flow rate is the parameter that can be altered most easily in order to vary recovery. At lower perfusion rates, there is more time for compounds to diffuse through the membrane into the dialysate, resulting in higher relative recoveries. Molecular weight is another primary determinant of compound recovery, with dramatically decreased recovery for analytes with molecular weight above 1 kDa. Ionic strength and pH of the perfusate should mimic the extracellular environment to minimize differences in the osmotic pressure at the probe tip. Moreover, the addition of an antioxidant in the perfusate is usually recommended in order to reduce oxidation and further degradation of the analyte.

Microdialysis has become an attractive tool for pharmacokinetic research, as it offers several distinct advantages over previous sampling techniques. This includes the possibility to simultaneously examine concentration changes of exogenous and endogenous analytes in extracellular fluid from discrete brain regions, with minimal disruption of the tissue and the blood-brain barrier. Investigations of the mechanisms of drug actions can thus be performed in very specific brain tissues . Also, it allows for continuous monitoring of extracellular levels of various neurochemicals and their

metabolites *in vivo*.[43] Moreover, it offers high-resolution concentration profiles of drugs, that enable calculations of kinetic parameters.

The membrane acts as an effective enzyme inhibitor excluding these molecules due to their large molecular weights, thus preventing continuous enzymatic degradation of neurotransmitters once they have entered the perfusion solution. Also, by preventing large molecules from entering the perfusion medium, the membrane partially purifies the samples, making direct injection into an analytical system possible.[44,45]

The sampling limits of microdialysis are usually set by the sensitivity of the assay techniques, thus the application of proper analytical techniques is essential for successful analysis.[46] With the progress of analytical methodology, especially with respect to acquiring low volume/low concentration measurements and simultaneous measurement of multiple compounds, microdialysis is playing an increasingly important and standard role in pharmacokinetic research.[47]

1.5 Analytical Methods

A great advantage of *in vivo* microdialysis is that it can be coupled with a wide range of analytical techniques. The small volumes typical of microdialysis samples preclude the use of preconcentration methods prior to analysis. Therefore, analytical methods providing high sensitivity are required. If the analytical method does not have sufficiently low detection limits, larger samples must be taken. This, however, requires a longer sampling time and leads to decreased temporal resolution. The techniques currently in use with *in vivo* microdialysis which allow the detection of multiple analytes in each sample are characterized as separation based methods of analysis.[48,49]

Samples obtained by microdialysis consist primarily of small hydrophilic analytes dissolved in a highly ionic matrix. In general, these characteristics have made liquid chromatography (LC) and capillary electrophoresis (CE) the analytical methods of choice for coupling to microdialysis sampling. Reversed-phase or ion-exchange chromatography combined with offline solid phase extraction are the modes of LC most compatible with direct injection of samples.[50,51,52] Capillary zone electrophoresis (CZE) and micellar electrokinetic chromatography (MEKC) are the most common CE modes used with microdialysis.[53,54,55,56]

The temporal resolution of a microdialysis experiment is often dependent on the sensitivity of the analytical method because of the volume of sample that must be pooled for accurate quantitation of the analytes. The detection method employed following the separation is also very important since methods with higher sensitivity will require smaller sample volumes to attain the same signal. In addition to high sensitivity, the detector must also be selective toward the analytes. In these experiments, analyte selectivity is provided by the membrane and the separation method, however, the detector must also provide additional selectivity to accurately quantitate similar analytes in a complex sample matrix. Immunoassay, ultraviolet absorbance, electrochemical, fluorescence and mass spectrometric, are the most common types of detectors for LC analysis and provide varying levels of sensitivity and selectivity.[57,58,59,60,61] For CE, electrochemical and laser-induced fluorescence detection have been more widely used for analysis.[62,63,64,65,66]

Clearly, the analytical method that combines high selectivity with the lowest detection limit and smallest sample volume requirement affords the best temporal resolution for a given microdialysis experiment.

1.6 Overcoming Limitations of Current Technologies

Though the technique of choice for measuring basal monoamine levels has traditionally been HPLC or CE using electrochemical, fluorescence or voltammetric detection, these methods require relatively long analysis times, high sample volumes, lengthy analyte derivatizations or ion-pairing reagents to achieve low detection limits. Additionally, it is not always possible to monitor all analytes of interest in a single run. Furthermore, conclusive identification of analytes is often impossible, as these conventional assay methods confirm the identity of analytes based solely on retention times determined from standards and may not accurately reflect the elution profile in a complex biological sample.[67]

In pharmacokinetic and behavioural research with animals, enhanced temporal resolution is essential in order to obtain detailed physiological information correlated to a specific drug and behaviour. Our laboratory focuses on the neurochemical and molecular events that affect sexual behaviour and neuroendocrine functions. More specifically, we are interested in the role of brain monoamine and neuropeptide systems involved in sexual excitement, arousal, inhibition, and copulatory behaviour in laboratory animals.[68,69] The importance of high temporal resolution is clear considering that a rat undergoes an entire cycle of copulation in ten minutes. For example, if a sample size of 10 μL is required for analysis with a typical perfusion flow rate of 1.0 μL/min, only one

sample can be obtained to describe the entire session. An increase in various excitatory neurotransmitters in many brain areas is expected, however, precise changes, the times at which they took place, and the behaviour they are correlated to can not be determined. Only an overall picture is presented.

It is evident that a new, rapid, and selective assay for the measurement of basal levels of monoamines must be developed in order to allow small volume sampling and relatively short analysis time, enabling high throughput analysis. The aim of this research was to measure basal levels of monoamines and their metabolites from a 2 μL microdialysis sample. One of the first steps was to establish a chromatographic method that provided adequate retention of all five analytes of interest and the internal standards on an analytical column. This was a challenge since DA is an extremely polar compound, and retention using classical reverse-phase columns was not satisfactory. Recently, a newer type of separation based on a normal phase mechanism in aqueous mobile phases termed hydrophilic interaction chromatography (HILIC) has been gaining popularity for the separation of highly polar analytes not amenable by reverse phase separation. For this research, a silica based column packed with fluorophenyl bonded phase was used to separate both monoamine neurotransmitters and their respective acid metabolites by a combination of reverse phase and HILIC modes. Retention was critical for online desalting of the microdialysis sample and separation of all the analytes for successful detection. The detection method of choice was mass spectrometry.

1.7 Mass Spectrometry

Microdialysis combined with liquid chromatography-mass spectrometric detection (LC-MS) is gaining momentum as an important tool in biochemical and pharmaceutical research. Mass spectrometry is a technique for separating ions by their mass-to-charge (*m/z*) ratios. A mass spectrometer consists of three elements: an ion source, a mass analyzer, and a detector. The ion source generates ions from a sample and introduces them into the vacuum chamber of the mass spectrometer. The mass analyzer selects or separates the ions and transmits them to the detector that records the current produced by ions leaving the mass analyzer.

Some of the advantages of mass spectrometry are that it enables the simultaneous analysis of many analytes in each polarity, excellent selectivity against any interfering compounds in the biological matrix, and more structural information and enhanced confidence of the identity of the analyte is obtained. Lastly, it offers the extremely low detection limits, in the sub-picogram range, required to measure basal neurotransmitter levels.

1.7.1 Electrospray Ionization

Techniques for ionization have been key in determining what types of samples can be analyzed by mass spectrometry. Electrospray ionization (ESI) has become one of the most important ionization techniques for the online coupling of liquid phase separation methods with mass spectrometry, allowing for extremely effective detection, characterization, and trace analysis of both biological and chemical materials. ESI is a soft-ionization technique that allows for controllable fragmentation of analytes and the ability to ionize small as well as large molecules. Furthermore, it can create highly

charged forms of very high molecular weight compounds, and it allows noncovalent interactions between molecules in solution to be preserved in the gas phase.[70,71] ESI-MS can be divided into three steps: production of electrically charged droplets from a sample solution, formation of the gas-phase ions, and transportation from the atmospheric pressure ionization source region into the vacuum of the mass analyzer.

Electrospray ionization is used to produce gaseous ionized molecules from a liquid solution by creating a fine spray of droplets in the presence of a strong electric field. In pneumatically assisted electrospray, a sample solution is pumped through a capillary tube held at a high voltage. The nebulizer gas that flows over the capillary tube shatters the liquid as it emerged from the capillary leading to aerosol formation, whereas the voltage charges the droplets as they are formed. The potential used is sufficiently high to disperse the emerging solution into a very fine spray of charged droplets, all of which have the same polarity. The solvent rapidly evaporates, shrinking the droplet size and increasing the charge concentration at the droplet's surface. Eventually, at the Rayleigh limit, Coulomb repulsion overcomes the droplet's surface tension and the droplet explodes. This Coulomb explosion forms a series of smaller, lower charged droplets. The process of shrinking followed by explosion is repeated until individually charged analyte ions are formed. This process is shown schematically in Figure 5. The charges are statistically distributed amongst the analyte's available charge sites, leading to the formation of multiply charged ions, given the proper conditions. Heated nitrogen gas is applied to enhance droplet desolvation, wherein the gas is introduced perpendicular to the spray. Electrospray can operate in both positive and negative ion modes resulting in

positively and negatively charged analytes. The ions formed are then introduced and analyzed by the mass spectrometer, in this case, a triple quadrupole.[72,73]

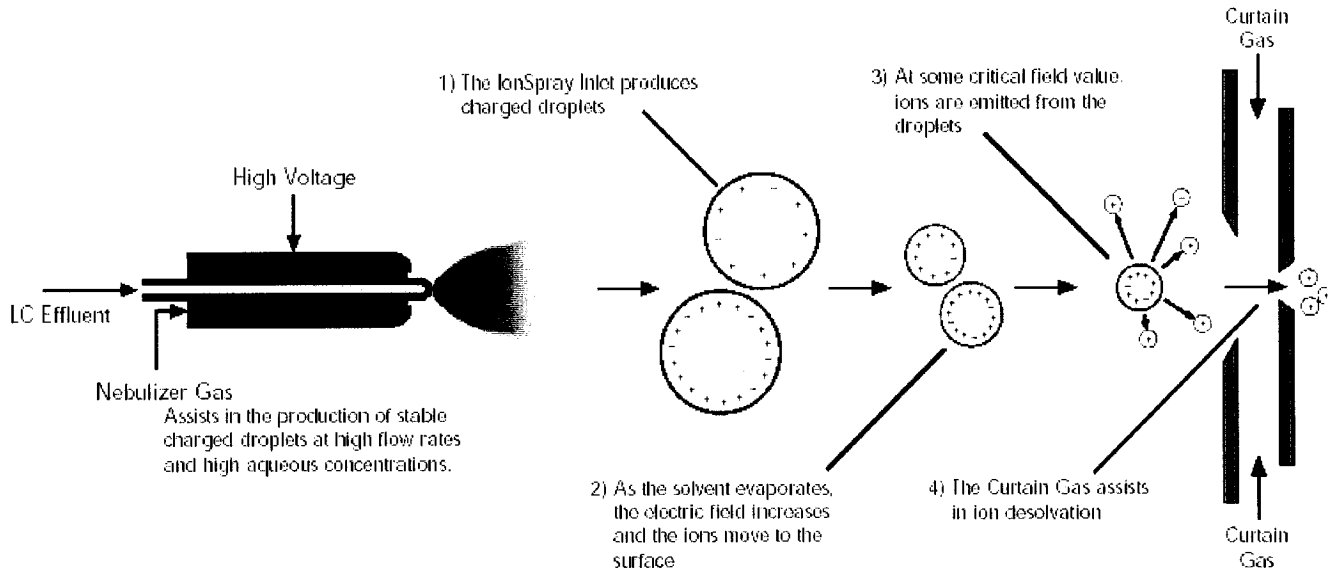

Figure 5 Diagram displaying the steps involved in pneumatically assisted electrospray ionization.[74]

1.7.2 Tandem Mass Spectrometry

The triple quadrupole mass spectrometer can be broken down into three main parts, two mass selective quadrupoles, operated with both r.f. and d.c. potentials, and one fixed r.f.-only quadrupole. In the first quadrupole (Q1), ions are separated according to their *m/z*. Only ions with the selected mass (actually *m/z*) are transmitted through to the second quadrupole. This second quadrupole (q2) is not a mass analyser, rather it has a fixed r.f. voltage, thus all ions are allowed to pass through. Instead, this chamber is used as a collision cell for fragmenting the precursor ion with an inert gas by a process known as collisional-induced dissociation. All of the ions from the second quadrupole are

transmitted through to the third quadrupole (Q3), where these product ions are filtered and detected.[75,76]

The product ion MS/MS spectrum is obtained using the selected reaction monitoring (SRM) scan mode, where only one or a few precursor-to-product ion transitions are monitored over a narrow scan range.[77] In this mode the first quadrupole transmits only the ions corresponding to the masses of the analytes. It does this by alternating from mass to mass in rapid succession. The third quadrupole then analyses the product ions for the masses known to be fragmentation products of the analytes. This provides extremely high selectivity since the probability of an interfering species having the same precursor mass and fragmentation masses is extremely low. The net result of this technology is an analytical method that affords selective detection of product ions that are unique signatures of the analyte of interest. Furthermore, this technique affords a high sensitivity as a result of chemical noise reduction.[78]

However, ESI is known to be susceptible to salts and impurities, which often cause a dramatic decrease in sensitivity due to the suppression of the ionization of the product of interest.

1.8 Liquid Chromatography

Due to the high ionic strength of microdialysis samples, they have to be desalted in order to be successfully analysed by MS. Most commonly, this challenge can be overcome with a range of offline sample pretreatment methods, including membrane-filtration cartridges and solid phase extraction (SPE).[79,80] However, the move towards small-volume samples puts more stringent requirements on sample preparation

techniques. Minimal sample handling is preferred in order to avoid any loss of sample and to reduce error. Moreover, most of these methods have laborious and time-consuming protocols. Since microdialysis samples are relatively clean of large molecules, an alternative is to desalt the samples online using typical liquid chromatographic techniques.

Liquid chromatography (LC) is one of the most commonly employed techniques for the analysis of microdialysis samples because it allows simultaneous detection of several analytes in a complex mixture.[81,82] Reverse phase or ion-exchange are the modes of liquid chromatography that are most compatible with direct injection of aqueous microdialysis samples.[83,84,85] The mode of chromatography chosen for analysis is dependent on the physiochemical properties of the analytes. Moreover, the type of column used (length, particle size and internal diameter) is determined by the sampling interval desired and the required sensitivity. In a typical LC assay, 5-10 μL of sample are needed. This means that the temporal resolution is 5-10 min if a perfusion flow rate of 1 μL/min is employed. If lower flow rates are used to increase recovery, temporal resolution is further decreased.

In principle, equivalent separations can be obtained with columns having the same length but different internal diameters, because column efficiency and analysis time are dependent on the linear velocity of the mobile phase. Thus, no resolution advantage is gained through the use of narrow bore LC columns. However, the use of microbore columns results in a tremendous increase in sensitivity, because peak dispersion is proportional to the square of the column diameter. Therefore, short (L = 5 cm) microbore (d = 1 mm) columns have become increasingly popular for the analysis of microdialysis

samples because they provide the optimum combination of high sensitivity and rapid analysis.[44,45]

However, highly polar low-molecular-weight compounds are often not sufficiently retained by reverse phases and represent a particular chromatographic challenge. In some cases, ion-pairing reagents are employed to offer some retention. This technique, however, is not very compatible with MS since suppression of the signal is often observed when such reagents enter the MS. Consequently, the requirement to retain and analyze polar molecules by HPLC-MS is one that has grown steadily over the last few years, and has been the driving force behind the generation of a range of new types of stationary phases dedicated to this purpose. The result of all this effort has been the development of a new type of stationary phase that appears to operate in both reverse phase and hydrophilic interaction modes.

1.8.1 Hydrophilic Interaction Chromatography

Hydrophilic interaction chromatography (HILIC) exhibits normal phase chromatographic behavior in aqueous mobile phases. This is usually accomplished by increasing the amount of organic modifier in the mobile phase in the neighborhood of 55-95%. As the percent of organic modifier is increased, increased retention is observed for more polar compounds while reduced retention is observed for hydrophobic compounds. In general, the elution profile observed is one where the least polar analyte elutes first and the most polar elutes last. Therefore, the more soluble the analyte is in water, the more retention is observed. Conversely, the less soluble the analyte is in mobile phase, the more retention is observed.

Recent developments in column technology have introduced fluorinated stationary phases capable of operating in reverse phase and HILIC modes. For example, these novel columns give new selectivity for halogenated and polar compounds in reverse phase analysis. Fluorinated packings offer additional modes of interaction compared to those of traditional alkyl bonded phases, and often provide different retention behavior and selectivity. Introducing fluorine groups into the stationary phase gives columns unique capabilities in solute-stationary phase interactions. The carbon-fluorine bond has greater dipole character than a carbon-hydrogen bond, giving greater interactions with polar and halogenated compounds.

In the present case, the column that provided the best retention for all the analytes of interest was the Thermo Hypersil Fluophase PFP. The stationary phase of Fluophase PFP contains a perfluorinated phenyl ring, where every hydrogen atom on the phenyl ring is substituted for a fluorine atom as shown in Figure 6. This substitution gives the phase extra interactions with polar samples to extend its selectivity capabilities.

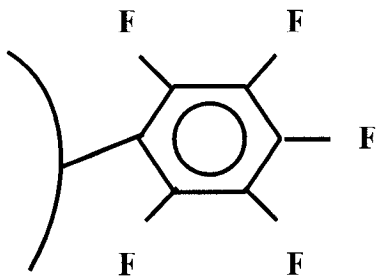

Figure 6 Diagram displaying the stationary phase of the Fluophase PFP column.

The combination of strong interaction with the carbon-fluorine dipole, and shape selectivity due to the more rigid nature of the fluorine-substituted alkyl chains, makes Fluophase PFP a packing capable of separating compounds with hydroxyl, carboxyl,

nitro, and other important polar functional groups frequently found in biomolecules. Moreover, this stationary phase is stable under 100% aqueous conditions, allowing for rapid and effective online desalting of microdialysis samples prior to entering the mass spectrometer.

In this study, a rapid and selective method using microdialysis-LC/MS/MS was developed for the *in vivo* analysis of the catecholamine dopamine, and its metabolites DOPAC and HVA, and the indolamine serotonin, and its metabolite 5-HIAA.

Sampling of the extracellular fluid by microdialysis enables continuous monitoring of intercellular chemical concentrations, that allows for the study of neuronal communications. Liquid chromatography using a column with a fluorinated phase provided sufficient separation to allow for all the analytes to be detected. Mass spectrometry was used to quantify molecules with a high degree of specificity, therefore, increasing the degree of confidence that other molecules are not interfering with, or contributing to, the signal produced by the molecule of interest.

The study was designed to monitor basal extracellular monoamine levels, and the quantitative responses of these neurotransmitters to three different drugs acting at various stages of neuronal processing including uptake, release and metabolism of monoamines. Performance and reliability of the method was assessed by treatments with these drugs having well-known effects on dopamine, serotonin and their metabolites. The three drugs investigated were amphetamine, pargyline and fluoxetine. This assay offers the advantages of high temporal resolution and, accordingly, the potential to assess the dynamics of dopamine and serotonin function in the nucleus accumbens of the male rat.

2. EXPERIMENTAL

2.1 Chemicals

Dopamine (DA), 3,4-dihydroxyphenylacetic acid (DOPAC), homovanillic acid (HVA), serotonin (5-HT), and 5-hydroxyindolacetic acid (5-HIAA) were obtained from Sigma (St. Louis, MO). The internal standards dopamine-d_4 (DA- d_4) and homovanillic acid-d_2 (HVA- d_2) were purchased from CDN Isotopes (St.-Laurent, Qc). Amphetamine was obtained from BDH (Mississauga, Ont.); licensed by Health Canada. Pargyline was purchased from RBI (Natick, MA) and fluoxetine from Fermion, Orion Corporation (Clifton, New Jersey). Sodium pentobarbital was purchased from MTC Pharmaceuticals (Cambridge, Ont.); licensed by Health Canada. All solvents and reagents were of HPLC or analytical grade. Eighteen megaohm cm^{-1} water, obtained from a Milli-Q system (Millipore, Bedford, MA), (Type 1) was used to prepare all the solutions.

The 1 mM stock solutions of DA, DOPAC, HVA, 5-HT, 5-HIAA, DA-d_4 and HVA-d_2 were prepared in 100% methanol and stored at 4 °C. The required working solutions were obtained by further dilution with 0.2% formic acid pH 3.0. Amphetamine (5 mg/kg/mL) and pargyline (100 mg/kg/mL) were prepared in Type 1 water. Fluoxetine (14 mg/kg/mL) was dissolved in 1% ethanol in water and sonicated until completely dissolved. Artificial cerebrospinal fluid (αCSF), solution used for microdialysis perfusion, consisted of 145 mM NaCl, 2.7 mM KCl, 1.2 mM $CaCl_2$, 1.0 mM $MgCl_2$, 0.2 mM ascorbic acid, 2 mM Na_2HPO_4, pH 7.4. All solutions were stored in the dark.

2.2 Animals

Male Long-Evans rats (Charles River, St.-Constant, Qc) weighing between 350 and 400 g were used for all experiments. Animals were housed in groups of four per cage in a temperature-controlled room (21 °C). Rats were kept on a 12 hour light-dark cycle, with lights on at 20 h. Food and water were available *ad libitum.*

2.3 Surgery

All surgical procedures and protocols followed the CCAC guidelines and were approved by the Animal Care Committee, Concordia University. Rats were anaesthetized with an intraperitoneal (i.p.) injection of sodium pentobarbital (65 mg/kg). Once deep anaesthesia was obtained, rats were transferred to a stereotaxic frame (David Kopf, Topanga, CA). A longitudinal incision was made to expose the skull. A small hole was drilled to allow implantation of a single guide cannula (Plastics One Inc., Roanoke, VA) into the nucleus accumbens at the following coordinates (relative to bregma and the skull surface) at a 10° angle: AP +3.1, ML +2.7 and DV -5.3. These coordinates place the cannula 1 mm above the shell of the nucleus accumbens. Three skull screws were implanted, and the cannula was fixed in place with dental cement. Following cannulation, the animals were housed individually in plastic cages (36 x 26 x 19 cm) and were given one week to recover prior to undergoing experimentation.

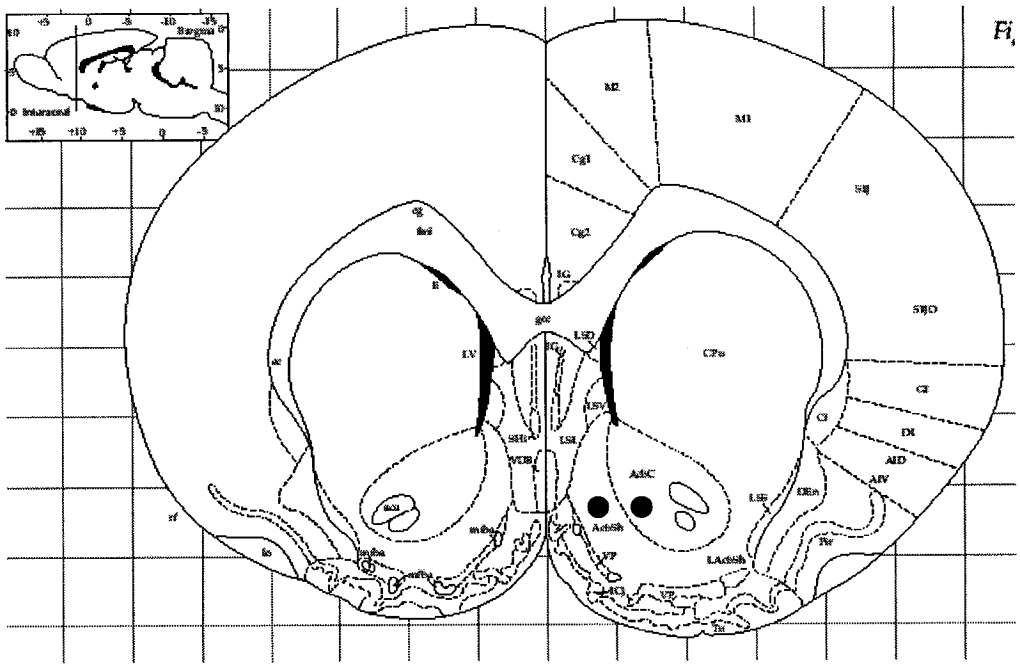

Figure 7 Coronal section showing the NAcc coordinates where probe was aimed.

2.4 Preparation of Microdialysis Probe

The dialysis probe consisted of a 2 mm length of semi-permeable membrane with a molecular weight cutoff of 13 000 Daltons (Spectrum Laboratories Inc., Ft. Lauderdale, FL). They were closed with epoxy at one end, and attached to a 21 mm length of 26 gauge stainless steel tubing at the other. The other end of the stainless steel tube was connected to a 50 cm length of PE-20 tubing (Becton Dickinson Primary Care Diagnostics, Sparks, MA) that attached to a single channel infusion swivel (Harvard Apparatus, Holliston, MA) positioned over the testing cage. Another piece of PE-50 tubing connected the other side of the swivel to a microliter syringe pump (Harvard Apparatus, South Natwick, MA). A bare fused-silica capillary with 150 μm O.D. and 75 μm I.D. (Polymicro Technologies, AZ) extended into the probe 0.5 mm from the end of

the tip; the other end exited the PE-20 tubing 35 cm below the infusion swivel. Extracellular sample fluid was collected from the other end of the capillary. Steel spring casings protected the tubing located inside the testing cage. The entire length of semi-permeable membrane extended below the guide cannula tip.

2.5 Probe Recovery

In order to be able to estimate the *in vivo* concentrations of DA, 5HT and their metabolites, it was necessary to determine the recovery of the microdialysis probe. This was accomplished by placing the microdialysis probe into a stirred standard solution (23 °C) containing known concentrations of all the analytes of interest, diluted in αCSF. The probes were perfused with αCSF at a flow rate of 1 μL/min. The relative recovery ($recovery_{in\ vitro} = C_{out} / C_{in}$) was calculated by comparing the area under the peaks in the ion chromatograms for each respective analyte, where C_{out} is the concentration in the dialysate and C_{in} the concentration in the medium.

2.6 *In Vivo* Microdialysis Procedure

2.6.1 Dialysis Probe Implantation

Twenty-four hours before the experiments, the animal was anaesthetized with an intraperitoneal injection of sodium pentobarbital (65 mg/kg). The guide cannula dummy was then removed and replaced with a microdialysis probe, with a 2 mm length active membrane, that was inserted into the nucleus accumbens. To minimize tissue damage, the probe was introduced and tightened very slowly. The animals were then placed in a

clear plexiglass chamber. The awake, freely moving rats had food and water available throughout the experiment as shown in Figure 8. To stabilize the tissue in the area of the probe, artificial cerebrospinal fluid was perfused overnight at a rate of 0.25 μL/min using the microliter syringe pump. The following day, the flow rate was increased to 1.0 μL/min one hour before sampling began.

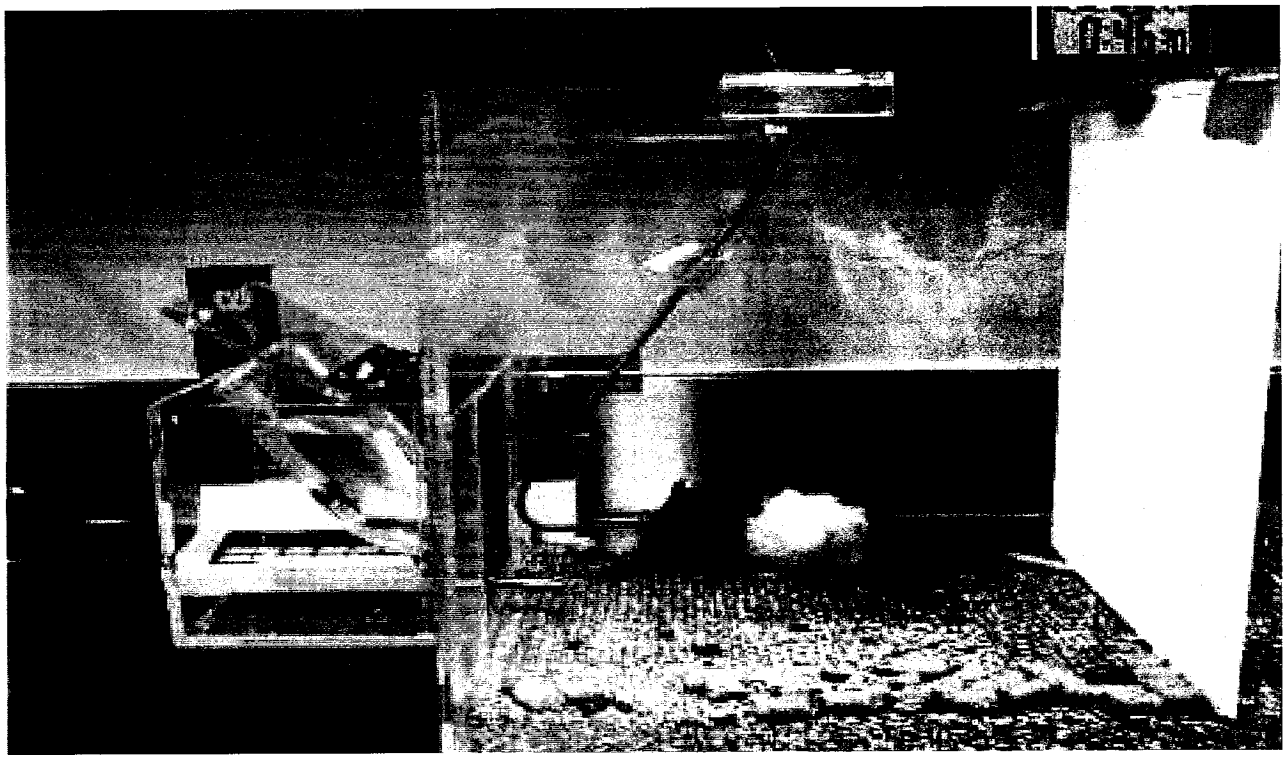

Figure 8 Awake, freely moving rat in the testing chamber connected to a microdialysis probe.

2.6.2 Collection of Dialysates

Basal levels of dopamine, serotonin and their metabolites were monitored for one hour before administration of the drug. Microdialysis fractions of 2 μL each were collected at 2 min intervals into 250 μL polypropylene microinserts with a conical point

for wide I.D. vials (Chromatographic Specialties Inc., Brockville, Ont.). Fraction collection was performed manually by positioning the outlet of the microdialysis probe into the collection vials, which were wrapped with aluminum foil. The samples were then diluted with 8 μL of 0.2% formic acid in water containing the two internal standards. The microinserts were placed into 1.8 mL AP2000 polypropylene sample vials purchased from VWR International (Mississauga, Ont.) and capped with a Snap-It seal with an 11 mm slit (Chromatographic Specialties Inc., Brockville, Ont.). The last step was to centrifuge for 30 sec in order to ensure that there were no drops left on the walls of the microinsert. The vials were positioned in the cooled autosampler at 5 °C for analysis.

2.7 Histology

At the end of the experiment, the animals were sacrificed in order to verify proper cannulae placement. They were injected with 1 ml of sodium pentobarbital and perfused intracardially using a 50 ml syringe filled with phosphate buffer saline, which acted to remove the blood, followed by 50 ml of 4% paraformaldehyde in 0.1 M phosphate buffer, which served as a fixative. The brains were placed in a 4% paraformaldehyde solution for 4 hours, and then into a 30% sucrose solution. Once removed from this solution, the brains were frozen using dry ice and sliced into coronal sections (40 μm thick) using a Leica cryostat (Meyer Instruments Inc., Houston, TX).

2.8 Chromatographic Analysis

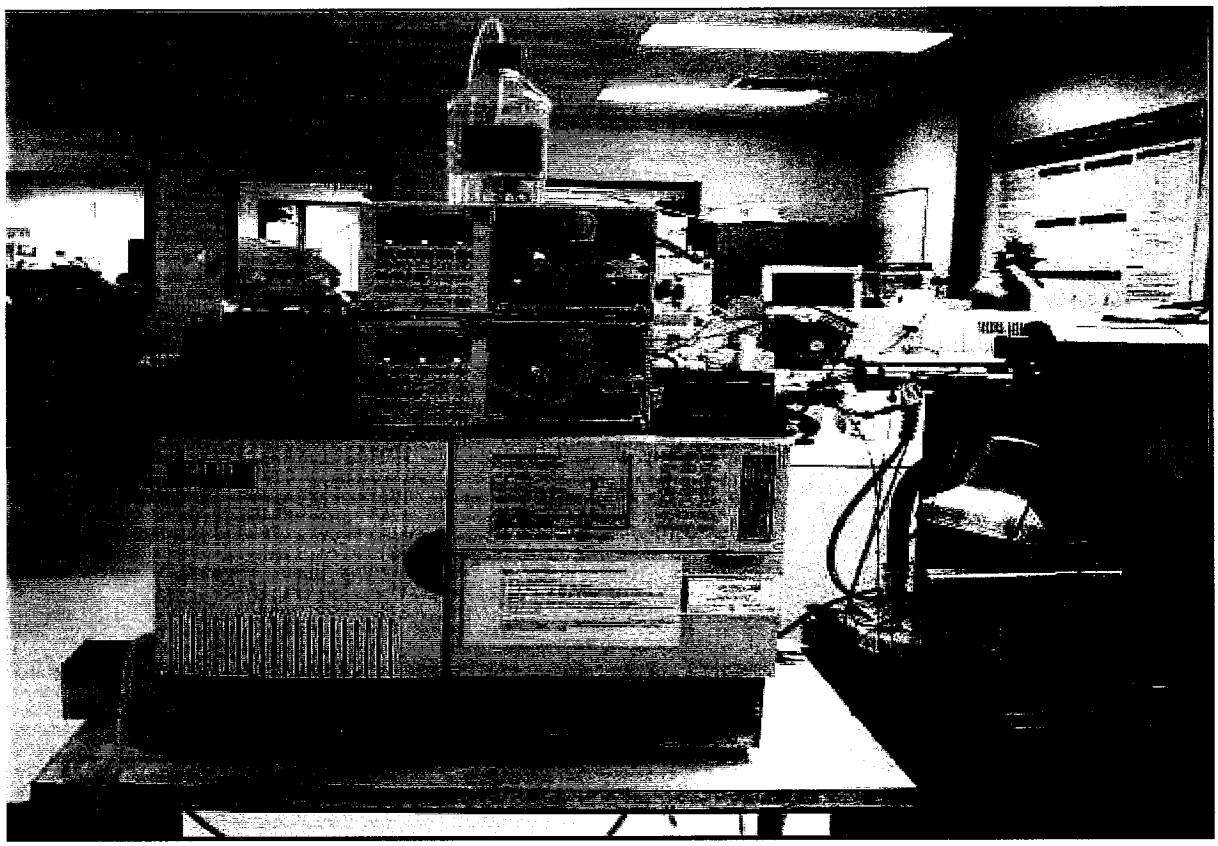

Figure 9 The liquid chromatography (LC) system consisted of the following components: a Shimadzu SIL-HTc autosampler, a set of Shimadzu LC-10ADVP pumps (Shimadzu Scientific Instruments, Inc., Columbia, MA), a two position microelectric actuator (Valco Instruments Co. Inc., Houston, Texas), an analytical column and a Waters 515 pump.

The Shimadzu autosampler was equipped with a 25 µL injection loop. The total volume from injector to source excluding the column was 35 µL. The mobile phase (Shimadzu Pump A) used to load the samples onto the column was 0.1% acetic acid in water pH 3.4. The mobile phase (Shimadzu Pump B) used to elute the analytes was a premixed solution of 35/65 (v/v) 0.2% formic acid/acetonitrile pH 3.0. All solutions were sonicated and degassed under vacuum to minimize bubble formation in the pump. The flow rate for both pumps was set at 0.1 mL/min. Samples (10 µL) were injected

from the autosampler using Pump A to deliver the sample to a two position microelectric actuator switch valve in the load position. During the first 1.5 min after each injection, the valve was used to divert the unretained artificial cerebrospinal fluid salts to waste. Thereafter, it functioned to direct effluent to the mass spectrometer. The valve was programmed to switch from elute back to the load position at 3.0 min.

The analytical column used was a Fluophase PFP (1.0 x 50 mm, 5 μm) from Thermo Hypersil-Keystone (Bellefonte, PA). The column was allowed to re-equilibrate for 1.5 min between injections.

Best sensitivity was obtained when the final organic content of the solvent entering the ion source was approximately 90%. This was accomplished through a process referred to as post column addition (PCA) using a Waters 515 pump (Pump C) delivering a solution of 100% acetonitrile at a flow rate of 0.25 mL/min. Pump C was connected through a tee immediately before entering the source of the mass spectrometer. PEEK (red color) tubing O.D. 1/16", 0.13 mm i.d. (Chromatographic Specialties Inc., Brockville, Ont.) was needed to minimize system dead volume. All connections were made using zero dead volume (ZDV) unions and tees (Valco, Houston, TX).

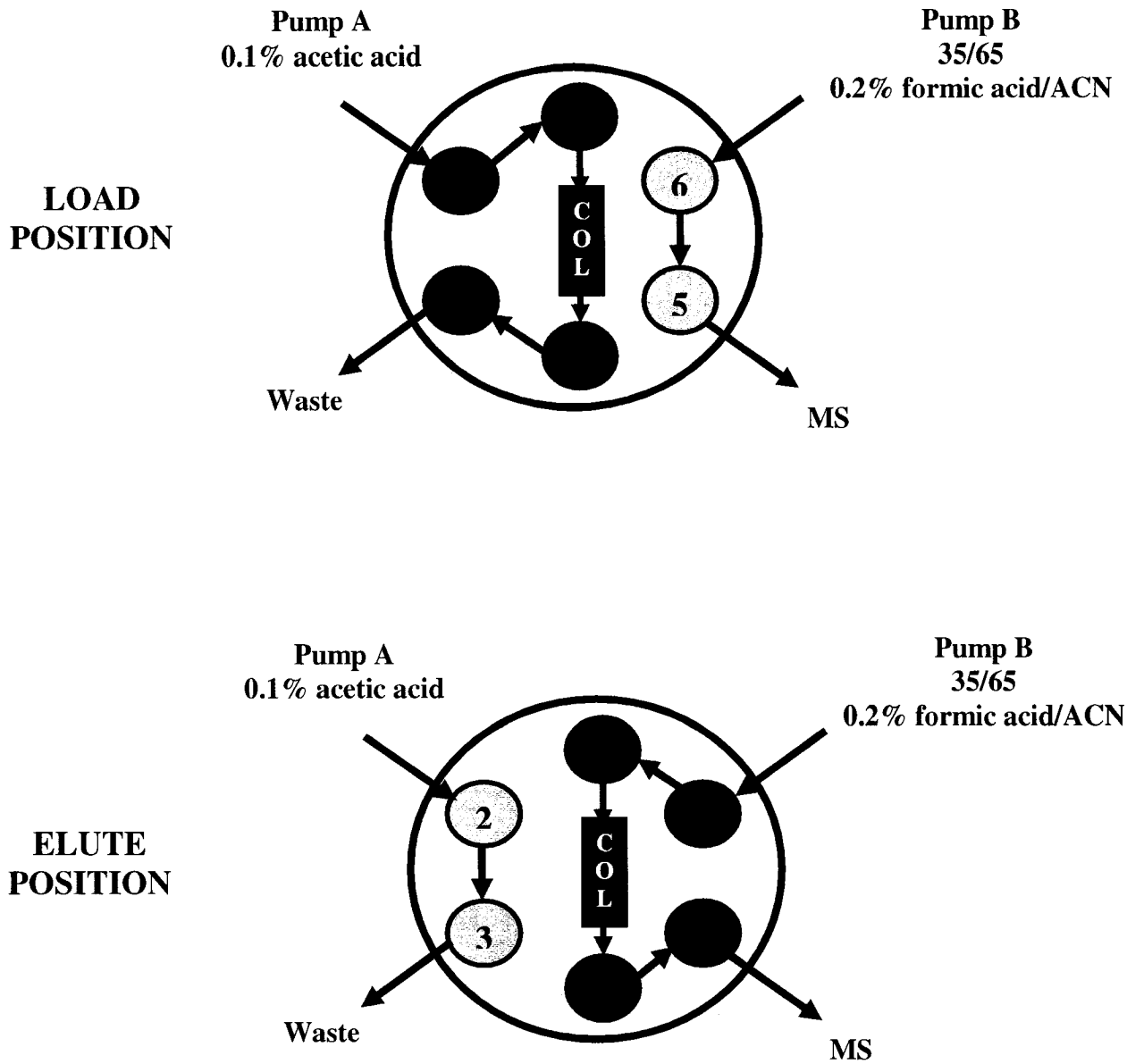

Figure 10 Schematic diagram of a Valco switch valve and its components. Port to port internal volume is 70 nL.

2.9 Mass Spectrometry

Mass spectrometry was performed using an Applied Biosystems / MDS Sciex API 3000 triple quadrupole mass spectrometer equipped with TurboIonSpray™ source and operating in selected reaction monitoring (SRM) mode. The source polarity was switched from negative to positive at 2.15 min.

The data was acquired on an Apple™ Macintosh G3 version 8.5 data system using the MassChrom 1.1.2 software. Further data analysis, peak integration and quantitation were performed using the MacQuan 2.1 and PHIRST 1.0 programs.

2.10 Experiment #1: Method Development

The following source parameters were optimized: TurboIonSpray™ voltage (ISV), source temperature (TEM), probe position, nebulizer gas (NEB), auxiliary gas (AUX). The curtain gas value (CUR) was set at 10 (arbitrary units). Orifice voltage (OR), ring voltage (RNG), ion transitions (Q1→Q3), collision gas pressure (CAD) and collision energy (CE) were optimized for each analyte. Mass calibration was performed for both resolving quadrupoles (Q1 and Q3) by infusion of a mixture of polypropylene glycols (PPGs) at a concentration of 10^{-4}M. The calibration range was established from *m/z* 59 to *m/z* 2242 for positive ions and *m/z* 45 to *m/z* 2211 for negative ions.

Response for each analyte (0.1 μg/mL) dissolved in 0.2% formic acid in water was optimized by infusion, using a Harvard Apparatus syringe pump (Holliston, MA, USA) operating at 5 μL/min. This in turn was plumbed via a zero dead volume (ZDV)

tee into a mobile phase stream containing [50/50] (v/v) [0.2% aqueous formic acid /acetonitrile] flowing at 100 μL/min into the ion source.

For positive ion mode, the ISV and OR were optimized at +3000 V and +30 V respectively. For negative ion mode, the ISV and OR were optimized at -3000 V and -15 V respectively. The source temperature was set to 500 °C. Ultra high purity (UHP, 99.99%) nitrogen was used for all gas supplies. The optimized values were determined to be: NEB = 10 (arbitrary units), AUX = 7 L/min, CAD = 10 (arbitrary units).

Each analyte of interest was tested in both polarities in order to maximize sensitivity as it is difficult to predict if the analyte will ionize more readily as a positive or negative ion. Once the superior polarity for each individual analyte was confirmed, the best ion transitions were determined. The following precursor to product ion transitions were monitored in negative ion mode: DOPAC *m/z* 167 → 123, HVA *m/z* 181 → 122, 5-HIAA *m/z* 190 → 116 and HVA-d_2 *m/z* 183 → 124 (internal standard). The following precursor to product ion transitions were monitored in positive ion mode: dopamine *m/z* 154 → 91, serotonin *m/z* 177 → 115 and dopamine-d_4 *m/z* 158 → 95 (internal standard).

Sample preparation consisted of desalting microdialysis samples in an online manner. This was achieved by using the analytical column to perform the wash and separation steps of the analysis. Critical to the success of the assay was to obtain adequate retention of all analytes prior to chromatographic separation of the acid metabolites from the monoamines. A successful separation was obtained using a commercial column packed with a fluorinated-phenyl phase bonded to a silica substrate.

The polarity of the mass spectrometer was programmed to operate in negative ion mode for the first 2.15 min in which all the acid metabolites elute at 1.98 min. The polarity was then switched to positive ion mode where DA and DA-d_4 elute at 2.25 min and 5-HT at 2.75 min. The total run time of the assay is 3.0 min. Mass chromatograms were recorded with a dwell time of 200 ms and a pause time of 5 ms per ion.

2.11 Experiment #2: Method Validation

Assay validation was obtained using the LC-MS/MS method described above. The assay validation consisted of three runs that included one standard curve. Quality control (QC) samples at three different concentrations were analyzed during validation. Linearity was established with spiked standards over a range of two orders of magnitude. Each standard was prepared with: **(1)** DA and 5-HT at the following concentrations: double blank (no analyte, No IS) (BLK), single blank (IS only) (STD A), 0.25 (STD B), 0.375 (QCA), 0.5 (STD C), 1.25 (STD D), 2.5 (QCA), 3.75 (STD E), 12.5 (STD F), 20.0 (QCC), 25.0 (STD G) pg/μL and **(2)** DOPAC, HVA, 5-HIAA at the following concentrations: double blank (BLK), single blank (STD A), 50 (STD B), 75 (QCA), 100 (STD C), 250 (STD D), 500 (QCB), 750 (STD E), 2500 (STD F), 4000 (QCC), 5000 (STD G) ng/mL. The standards were diluted with artificial CSF yielding a final solution containing 95% αCSF. This was the solution simulating the biological matrix used for the calibration curves and validation. It was necessary to compare between a standard solution prepared in 0.2% formic acid and a simulated microdialysis sample containing αCSF in order to establish if the same sensitivity could be obtained (i.e., no ion suppression from the salts or matrix effect).

Prior to injection, standards (2 μL) were diluted with 8 μL of 0.2% formic acid containing the internal standards. Thus for a 10 μL injection, the limit of quantitation (LOQ) for DA and 5-HT was 0.5 pg on column. The limit of detection (LOD = S/B 3) was estimated to be 75 fg (or ~500 attomoles) on column.

2.12 Experiment #3: Microdialysis-LC/MS/MS

The final stage of testing was live, *in vivo* microdialysis samples. Quantitation of basal neurotransmitter levels in rat microdialysis samples (2 μL) was achieved using the protocol described above. Samples were diluted with 8 μL of 0.2% formic acid containing the internal standards. No further sample preparation was required.

Once the baseline extracellular levels were determined, the rat was subjected to drug testing. The animal's response was monitored and neurotransmitter levels quantified. The rat was injected with one of the following drugs: amphetamine (5 mg/kg/mL i.p.), pargyline (100 mg/kg/mL i.p.) or fluoxetine (14 mg/kg/mL i.p.). Sample collection started immediately after injection and lasted for two hours when the rat was injected with AMPH and two and a half hours with pargyline. When the animal was tested with fluoxetine, which has a longer half-life, microdialysis samples were collected between 2-6 hours after injection of the drug.

3. RESULTS AND DISCUSSION

3.1 Experiment #1: Method Development

Mass Spectrometry

The first step was to establish whether mass spectrometry was a viable detection method for the analysis of monoamine neurotransmitters and their metabolites. As described in section 2.10, each analyte of interest was tested separately in both polarities and mass spectrometric parameters were optimized in order to maximize sensitivity. This was achieved by setting the first quadrupole (Q1) to scan a range of *m/z* 50 to 200 and observing the response of the analyte in each polarity separately. DA and 5-HT were most sensitive in positive ion mode observed as the protonated molecule ($M+H^+$) at *m/z* 154 and 177, respectively. The acid metabolites DOPAC, HVA and 5-HIAA were most sensitive in negative ion mode observed as deprotonated molecules ($M-H^+$) at *m/z* 167, 181 and 190, respectively.

A key element was to find a suitable compound to serve as the internal standard. The internal standard must resemble as closely as possible the analytes in the sampling procedure, desalting and chromatographic behaviour while being sufficiently different to allow the two signals to be easily distinguished by the detection instrument. The ratio of analyte to internal standard signals, in this case peak areas, serves as the analytical parameter for quantitation. Two internal standards were selected for this study: in negative ion mode, HVA-d_2 was used which is chemically identical to HVA except that two hydrogen are replaced by two deuterons at *m/z* 183 while in positive ion mode, DA-

d_4 is identical to DA except for the replacement of four hydrogen for four deuterons at *m/z* 158.

Once the optimal polarity for each individual analyte was confirmed, the best ion transitions were determined. This was accomplished by setting Q1 to allow only the precursor ion of interest to enter the collision cell (q2) an rf only quadrupole and undergo collision-induced dissociation (CID). Two key parameters are required to achieve collision-induced dissociation in an RF quadrupole: (1) an inert gas (nitrogen) at a pressure high enough (1-4 mTorr) to reduce the mean free path and allow multiple collisions and (2) impart adequate translational kinetic energy into an ion to undergo fragmentation. In a selected reaction monitoring (SRM) experiment, the gas pressure inside the collision cell is constant for all ions in all polarities. However, the translational kinetic energy or collision energy (CE) is unique for each ion transition monitored and is adjusted by varying the voltage potential between the RF only quadrupole (q0) situated immediately before Q1 and the collision cell (q2) which is situated immediately after Q1. The selected ion of interest is accelerated towards q2 to produce collisions by converting translational kinetic energy into internal energy with the most labile bonds in an ion breaking to produce product ions. Product ions exiting the collision cell proceed to Q3 which is set to scan a range of *m/z* 50 to 200 allowing for all the product ions to reach the detector. The most sensitive and/or selective product ion is selected for each analyte.

Negative Ion Mode

The following precursor to product ion transitions (Q1 → Q3) were monitored in negative ion mode: DOPAC *m/z* 167 → 123, HVA *m/z* 181 → 122, 5-HIAA *m/z* 190 → 116 and HVA-d_2 *m/z* 183 → 124 (internal standard). Figures 11 to 14 show the product ion scans for each analyte displaying all the peaks including the precursor ion and their respective product ions, with their structures and molecular formulae.

For DOPAC, as can be seen from Figure 11, most of the molecular ion is converted to only one major product at a *m/z* 123. This is produced by a loss of 44 Da that corresponds to a loss of carbon dioxide (CO_2). Thus, the mass transition *m/z* 167 → 123 was monitored yielding a strong signal response. The lack of any other product ions being produced of any significant intensity precluded selecting a different product ion. Moreover, there is minimal background noise observed at this transition, generating a chromatogram free of chemical noise.

For HVA, the principal product ion is observed at *m/z* 137 resulting from the non-selective loss of CO_2. In addition, high background noise observed at this transition leads to a poor signal to baseline ratio that limits the detection. Increasing the ion's collision energy resulted in a more energetic and more selective fragmentation product at *m/z* 122 that appears to result from an additional loss of 15 Da corresponding to a loss of a methyl radical. The ion transition *m/z* 181 → 122 proved to be more selective for HVA and therefore was selected for monitoring.

The metabolite 5-HIAA, yields a major product ion at low collision energy resulting in a non-selective product ion at *m/z* 146 due to loss of CO_2. Again as with HVA this ion transition displays high chemical noise, permitting detection only at higher

concentrations of the analyte. As the microdialysis samples contain very low levels of these neurotransmitters this was not acceptable and a more selective ion transition was needed. This was obtained by increasing the collision energy, which gave rise to a product ion at *m/z* 116. The product ion at *m/z* 146 is not seen in Figure 13 as it is completely dissociated once high energy is applied to the precursor ion to form other product ions. The ion transition that provided maximum sensitivity was *m/z* 190 → 116. This results in a loss of 74 Da from the precursor ion that is characteristic of a loss of CO_2 followed by a loss of formaldehyde (MW of CH_2O = 30 Da). The higher collision energy applied to the ion causes the ring to break open, and therefore, facilitates the loss of CH_2O.

The internal standard, HVA-d_2, follows the same fragmentation pattern as HVA where the *m/z* is shifted by two Daltons for the precursor and product ion due to the presence of the two deuterons. Collision induced fragmentation produces the mass transition *m/z* 183 → 124 caused by the loss of CO_2 and a methyl radical. HVA-d_2 was the internal standard selected for the negative ion mode since it is chemically identical to HVA while possessing an easily distinguishable signal.

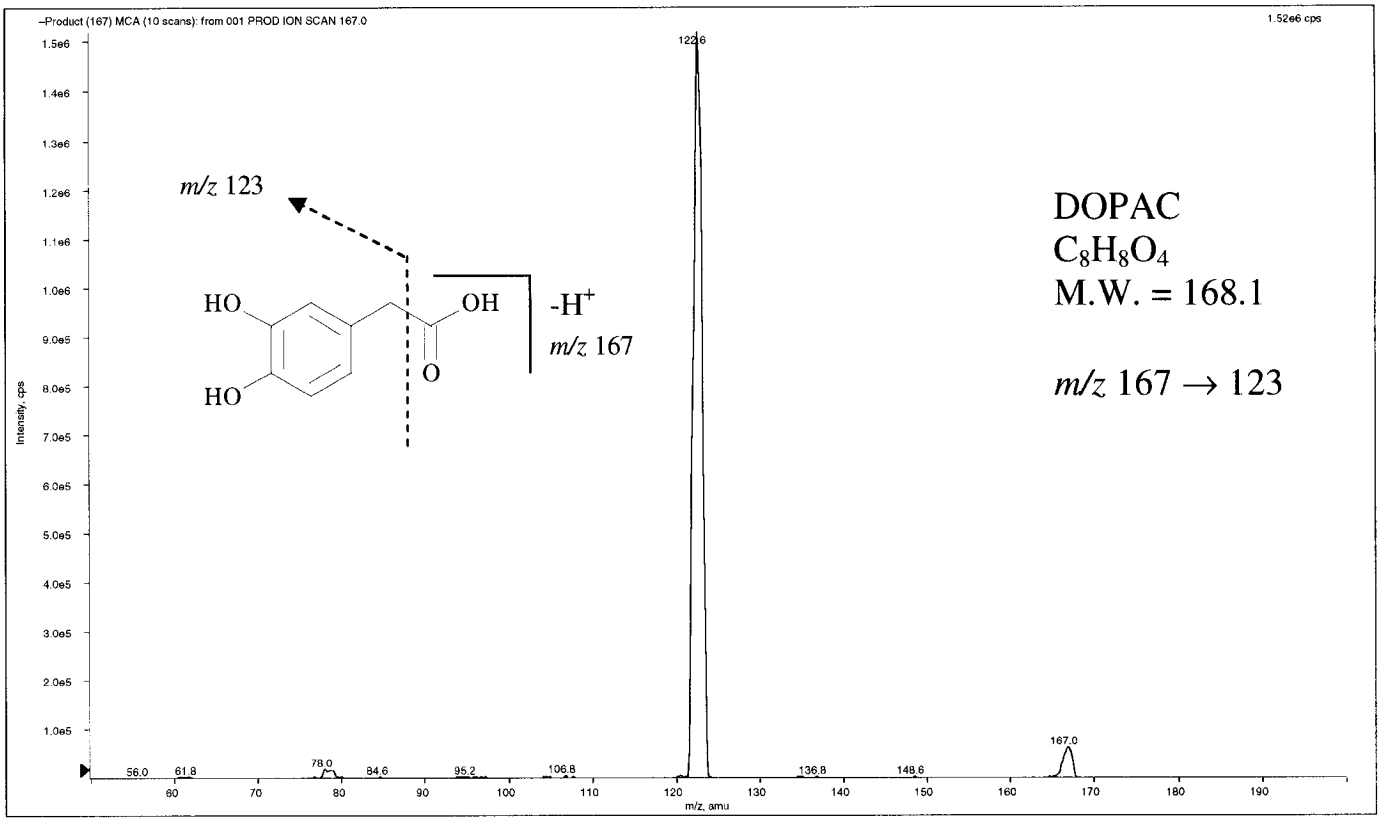

Figure 11 Product Ion Scan of *m/z* 167

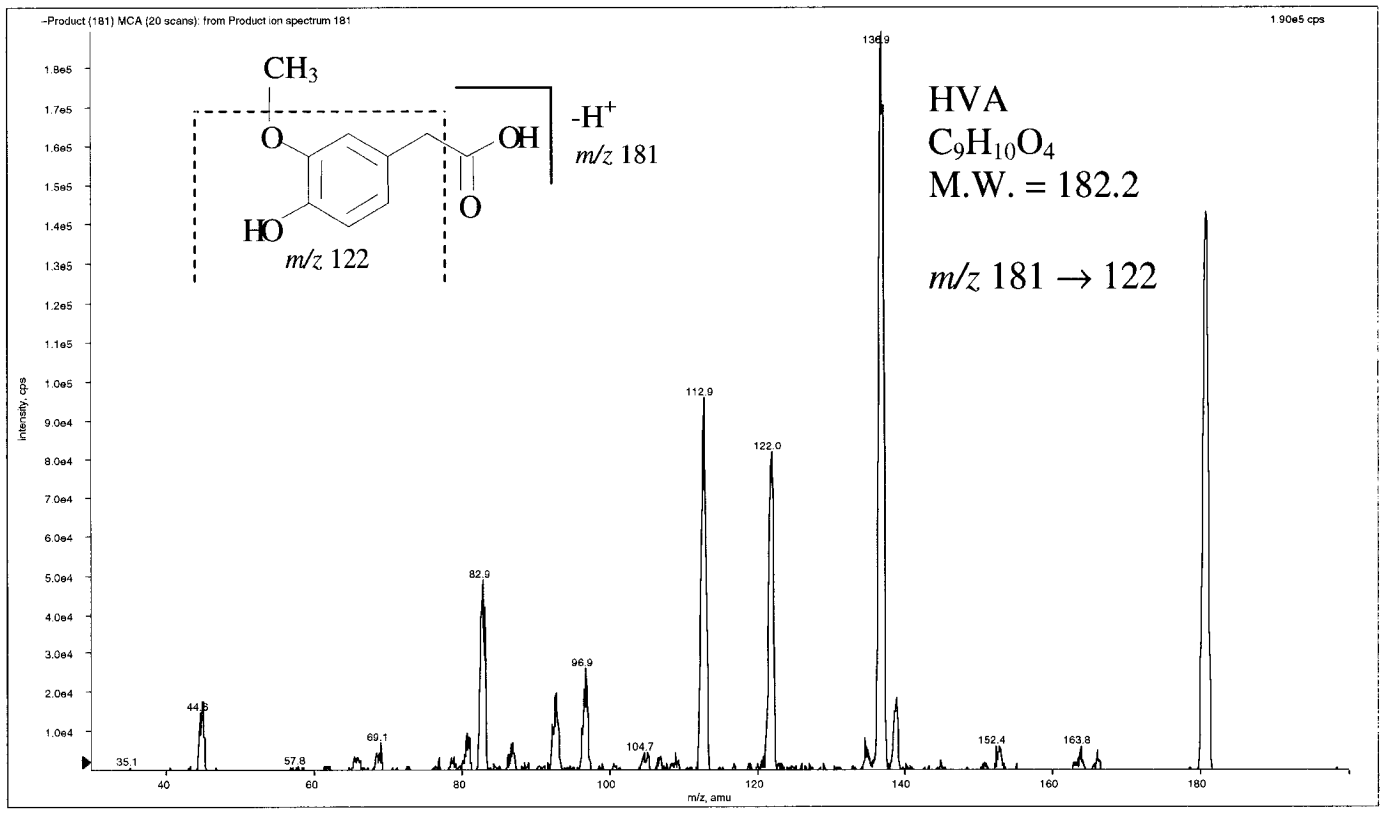

Figure 12 Product Ion Scan of *m/z* 181

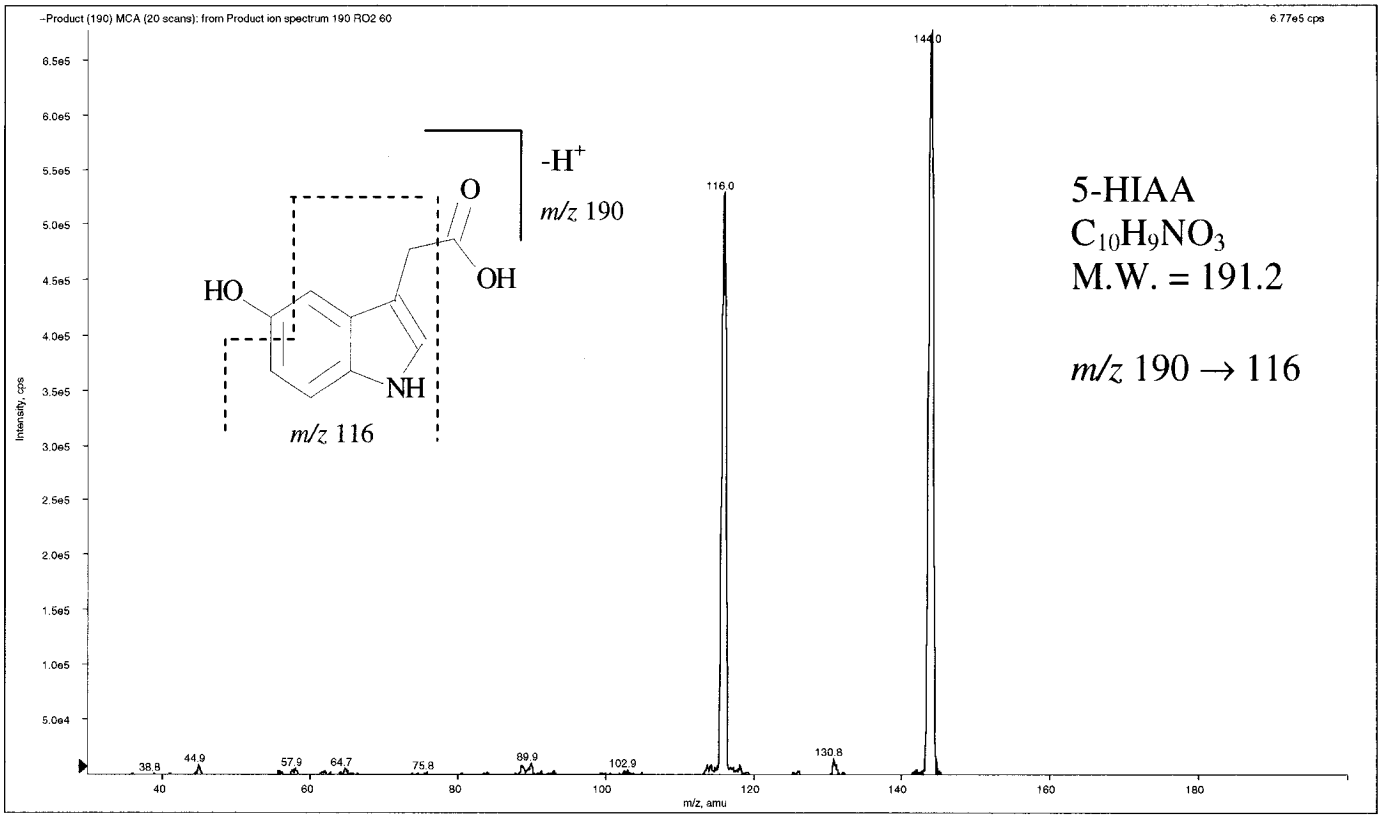

Figure 13 Product Ion Scan of *m/z* 190

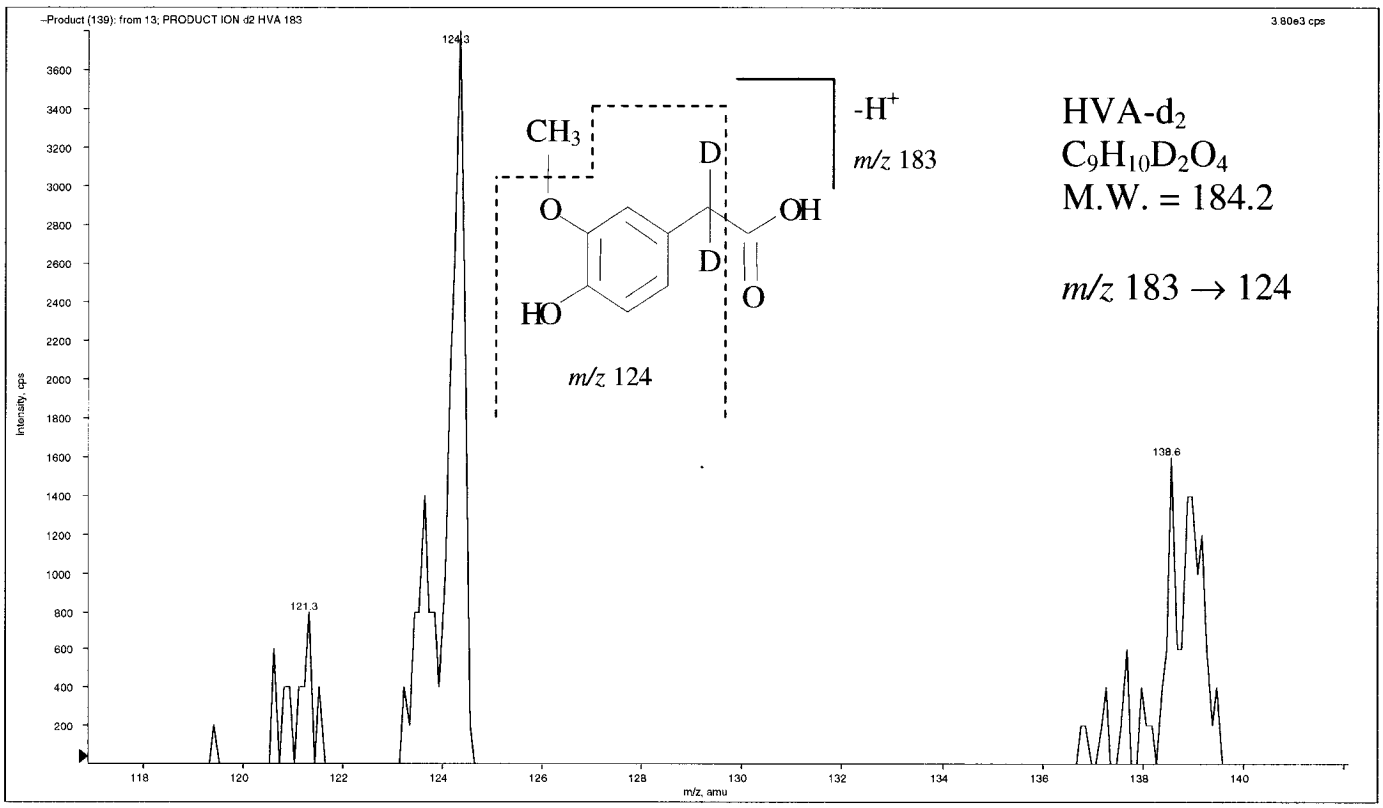

Figure 14 Product Ion Scan of *m/z* 183

Positive Ion Mode

The following precursor to product ion transitions were monitored in positive ion mode: DA *m/z* 154 → 91, 5-HT *m/z* 177 → 115 and DA-d_4 *m/z* 158 → 95 (internal standard). Figures 15 to 17 show the product ion scans for each analyte displaying all the peaks including the precursor ion and their respective product ions, their structures and molecular formula.

For DA, the largest peak at *m/z* 137, seen in the product ion scan (Figure 15), corresponds to the non-selective loss of the ammonium ion (NH_3). The second largest peak at *m/z* 119 is produced by a subsequent loss of water, giving rise to another non-selective product ion. An additional loss of carbon monoxide (CO) and a molecular rearrangement results in the formation of a delocalized carbenium ion more commonly known as a tropylium ion. This product ion is detected at *m/z* 91 and is more selective to DA than the other product ions previously discussed.

For 5-HT, the two first peaks displayed in the product ion scan (Figure 16) represent the non-selective loss of NH_3 (*m/z* 160) followed by the loss of ethylene (C_2H_4) (*m/z* 132). A subsequent loss of the hydroxyl group (OH) results in the selective ion product at *m/z* 115. For 5-HT, the precursor to product ion transition at *m/z* 177 → 115 displays minimal background noise and strong signal response.

The internal standard, DA-d_4, was selected for the positive ion mode since it matches the chemical properties of DA. The same fragmentation pattern as DA is observed where the *m/z* is shifted by four Daltons for the precursor and product ions due to the presence of the four deuterons atoms. Again as with DA, collision induced fragmentation produces the precursor to product ion transition *m/z* 158 → 95,

corresponding to a loss of NH_3, water and CO with a molecular rearrangement. As all the deuterons atoms are conserved after fragmentation, it can easily be distinguished from DA.

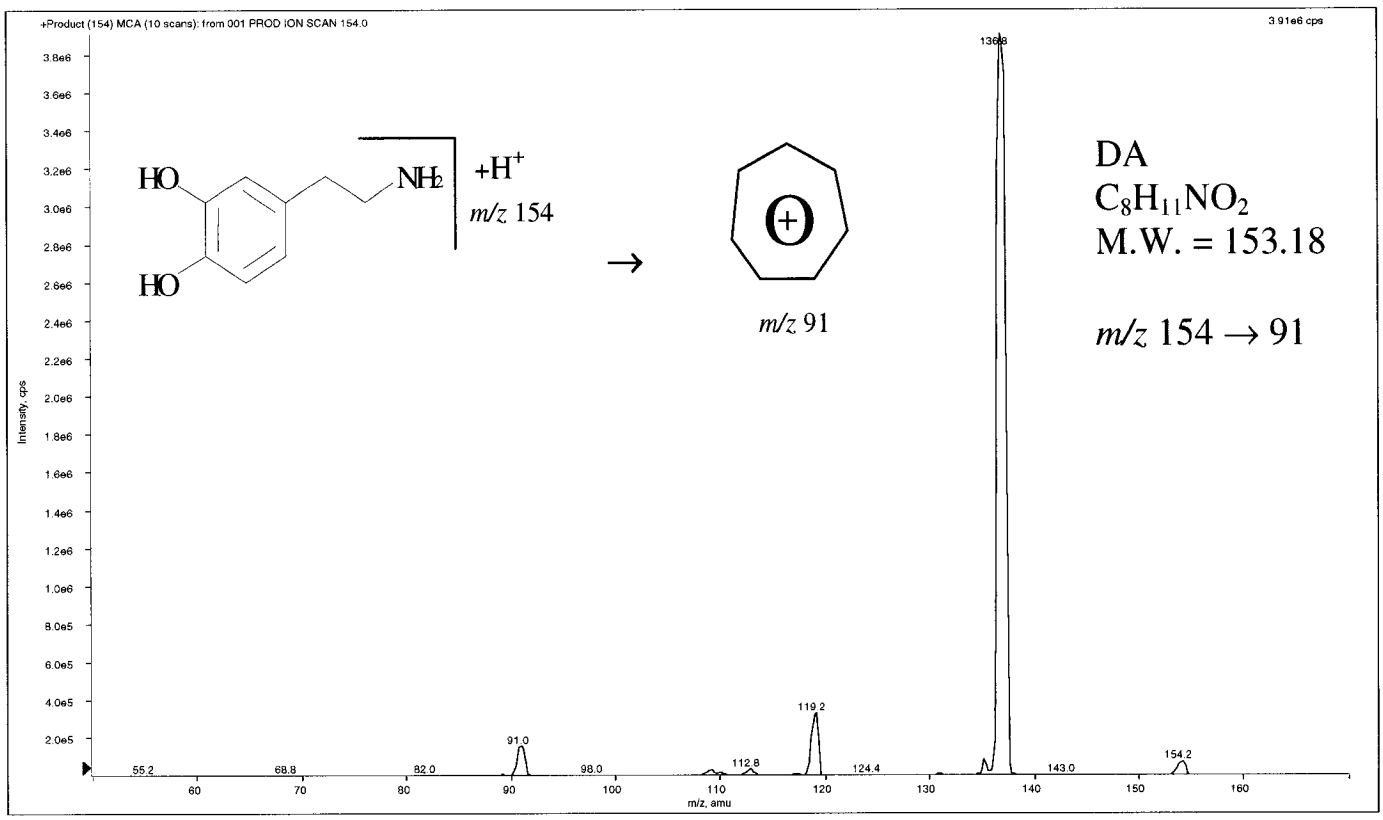

Figure 15 Product Ion Scan of *m/z* 154

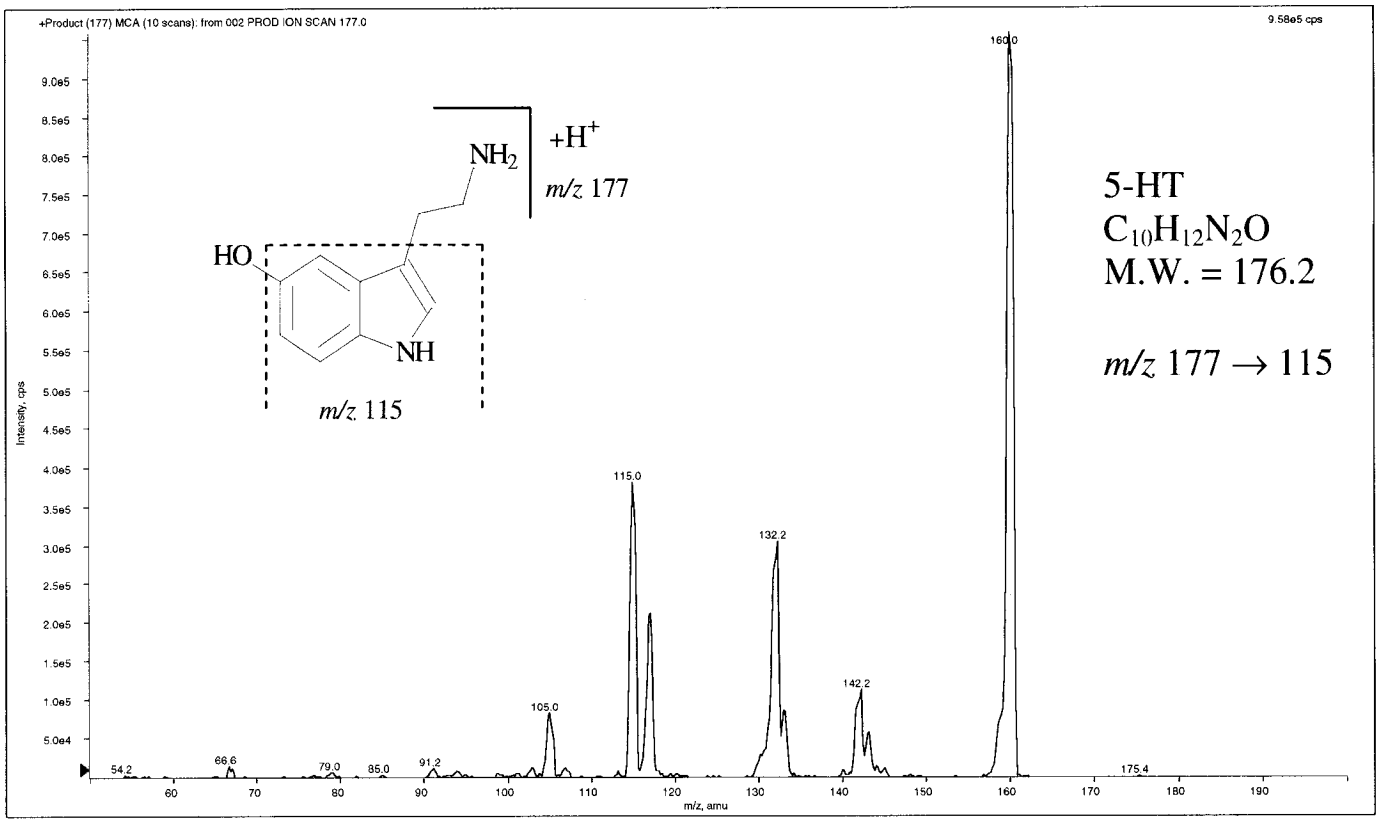

Figure 16 Product Ion Scan of *m/z* 177

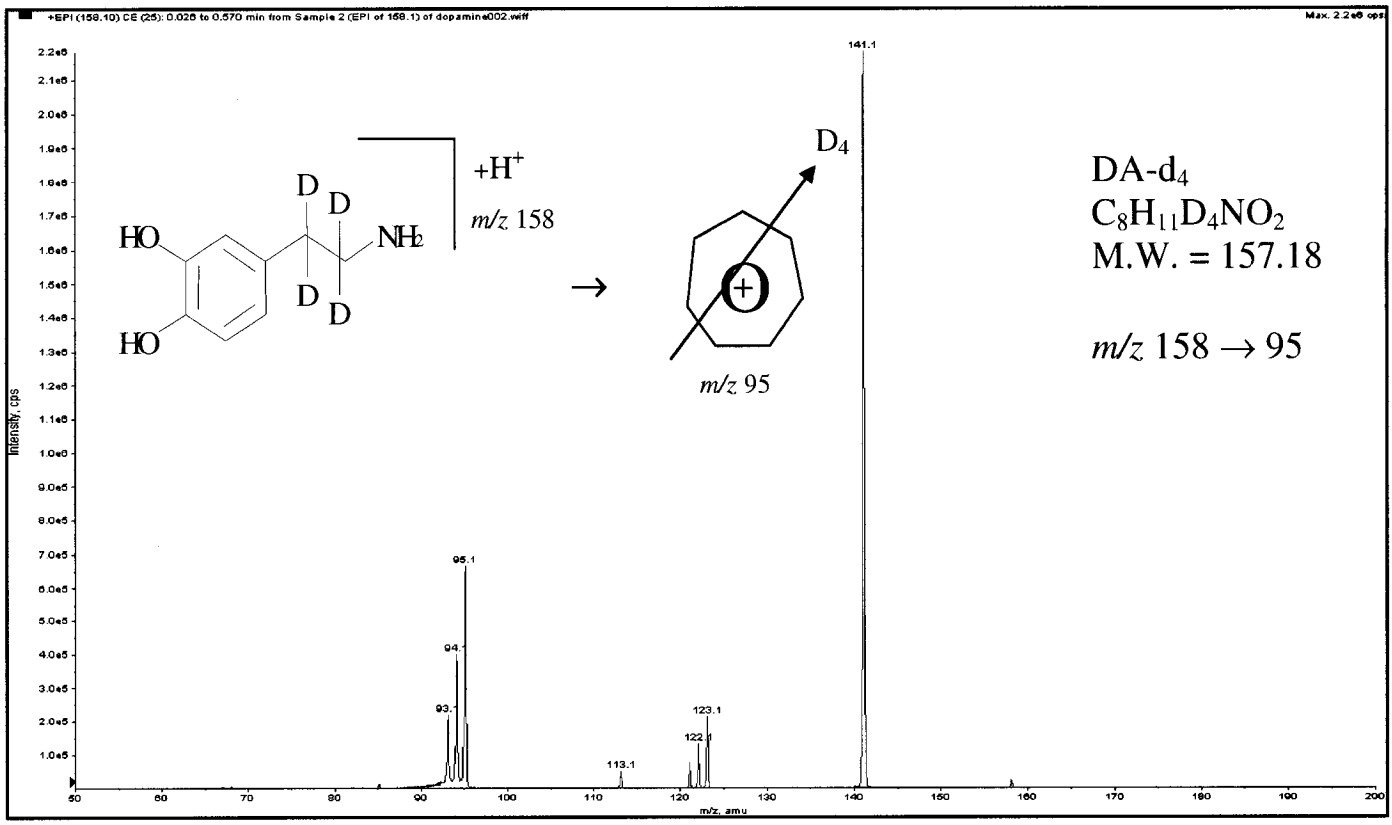

Figure 17 Product Ion Scan of *m/z* 158

Table 1, shown below, summarizes all the optimal parameters and conditions of the ion source and the mass spectrometer in order to achieve the highest sensitivity for all the analytes.

Table 1 Mass spectrometric parameters for each analyte.

Analyte	Polarity	*m/z* Q1	*m/z* *Q3*	OR (V)	RNG (V)	Q0 (V)	RO2 (V)	CE (RO2 – Q0) (V)
DOPAC	-	167	123	-15	-55	5	46	41
HVA	-	181	122	-15	-55	5	26	21
5-HIAA	-	190	116	-15	-55	5	58	53
HVA-d_2	-	183	124	-15	-55	5	26	21
DA	+	154	91	30	100	-5	-38	-33
5-HT	+	177	115	30	100	-5	-40	-35
DA-d_4	+	158	95	30	100	-5	-38	-33

Notes: The ion spray voltage was set at -3000 V in negative ion mode and +3000 V in positive ion mode. Source temperature was constant at 500 °C.

Chromatography

Successful development of this assay relied on the fact that the chromatography fulfills two key requirements. The first requirement is that in order to detect all five analytes in a single injection, sufficient temporal separation of the monoamine neurotransmitters from their acid metabolites was required, since the mass spectrometer can only operate in one polarity at any given time. The problem is exemplified if one of the acid metabolites co-elutes at the same time as DA or 5-HT. In this case, only one of the two analytes can be accurately detected during that run. However, the detector can be set to switch polarities (~700 ms per switch) at any point during the run as long as the analytes are separated in time. The second requirement is that rat *in vivo* microdialysis samples must be adequately desalted prior to MS detection. Even small amounts of salt

content entering the mass spectrometer ion source can suppress the ion signals leading to poor detection limits. The more common method of sample preparation by offline solid phase extraction procedures was too difficult if not impossible in our case without incurring significant sample losses due to the sample size (2 μL). Minimal sample handling is preferred in order to avoid these losses and to reduce error. Due to the sieving effect of the dialysis membrane, microdialysis samples are relatively free of larger molecules making them amenable to online desalting using liquid chromatographic techniques.

The first step in the chromatographic method development required adequate retention of all five analytes of interest and the internal standards on an analytical column. This can be difficult as highly polar low-molecular-weight compounds, such as DA, are often not sufficiently retained by a classical reverse phase mechanism and represent a particular chromatographic challenge. Other methods have used ion-pairing reagents to obtain some retention but this was not a viable option as these reagents are not compatible with MS. The use of volatile ion-pairing reagents may be compatible with MS, but they always lead to some type of signal suppression.

Consequently, the requirement to retain and analyze polar molecules by HPLC-MS is one that has grown steadily over the last few years, and has been the driving force behind the generation of a range of new types of stationary phases dedicated to this purpose. Recently, a newer type of separation based on a normal phase mechanism in aqueous mobile phases termed hydrophilic interaction chromatography (HILIC) has been gaining popularity for the separation of highly polar analytes not amenable by reverse phase separation. The result of all this effort has been the development of a new type of

stationary phase that appears to operate in both reverse phase and hydrophilic interaction modes.

For this research, sample preparation consisted of desalting microdialysis samples online. Critical to the success of the assay was obtaining adequate retention of all analytes prior to chromatographic separation of the acid metabolites from the monoamines. This was achieved using an analytical column packed with porous spherical particles in which a fluorophenyl phase bonded is to a silica substrate, commercially known as Fluophase PFP. The column and conditions were chosen to adsorb all of the analytes, and internal standards, while the salts were washed out and diverted to waste.

The loading HPLC pump (Pump A), connected to the autosampler, was set to deliver 100 μL/min of 0.1% acetic acid for the first 1.5 min of the run. Under mobile phase "A" conditions all analytes appear to be retained by a reverse phase mechanism where the mobile phase is more polar than the stationary phase. This was sufficient time to allow for complete desalting of the sample. At 1.5 min, the switch valve was programmed to allow the elution HPLC pump (Pump B), delivering 100 μL/min of 35/65 0.2% formic acid/acetonitrile, to come inline with the column and deliver the analytes to the mass spectrometer. Under these mobile phase "B" conditions the acid metabolites appear to elute in a manner consistent with reverse phase behaviour. However, under the same mobile phase "B" conditions the increased retention of the monoamines relative to the acid metabolites seems to suggest retention behaviour different from reverse phase. In the case of DA, which is very polar and basic in nature mobile phase "B" may facilitate retention of DA through a HILIC mechanism. Previous testing showed that as

the percentage of organic modifier increased so did DA retention. The more non-polar the mobile phase the greater the affinity of DA for the stationary phase and the greater the retention. Retention also increased when formic acid was used in place of acetic acid. The stronger acid favours the more polar charged form of DA, which in turn would increase the affinity of DA for the polar stationary phase. In the case of serotonin (5HT), which is less polar than DA but also basic in nature, mobile phase "B" may facilitate retention by a combination of reverse phase and HILIC mechanism. Previous testing showed that as the percentage of organic modifier is increased from (0-50%) serotonin retention decreased initially (reverse phase) and then increased again as the percentage of organic modifier exceeds approximately 60% (HILIC). Both monoamines are retained under reverse phase in mobile phase "A" conditions, but 5HT elutes after DA when mobile phase "B" conditions are introduced even though DA is the more polar analyte. The elution order suggests that the overall greater retention displayed by 5HT may be due to its stronger reverse phase retention with respect to DA and thereby is consistent with chromatographic behaviour that is a combination of reverse phase and HILIC.

Short (L = 5 cm) microbore (d = 1 mm) columns have become increasingly popular for the analysis of microdialysis samples because they provide the optimum combination of high sensitivity and rapid analysis.[44] This is observed since peak dispersion is proportional to the square of the column diameter. However, an important consideration in the use of microbore columns is the reduction of extra-column contributions to band broadening. Reductions in the length of the connecting tubing and dead volume in the connectors and injector are necessary to take full advantage of the benefits afforded by microbore chromatography. PEEK (red color) tubing O.D. 1/16"

and 0.13 mm id was required in order to minimize system dead volume. Ten centimeters of this tubing would contribute approximately 1.33 μL of system volume. Based on actual injections performed without the column, the system volume was measured at approximately 35 μL. As no more than 30 cm (maximum of 5 μL) of tubing were used outside the injector, this leads one to conclude that the bulk of the volume was contributed by the auto-injector. As a 25 μL injector loop was installed, this leaves approximately 5 μL of system volume that may be accounted for by the multiple plumbing connections resulting in minimal contribution to the system volume. All connections were made using zero dead volume (ZDV) unions and tees.

The polarity of the mass spectrometer was programmed to operate in negative ion mode for the first 2.15 min during which all the acid metabolites elute at 1.98 min. The polarity was then switched to positive ion mode where DA and DA-d_4 elute at 2.25 min and 5-HT at 2.75 min. The polarity switch itself requires approximately 700 ms (<1 second) to occur and for the power supply to equilibrate. The total run time of the assay is 3.0 min. The column was allowed to re-equilibrate for 1.5 min between injections. The detailed total ion chromatogram (TIC) along with the extracted mass chromatograms for each analyte is displayed in Figure 18 below.

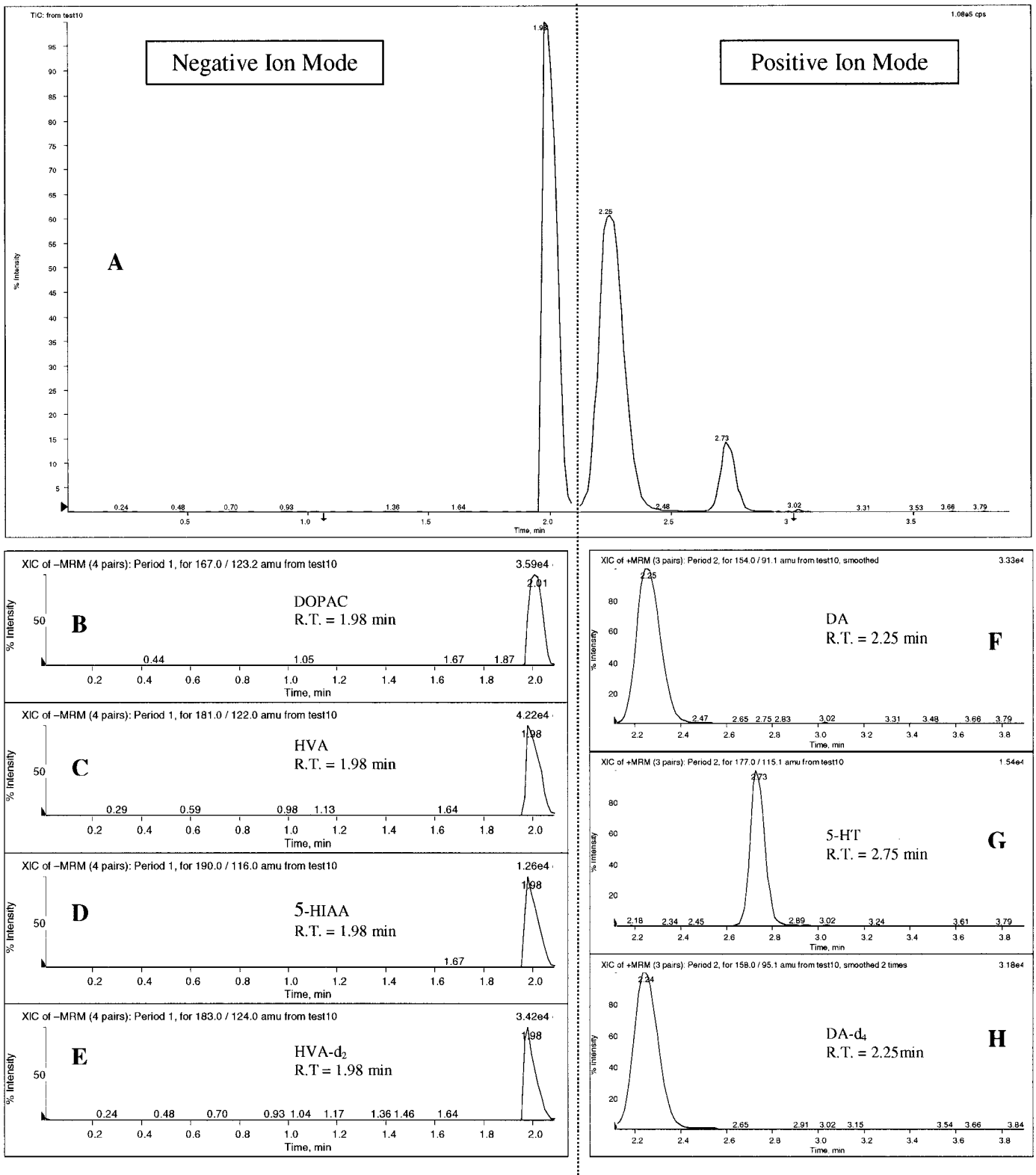

Figure 18 Solution standard of ULOQ showing TIC (A) and corresponding mass chromatograms of DOPAC (B), HVA (C), 5-HIAA (D), HVA-d_2 (E), DA (F), 5-HT (G) and DA-d_4 (H).

Post Column Addition

Best sensitivity was obtained when the final organic content of the solvent entering the ion source was approximately 90%. This was accomplished through a process referred to as post column addition (PCA) using a Waters 515 pump (Pump C) delivering a solution of 100% acetonitrile at a flow rate of 250 μL/min. Pump C was connected through a tee immediately before entering the source of the mass spectrometer (shown below in Figure 19). Before PCA (A) was introduced, the total organic content entering the ion source was only 65 %. It can be seen that once PCA was added to the system (B), the final organic content was increased to 90%. This results in a more stable spray, which increases the rate of droplet desolvation and ultimately increases ion yield in the ion source. The incorporation of PCA into the system results in a significant increase of three times the signal. When dealing with such small concentrations found in microdialysis samples, this is a considerable increase.

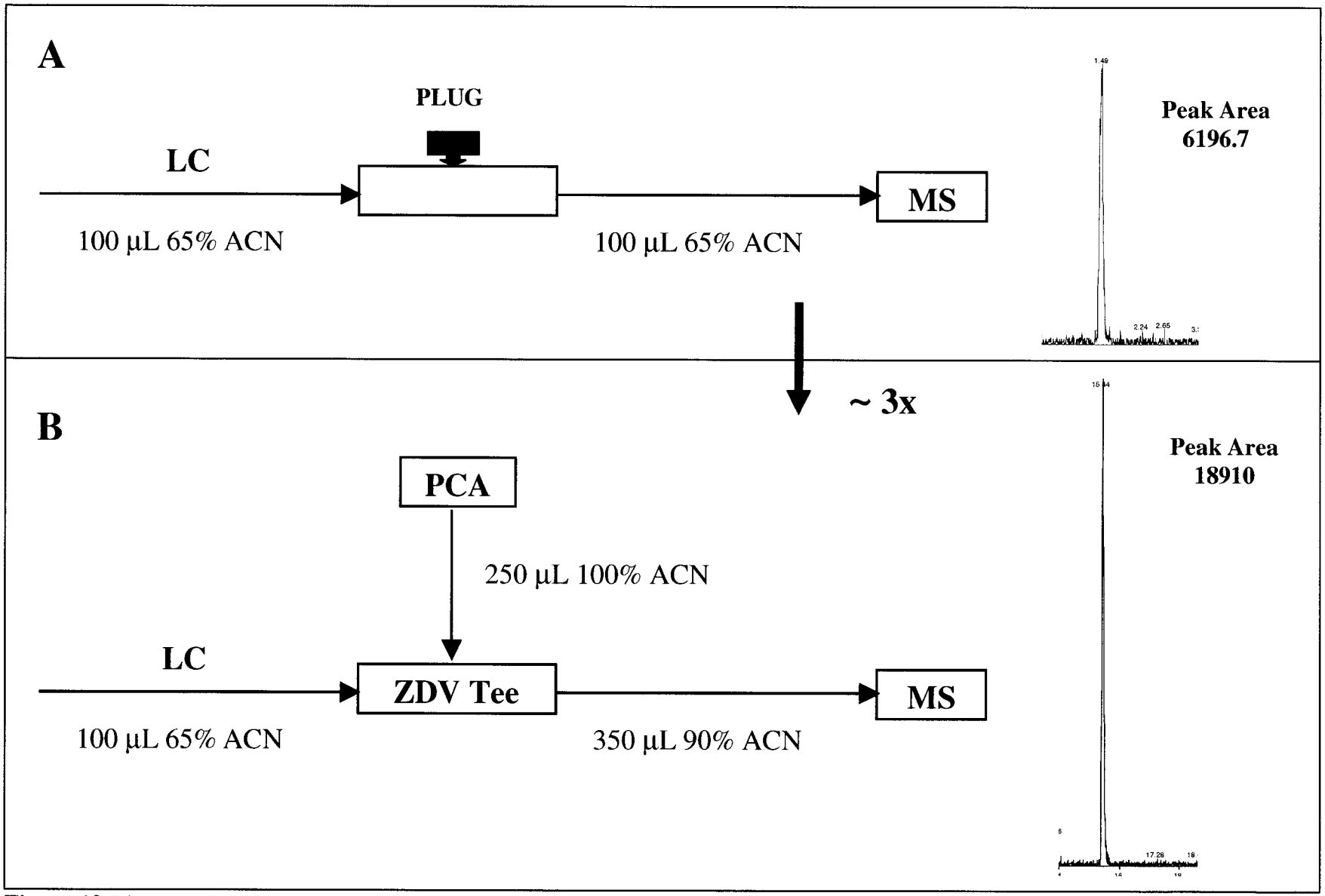

Figure 19 Diagram illustrating the response of 5pg of DA without (A) and with (B) post column addition (PCA). This can be directly determined by comparing the peak areas for each mass chromatogram.

Matrix Effect

When matrix components are not efficiently removed from a sample they may adversely affect detection. In MS/MS detection systems, matrix contaminants have been shown to reduce the efficiency of the ionization. A loss in response is observed and this phenomenon is referred to as ionization suppression or matrix effect. This effect can lead to decreased reproducibility and accuracy for an assay, failure to reach the desired limit of quantitation (LOQ) due to accumulation of matrix on the analytical column which can affect the internal standard (IS) and drug differently. There are different sources that can contribute to the matrix effect, including endogenous matrix components such as proteins and salts, other potential interference substances such as decomposition products and exogenous material or matrix from a component included in the method of analysis.

Generally, there are two types of matrix effects that can be observed. The first type suppresses or enhances the analyte signal. Suppression (in most cases) results from competitive ionization in the source area. Enhancement is observed when there is formation of adduct(s) with the analyte of interest that make the analyte more volatile or easier to ionize. The second type results from an interference peak from matrix in the retention region of the analyte.

In order to determine the influence of the artificial matrix on the analysis, a matrix effect test had to be performed. This was accomplished by comparing the results of a standard solution with the internal standards without any matrix to a standard solution prepared with the same concentrations of analytes and internal standards in the artificial CSF matrix. The matrix effect is calculated by dividing the area of the peak for the sample in matrix by the area of the peak for the sample clean of matrix. The absence of a

matrix effect is indicated by a ratio of 1.0. Suppression of ionization results in reduced analyte response (ratio < 1.0) whereas total matrix suppression yields a value of zero.

It can be seen from Figure 20, that there is no significant effect contributed by the matrix. For example, the matrix effect was calculated to be $2.544x10^5 / 2.587x10^5 = 0.98$ or less than 2% difference in peak areas.

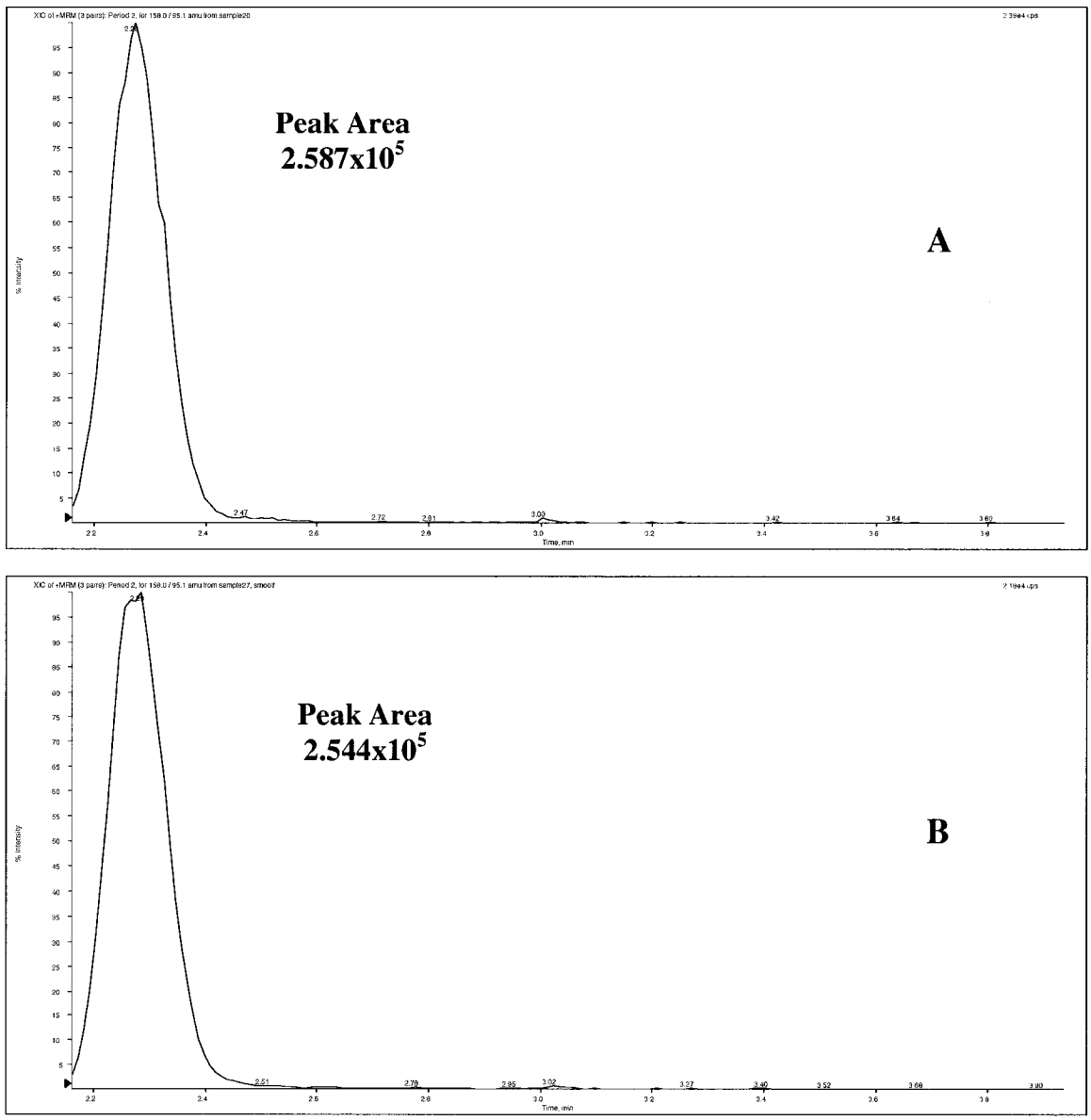

Figure 20 Standard solution prepared without (A) and with (B) αCSF in matrix.

3.2 Experiment #2: Method Validation

Assay validation was performed using the LC-MS/MS method described above. The assay validation consisted of two runs that included three standard curves each. These were analyzed on two different days providing intra and inter day calibration curves. Quality control (QC) samples at three different concentrations, including a QC at 1.5 times the lower limit of quantitation (LLOQ) (0.375 ng/mL), a QC at 10% of the upper limit of quantitation (ULOQ) (500 ng/mL) and a QC at 80% of the ULOQ (4000 ng/mL), were analyzed during validation.

Linearity was established over a concentration range of two orders of magnitude with spiked standards. The standards were then diluted with artificial CSF yielding a final solution containing 95% αCSF, 5% standard at the above concentrations. This was the solution simulating the biological matrix used for the calibration curves during validation and sample analysis. It was necessary to compare between a standard solution prepared in 0.2% formic acid and a simulated microdialysis sample containing αCSF in order to establish if the same sensitivity could be obtained (i.e., no ion suppression from the salts or matrix effect). Prior to injection, 2 μL of standards at the concentrations noted above were diluted with 8 μL of 0.2% formic acid containing the internal standards.

The highest precision and accuracy for quantitative chromatography is obtained by use of internal standards because the uncertainties introduced by random and systematic errors can be compensated for. A constant measured quantity of an internal standard substance is introduced into each blank, calibration standard and sample.

Calibration then involves plotting the ratio of the analyte signal to the internal standard signal as a function of the analyte concentration of the standards. This ratio for the samples is then used to obtain their analyte concentrations from the calibration curve. Thus, if the analyte and internal standard signals respond proportionally to random instrumental and method fluctuations or matrix effects, the ratio of these signals is independent of these differences.

Calculated concentrations of all the analytes were obtained by peak area measurements. The peak area ratio for DA and 5-HT to the internal standard, DA-d_4, and DOPAC, HVA and 5-HIAA to the internal standard, HVA-d_2, and the concentrations of the calibration curve were fitted using a linear 1/concentration (1/c) regression algorithm. The regression equation is as follows: $y = mx + b$, where y = peak area ratio of the analyte to its internal standard, x = concentration of the analyte and slope (m) and intercept (b) are curve parameters.

The following validation criteria are applicable to the standards and QCs (relative intra-batch precision and accuracy):

Linearity: Curve acceptance criteria must include a minimum of six standards (including at least one at both the bottom and top of the range) back-calculated to ± 20% of their nominal concentrations and a correlation coefficient of 0.9900 or greater.

QC Acceptance: At least 67% of the QCs must be evaluated, including at least 50% at each concentration level.

Precision: Within-batch CVs must be less than or equal to 20% for low QCs and less than or equal to 15% for mid and high QCs.

Accuracy: The mean value for the LLOQ and low QCs should be within 80-120% of the nominal, and for the mid and high QCs within 85-115% of the nominal.

Sensitivity: The lowest standard is accepted as the limit of quantitation if the typical response at this concentration is at least five times greater than any interference in the blanks at the t_R of the analyte(s).

Specificity: The response ratio of any interfering peak(s) in the matrix blanks at the t_R of the analyte(s) should be less than or equal to 25% of the response ratio of the LOQ standard only when the IS has been added. The response of any interfering peak(s) in the matrix blanks at the t_R of the IS must be less than 5% of the mean response of the IS concentration to be used in the study.

The theoretical and calculated concentrations in artificial CSF matrix for the validation standard curves and the standard deviations of their means from nominal concentrations and %CV (coefficient of variation) for DA, 5-HT, DOPAC, HVA, 5-HIAA are shown in Tables 2 to 6. Summaries of standard curve parameters for assay validation for all the analytes are shown in Tables 7 to 11. The theoretical and calculated quality control concentrations in artificial CSF matrix for the validation standard curves, standard deviations of their means from nominal concentrations and %CV (coefficient of variation) for all of the analytes are shown in Tables 12 to 16.

Table 2 Summary of calculated concentrations for DA in artificial CSF matrix during validation compared to expected concentrations.

	Expected DA Concentrations (ng/mL)					
Run ID	0.25	0.50	1.25	3.75	12.50	25.00
	Calculated DA Concentrations (ng/mL)					
Run 1	0.25	0.55	1.29	3.82	12.82	24.98
	0.26	0.53	1.16	3.68	13.38	24.92
	0.25	0.43	1.15	3.83	12.55	23.91
Run 2	0.27	0.46	1.24	3.41	12.58	24.75
	0.27	0.49	1.28	3.49	12.71	25.01
	0.27	0.50	1.25	3.43	12.77	25.12
Mean	0.26	0.49	1.23	3.61	12.80	24.78
SD	0.0098	0.04412	0.0598	0.1919	0.3022	0.4440
% CV	3.76	8.94	4.87	5.32	2.36	1.79
N	6	6	6	6	6	6
% nominal	104.00	98.00	98.40	96.27	102.40	99.12

Table 3 Summary of calculated concentrations for 5-HT in artificial CSF matrix during validation compared to expected concentrations.

	Expected 5-HT Concentrations (ng/mL)					
Run ID	0.25	0.50	1.25	3.75	12.50	25.00
	Calculated 5-HT Concentrations (ng/mL)					
Run 1	0.29	0.38	1.08	3.46	11.39	22.38
	0.26	0.51	1.19	4.35	14.54	26.40
	0.22	0.53	1.27	4.03	12.62	24.83
Run 2	0.25	0.49	1.33	3.37	12.82	25.47
	0.25	0.50	1.27	3.47	12.53	24.77
	0.27	0.51	1.38	3.49	13.03	24.97
Mean	0.26	0.49	1.25	3.70	12.82	24.80
SD	0.0234	0.0539	0.1063	0.3987	1.0170	1.3339
% CV	9.11	11.08	8.48	10.79	7.93	5.38
N	6	6	6	6	6	6
% nominal	104.00	98.00	100	98.67	102.56	99.20

Table 4 Summary of calculated concentrations for DOPAC in artificial CSF matrix during validation compared to expected concentrations.

	Expected DOPAC Concentrations (ng/mL)					
Run ID	50	100	250	750	2500	5000
	Calculated DOPAC Concentrations (ng/mL)					
Run 1	52.00	93.74	218.39	615.68	R	4786.87
	62.31	102.39	227.34	680.55	2057.81	5317.26
	62.35	111.37	238.88	718.62	2347.67	5755.13
Run 2	61.69	96.93	259.05	651.27	26.72.09	5512.09
	59.42	111.91	242.39	608.76	2414.10	4971.33
	58.87	108.68	246.75	630.55	2573.70	5424.98
Mean	59.44	104.17	238.80	650.91	2493.90	5294.61
SD	3.94	7.70	14.38	42.18	112.85	357.55
% CV	6.62	7.39	6.02	6.48	4.53	6.753
N	6	6	6	6	5	6
% nominal	118.88	104.17	95.52	86.79	99.76	105.89

R – Rejected, not included in statistics.

Table 5 Summary of calculated concentrations for HVA in artificial CSF matrix during validation compared to expected concentrations.

	Expected HVA Concentrations (ng/mL)					
Run ID	50	100	250	750	2500	5000
	Calculated HVA Concentrations (ng/mL)					
Run 1	48.57	106.83	261.70	767.06	2382.92	4858.68
	51.02	85.76	247.61	773.75	2486.65	5160.34
	43.37	106.80	261.88	785.67	2521.49	4999.91
Run 2	46.98	108.02	274.45	619.93	2641.38	4950.43
	45.37	102.47	270.96	621.29	2620.94	5070.64
	47.89	105.95	271.68	616.00	2661.67	4977.39
Mean	47.2	102.64	264.71	697.28	2552.51	5002.90
SD	2.65	8.48	9.92	85.90	108.22	103.53
% CV	5.61	8.26	3.75	12.32	4.24	2.07
N	6	6	6	6	6	6
% nominal	94.40	102.64	105.88	92.97	102.10	100.06

Table 6 Summary of calculated concentrations for 5-HIAA in artificial CSF matrix during validation compared to expected concentrations.

	Expected 5-HIAA Concentrations (ng/mL)					
Run ID	50	100	250	750	2500	5000
	Calculated 5-HIAA Concentrations (ng/mL)					
Run 1	53.32	94.36	264.52	773.73	2439.50	5001.31
	48.10	90.15	262.72	783.46	2418.81	5105.82
	46.88	101.81	264.68	762.18	2291.74	5146.92
Run 2	45.61	99.36	286.69	706.16	2611.91	4813.96
	43.50	102.21	293.47	710.43	2553.39	5040.62
	43.81	101.88	265.16	708.82	2626.21	5036.36
Mean	46.87	98.30	272.87	740.80	2490.26	5024.17
SD	3.62	4.97	13.52	36.07	129.89	115.64
% CV	7.72	5.06	4.96	4.87	5.22	2.30
N	6	6	6	6	6	6
% nominal	93.74	98.30	109.15	98.77	99.61	100.48

Table 7 Summary of standard curve parameters for DA in artificial CSF matrix during validation.

Run ID	Correlation Coefficient (r)	Correlation Coefficient (r^2)	Curve Parameters m	b
Run 1	0.9993	0.9986	0.0456	0.0001
Run 2	0.9995	0.9989	0.0401	-0.0003
Average Correlation Coefficient	0.9994	0.9988		

Table 8 Summary of standard curve parameters for 5-HT in artificial CSF matrix during validation.

Run ID	Correlation Coefficient (r)	Correlation Coefficient (r^2)	Curve Parameters m	b
Run 1	0.9957	0.9914	0.0128	0.0010
Run 2	0.9991	0.9983	0.0106	0.0008
Average Correlation Coefficient	0.9974	0.9949		

Table 9 Summary of standard curve parameters for DOPAC in artificial CSF matrix during validation.

Run ID	Correlation Coefficient (r)	Correlation Coefficient (r^2)	Curve Parameters m	b
Run 1	0.9934	0.9868	0.0002	-0.0043
Run 2	0.9957	0.9915	0.0003	-0.0070
Average Correlation Coefficient	0.9946	0.9892		

Table 10 Summary of standard curve parameters for HVA in artificial CSF matrix during validation.

Run ID	Correlation Coefficient (r)	Correlation Coefficient (r^2)	Curve Parameters M	b
Run 1	0.9995	0.9990	0.0002	0.0035
Run 2	0.9973	0.9947	0.0003	0.0043
Average Correlation Coefficient	0.9984	0.9969		

Table 11 Summary of standard curve parameters for 5-HIAA in artificial CSF matrix during validation.

Run ID	Correlation Coefficient (r)	Correlation Coefficient (r^2)	Curve Parameters m	b
Run 1	0.9992	0.9985	0.0001	0.0001
Run 2	0.9987	0.9975	0.0001	0.0011
Average Correlation Coefficient	0.9990	0.9980		

Table 12 Summary of quality control concentrations for DA in artificial CSF matrix during validation.

	Theoretical DA Concentrations (ng/mL)		
Run ID	0.375	2.50	20.00
	Calculated DA Concentrations (ng/mL)		
Run 1	0.33	2.42	18.08
	0.38	2.30	18.36
	0.35	2.52	17.75
Run 2	0.36	2.47	18.32
	0.36	2.45	18.10
	0.38	2.48	18.84
Mean	036	2.44	18.24
SD	0.0190	0.0762	0.3650
% CV	5.27	3.12	2.00
N	6	6	6
% nominal	96.00	97.60	91.20

Table 13 Summary of quality control concentrations for 5-HT in artificial CSF matrix during validation.

	Theoretical 5-HT Concentrations (ng/mL)		
Run ID	0.375	2.50	20.00
	Calculated 5-HT Concentrations (ng/mL)		
Run 1	0.32	2.18	19.65
	0.38	2.53	22.54
	0.38	2.81	20.41
Run 2	0.36	2.55	20.58
	0.33	2.47	20.50
	0.37	2.57	20.47
Mean	0.36	2.52	20.69
SD	0.0258	0.2028	0.9674
% CV	7.24	8.05	4.68
N	6	6	6
% nominal	96.00	100.80	103.45

Table 14 Summary of quality control concentrations for DOPAC in artificial CSF matrix during validation.

Run ID	Theoretical DOPAC Concentrations (ng/mL) 75	500	4000
	Calculated DOPAC Concentrations (ng/mL)		
Run 1	81.21	377.08	3811.25
	84.82	431.55	4537.45
	89.14	470.14	4738.19
Run 2	77.05	451.42	3645.86
	85.47	459.79	4032.89
	R	472.09	4275.99
Mean	83.54	443.68	4173.61
SD	4.59	35.80	422.19
% CV	5.49	8.07	10.12
N	5	6	6
% nominal	111.39	88.74	104.34

R – Rejected, not included in statistics.

Table 15 Summary of quality control concentrations for HVA in artificial CSF matrix during validation.

Run ID	Theoretical HVA Concentrations (ng/mL) 75	500	4000
	Calculated HVA Concentrations (ng/mL)		
Run 1	79.77	503.44	4123.81
	79.22	501.19	4247.39
	77.29	515.07	4127.72
Run 2	60.66	559.86	3900.59
	60.86	547.73	3938.20
	65.77	538.97	4003.55
Mean	70.60	527.71	4056.88
SD	9.17	24.55	132.02
% CV	12.99	4.65	3.25
N	6	6	6
% nominal	94.13	105.54	101.42

Table 16 Summary of quality control concentrations for 5-HIAA in artificial CSF matrix during validation.

	Theoretical 5-HIAA Concentrations (ng/mL)		
Run ID	75	500	4000
Run 1	85.92	534.64	3793.33
	76.18	515.79	3917.74
	81.11	507.33	3722.85
Run 2	64.12	553.12	3523.72
	68.89	545.67	3538.64
	69.64	540.98	3581.81
Mean	74.31	532.92	3679.68
SD	8.24	17.81	158.27
% CV	11.09	3.34	4.30
N	6	6	6
% nominal	99.08	106.58	91.99

A typical chromatogram obtained upon analysis of an ULOQ standard (STD G) prepared with 25 ng/mL of DA and 5-HT and 5000 ng/mL for DOPAC, HVA and 5-HIAA is shown in Figure 21. A representative chromatogram obtained upon analysis of a blank standard in artificial CSF is shown in Figure 22. The blank chromatogram shows no interference in the area where the peaks of interest elute (no signal was obtained for each analyte, only baseline chemical noise was observed). Moreover, the blank was immediately analysed after an upper level standard in order to test for carryover across the dynamic range. A typical representative chromatogram obtained upon analysis of a LLOQ standard (STD B) of 0.25 ng/mL for DA and 5-HT and 50 ng/mL for DOPAC, HVA and 5-HIAA is shown in Figure 23. All chromatograms shown below are plotted with relative percent intensity (signal peak response) in the y axis and time (minutes) in the x axis. The instrument operates in negative ion mode for 2.15 min. The polarity then switches to positive ion mode.

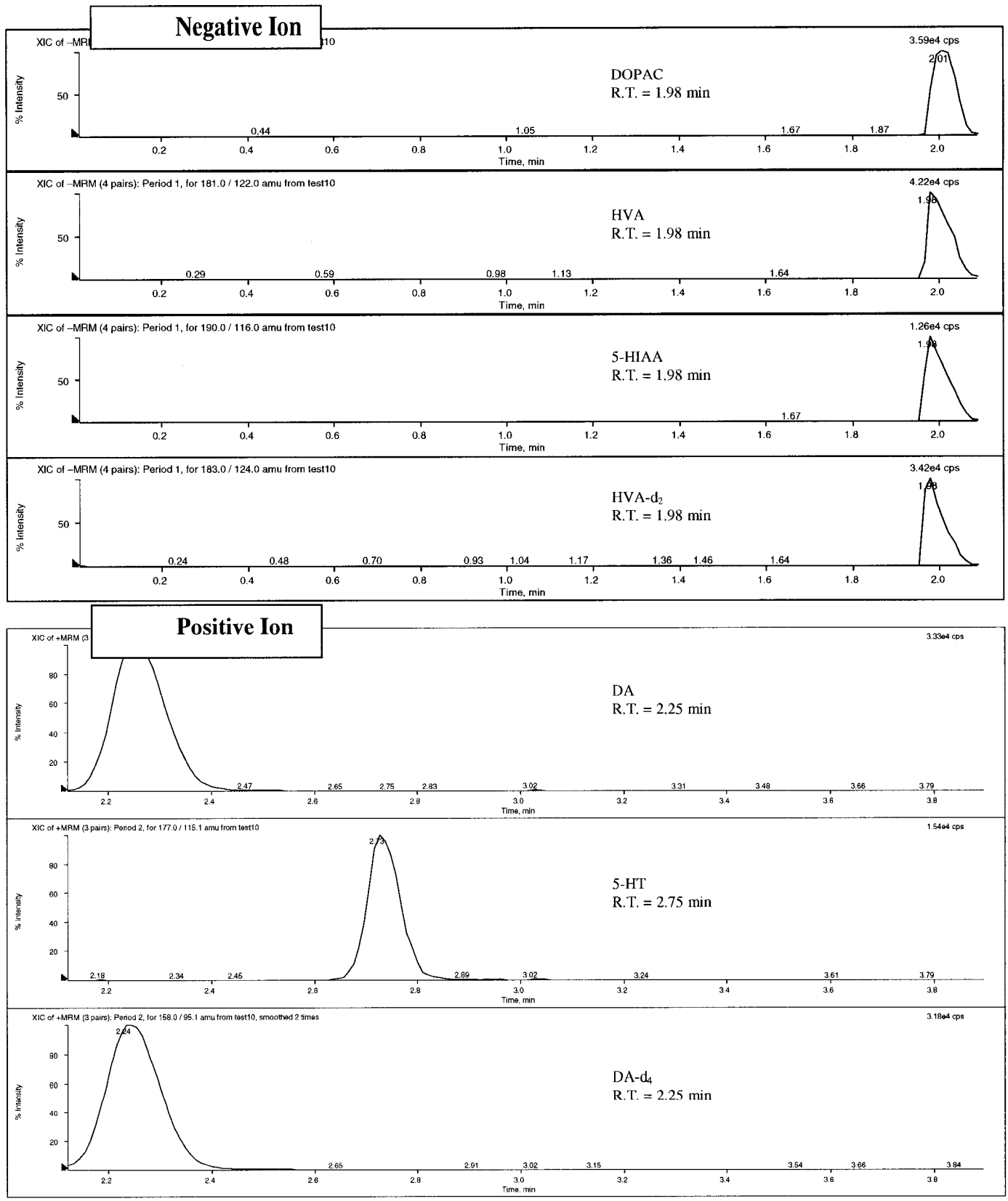

Figure 21 A representative chromatogram obtained upon analysis of a High Standard (STD G) in artificial CSF matrix.

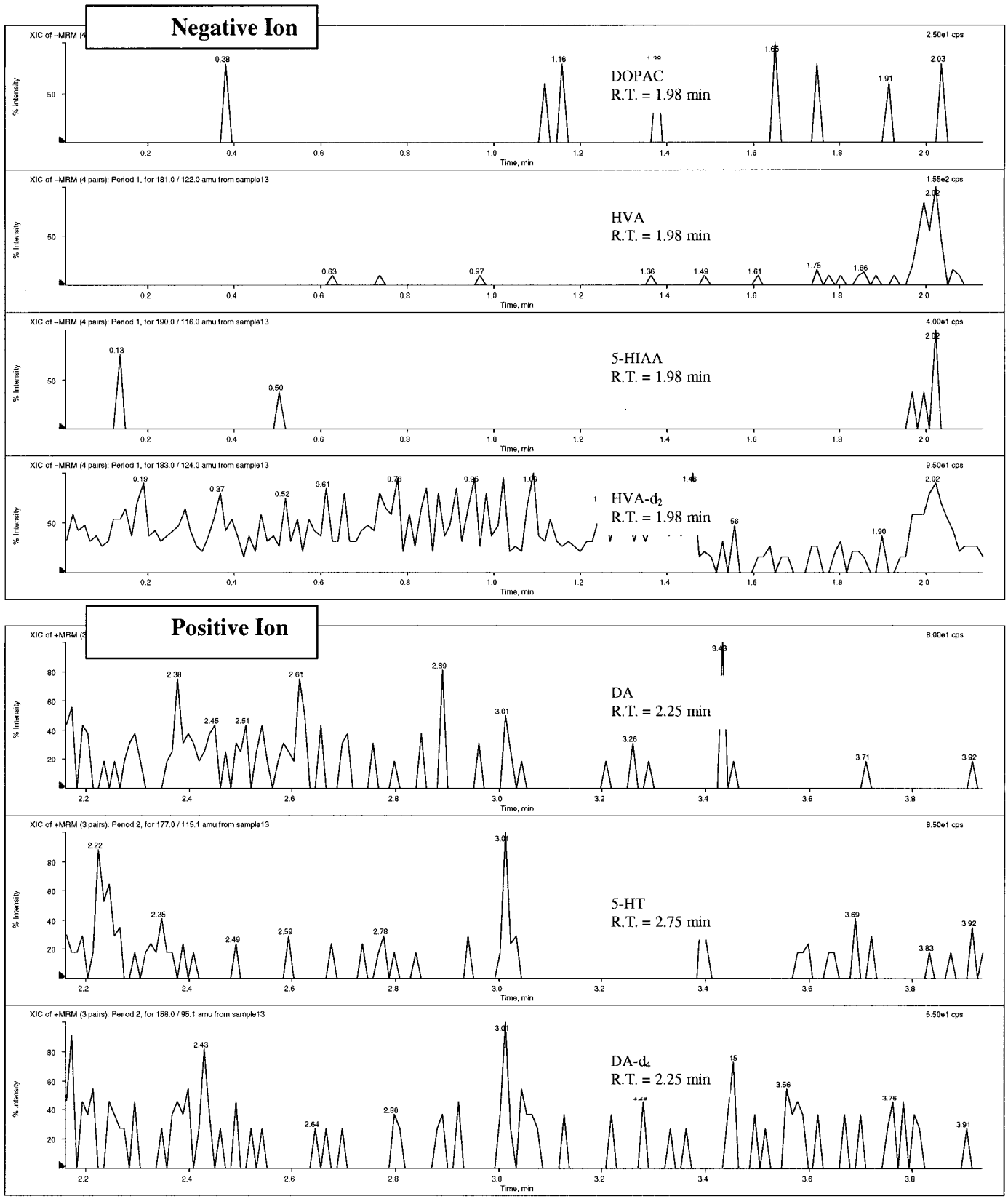

Figure 22 A representative chromatogram obtained upon analysis of a Double Blank in artificial CSF matrix.

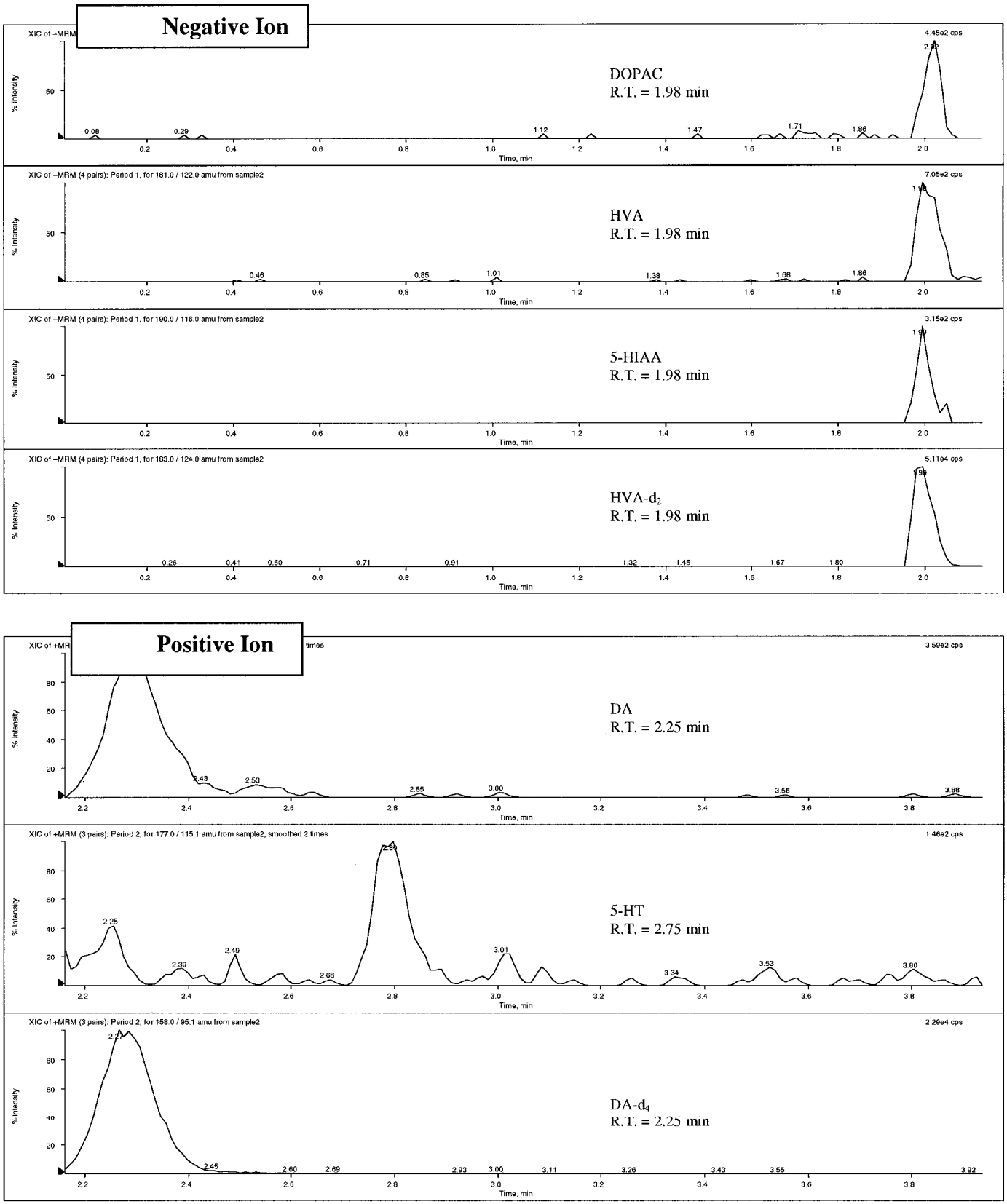

Figure 23 A representative chromatogram obtained upon analysis of a Low Standard (STD B) in artificial CSF matrix.

Limit of Quantitation

The method was validated with a conservative limit of quantitation (LOQ) at 500 fg on column for DA and 5-HT and at 100 pg on column for DOPAC, HVA and 5-HIAA. At this mass load, a signal-to-baseline (S/B) of at least 25 was obtained for DA and 5-HT and S/B of at least 50 is obtained DOPAC, HVA and 5-HIAA.

Theoretically, quantitation can be easily achieved at 100 fg (DA or 5-HT) and 10 pg (DOPAC, HVA and 5-HIAA) for a 2 µL sample resulting in a S/B of 5. The limit of detection (LOD) can be estimated at 60 fg for DA and 5-HT and 6 pg for DOAPC HVA and 5HIAA for a 2 µL sample resulting in a S/B of 3. This is illustrated in Figure 24 for DA.

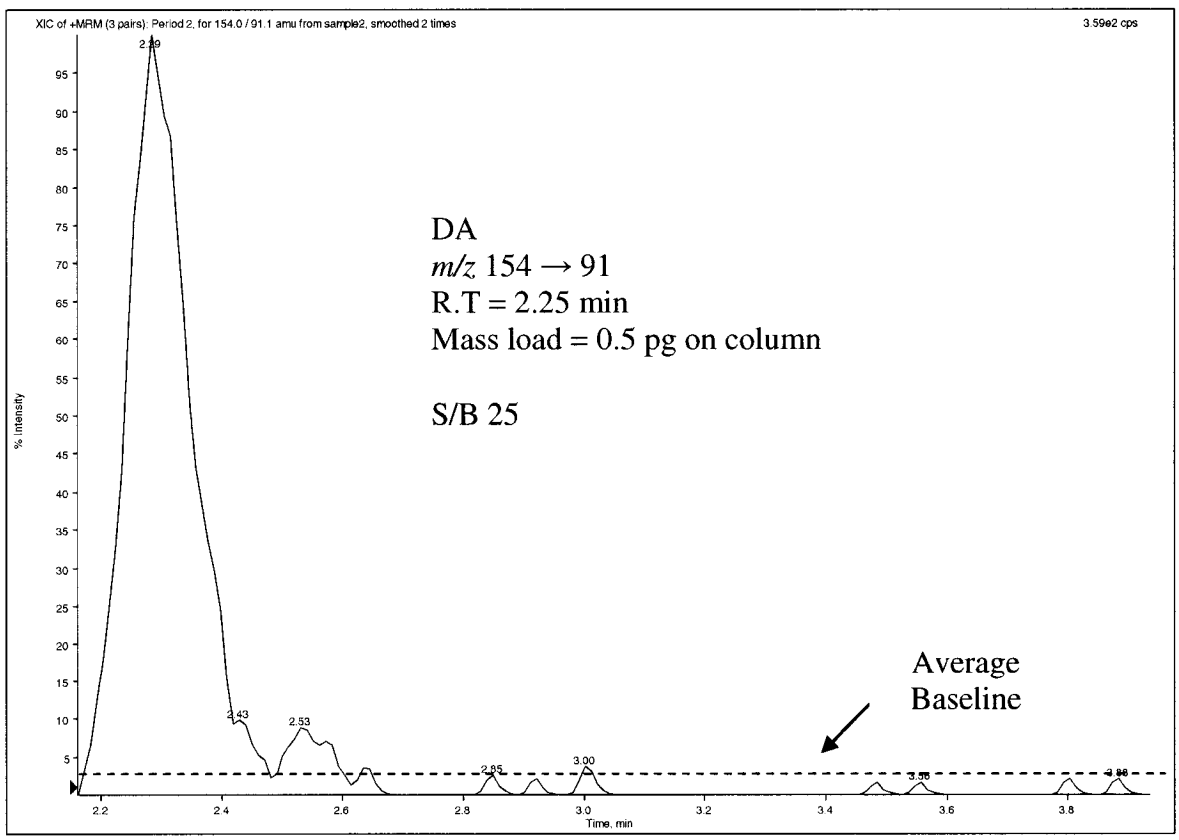

Figure 24 A representative mass chromatogram of DA at LOQ prepared in artificial CSF matrix.

Probe Recovery

Microdialysis probes were built in house from raw materials. In order to be able to measure *in vivo* levels of neurotransmitters collected through a microdialysis probe, it was essential to determine the efficiency, more specifically, the percent recovery of the probe. Probe recovery was tested using four different probes in order to verify efficiency and reproducibility of the probes. Results of this experiment are shown in Table 17.

Table 17 Summary of *in vitro* percent recoveries of microdialysis probes.

	DA	5-HT	DOPAC	HVA	5-HIAA
% Recovery Probe 1	8.52	10.62	7.99	8.54	8.08
% Recovery Probe 2	11.71	14.16	12.52	12.31	10.45
% Recovery Probe 3	11.18	13.81	11.98	11.53	9.12
% Recovery Probe 4	10.04	11.50	10.39	9.27	7.60
Mean	10.36	12.52	10.72	10.41	8.81
SD	1.41	1.73	2.03	1.79	1.26
%CV	13.63	13.83	18.96	17.23	14.33

Probes were perfused with αCSF at a flow rate of 1 μL/min.

3.2 Experiment #3: Microdialysis-LC/MS/MS.

It was critical to determine whether the analytical method developed combined with the microdialysis sampling technique was a viable method for quantifying neurotransmitter levels at basal concentrations from the rat brain. Microdialysis samples have previously been analysed by LC/MS, however, longer sampling times were required in order to be able to detect basal levels. An important element to this research was to increase temporal resolution. In order to achieve this, it was essential to decrease the sample volume collected for analysis.

The final stage of testing was the analysis of *in vivo* microdialysis samples. Quantitation of basal neurotransmitter levels in rat microdialysis samples (2 μL) was achieved using the protocol described in Section 2.12. Samples were diluted with 8 μL of 0.2% formic acid containing the internal standards. No further sample preparation was required.

The microdialysis probe (2 mm in length) was implanted and secured into the NAcc the night before testing. The flow rate of the perfusion pump was set to operate at 0.25 μL/min overnight. The rat was given 12-18 hours prior to testing in order to re-establish neurochemical equilibrium that might have been disturbed by the insertion of the probe. The day of the experiment, the flow rate of the perfusion pump was increased to 1 μL/min. The rat was given one hour before the first microdialysis sample was collected. Samples were collected and injected into the mass spectrometer to ensure that baseline levels were stable. Once a stable response was obtained, baseline samples were collected every two minutes for one hour. These thirty samples were then analysed and the basal concentrations of monoamines and their metabolites were determined. Samples

were kept in the dark by covering them with aluminium to avoid oxidation. Once five samples were collected, they were transferred to the autosampler where they waited to be injected. The autosampler was refrigerated with the temperature set to 5 °C. This was an additional precaution taken to prevent degradation of the samples.

Basal levels, measured from 2 μL microdialysis samples, of the monoamine neurotransmitters and their metabolites varied between rats. These can vary as a function of placement in the nucleus accumbens. For example, the shell has more dopamine than the core of the NAcc.

Table 18 Summary of the calculated values for the basal concentrations of the monoamines and their metabolites from a 2 μL microdialysis sample.

Analyte	DA	5-HT	DOPAC	HVA	5-HIAA
Concentration (ng/mL)	0.1-0.5	0.2-0.3	45-55	20-30	30-45

Figure 25 displays a typical representative chromatogram obtained upon analysis of a microdialysis sample at basal levels from the NAcc. Thus, a 2 μL sample volume was sufficient to monitor and determine baseline levels of the monoamines and their metabolites from the extracellular space in the NAcc.

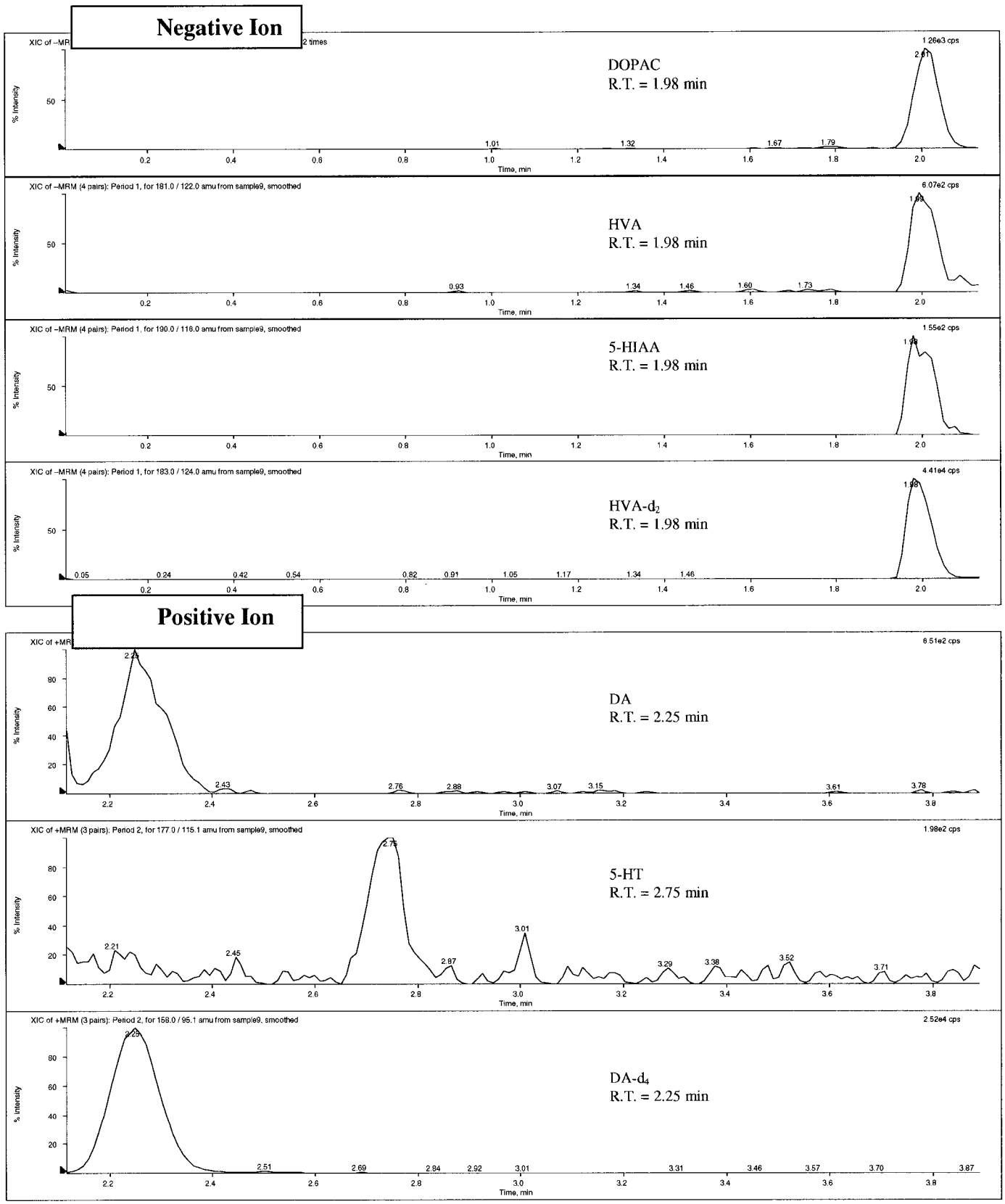

Figure 25 A representative chromatogram obtained upon analysis of a microdialysis sample at a low concentration (basal levels) from the nucleus accumbens.

This is an attractive technique because it offers the ability of conducting pharmacokinetic studies with high temporal resolution. For this final experiment, once the baseline extracellular levels were determined, the response of three different drugs acting at various stages of neuronal processing including uptake, release and metabolism of monoamines was monitored.

The rat was injected with one of the following drugs: amphetamine (5 mg/kg/mL i.p.), pargyline (100 mg/kg/mL i.p.) or fluoxetine (14 mg/kg/mL i.p.). Each drug is known to increase the monoamine neurotransmitter levels via different mechanisms and pathways. Amphetamine (AMPH) is a psychomotor stimulant known to cause the release of the excitatory neurotransmitter DA from storage vesicles in the CNS and to block the re-uptake process. Pargyline is a monoamine oxidase (MAO) inhibitor, which blocks the catabolism of dopamine, increasing its extracellular concentration. Fluoxetine is an antidepressant and a selective serotonin re-uptake inhibitor, thus administration of fluoxetine results in increased serotonin levels in the CNS. Sample collection started immediately after injection. Data were collected for two hours when injected with AMPH, two and a half hours with pargyline and between 2-6 hours with fluoxetine. The longer testing period was required with fluoxetine due to its longer half-life.

Figure 26 shows a mass chromatogram of each analyte of a microdialysis sample from the NAcc taken 35 minutes after injection of AMPH. An important increase in DA levels is expected due to the stimulated release of this monoamine in response to AMPH. This can easily be seen and confirmed in Figure 26.

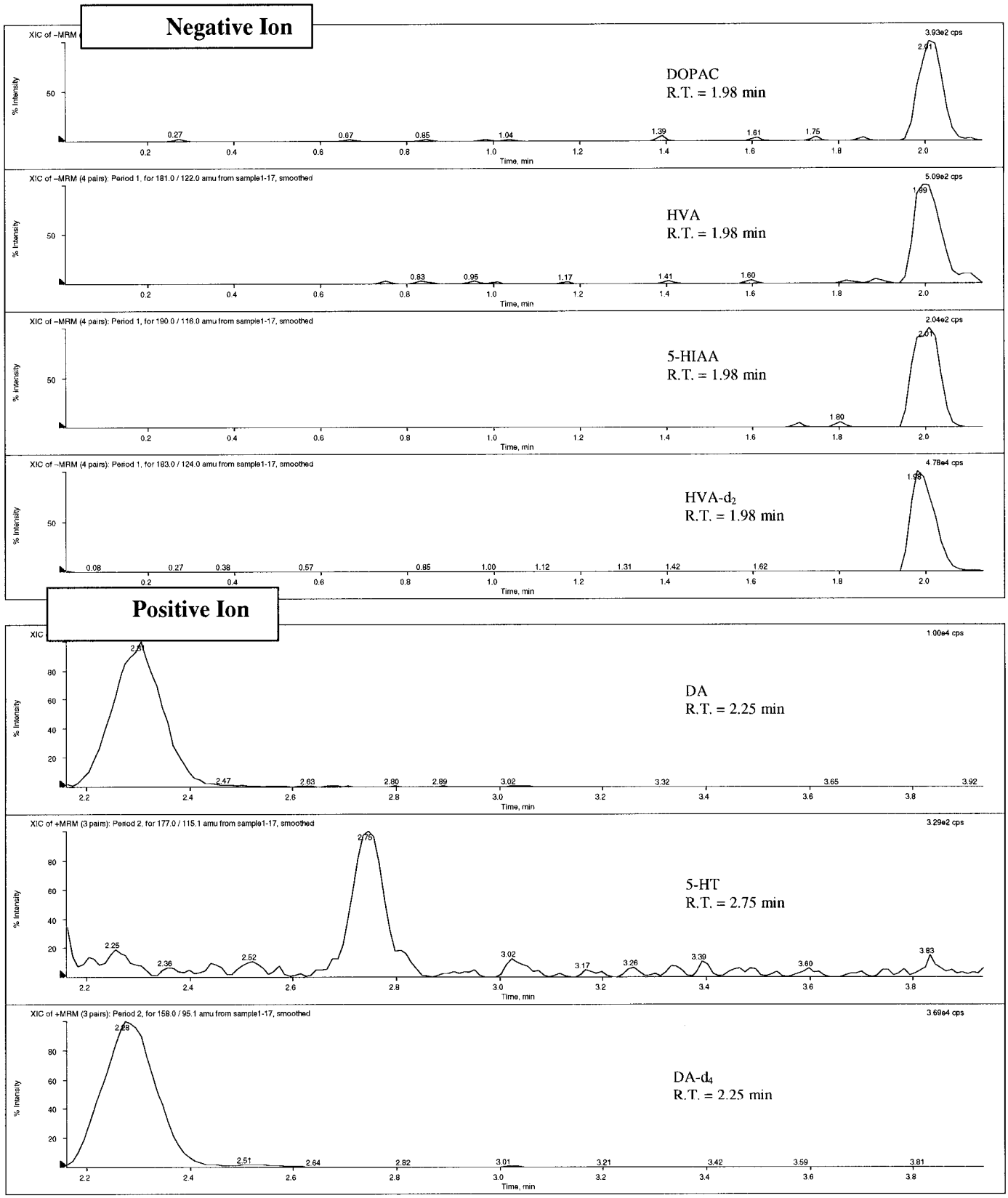

Figure 26 A representative chromatogram obtained upon analysis of a microdialysis sample at a high concentration from the nucleus accumbens.

The goal of this last experiment was to demonstrate that neurochemical responses can be monitored and a pharmacokinetic profile can be elicited with a data point obtained every two minutes. The temporal resolution afforded by this method provides a more accurate graphic portrayal of rapid fluctuations in extracellular neurochemical concentrations. A response curve can be plotted with more data points across the curve. Most current methods, with temporal resolution between 10 to 30 minutes, do not have the potential for such detailed information obtained with lower temporal resolution. In these cases, data are extrapolated and estimated between distant time points.[35,35,86,87,88,89,90,91,92]

As most of the animals were tested more than once, sensitization of monoamine responses to pharmacological stimulation likely occurred. As such, the figures shown below constitute an assessment of the ability of microdialysis-LC/MS/MS to detect monoamine changes, but can not correlate responses with a specific pattern of drug stimulation.

Figure 27 represents the concentration versus time response of DA after the rat has been injected with a high dose of AMPH. This set of data is the only data collected where the animal had no previous exposure to other drugs. Therefore, it can be directly compared to monoamine response curves from earlier published work, where similar dosing and testing conditions were applied. A pharmacokinetic profile showing an initial increase of dopamine was observed after AMPH was administered. A peak maximum, concentration of DA (Cmax) of approximately 30 times the baseline, was detected between 30 and 40 min after injection. A steady but slower decrease of the concentration of DA was measured after this point. It can be seen from Figure 27 that in the last sample

collected two hours after the beginning of the experiment, the DA levels had not yet reached their basal concentrations. These results correlate with the findings seen in previously published work. The magnitude and the time course of DA response are comparable to what other researchers have reported at similar doses.

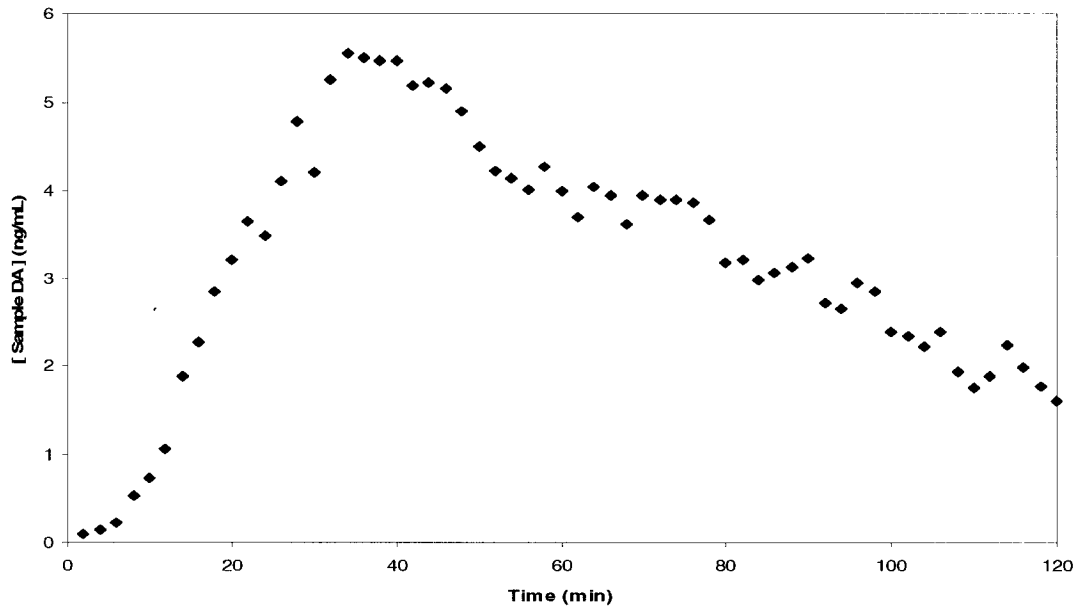

Figure 27 Concentration versus time profile of DA in the NAcc following administration of amphetamine.

The results presented for pargyline and fluoxetine can not be directly compared to earlier published data since the rat had experienced previous injections with different drugs leading to a sensitized response. The magnitude of the response (the extent of increase or decrease of the neurotransmitters), the exact time of onset, and the duration of the effect of the drug can not be compared, however, it can be seen that the results shown below exhibit a similar trend to what was expected and reported when a rat was administered with a drug that has a known effect on the neurotransmitter levels. In Figures 28 and 29, it can be seen that the extracellular concentrations of DA and 5-HT

initially increased when the rat was injected with pargyline. Pargyline, an MAO inhibitor, blocks the breakdown of these neurotransmitters, resulting in an accumulation in the extracellular space. The response slope was not as sharp, the onset was slower, compared to when the rat was injected with AMPH. This agrees with the earlier work scientists have observed with pargyline administration and its effects on monoamine levels. A Cmax was obtained between 60-100 minutes after injection. Baseline levels were reached by the last sample at 150 minutes. Moreover, the levels of the metabolites, DOPAC, HVA and 5-HIAA, were almost immediately affected (10-15 min) after administration of the drug. This was expected since pargyline directly affects the metabolites by not allowing the monoamines to metabolise. There was a sharp decrease observed and baseline levels were not reached by the end of the experiment. These results are also in agreement with what others have seen with pargyline administration.

Finally, fluoxetine was used to selectively increase the 5-HT levels in the NAcc. This was accomplished since fluoxetine blocks the reuptake mechanism, which is the primary pathway of serotonin clearance from the extracellular fluid. Fluoxetine has a longer half-life than the other two drugs tested displaying a slower onset. Samples were collected for four hours, starting two hours after injection, monitoring a segment of the onset of 5-HT response to fluoxetine. The metabolic pathway of 5-HT was unaffected by fluoxetine. An increase in the 5-HT metabolite, 5-HIAA, was also detected. Since there is an increased concentration of 5-HT, the monoamine oxidase breaks it down to 5-HIAA. Thus, an abundance of 5-HT resulted in increased formation of 5-HIAA. These findings concur with previously published data on fluoxetine.

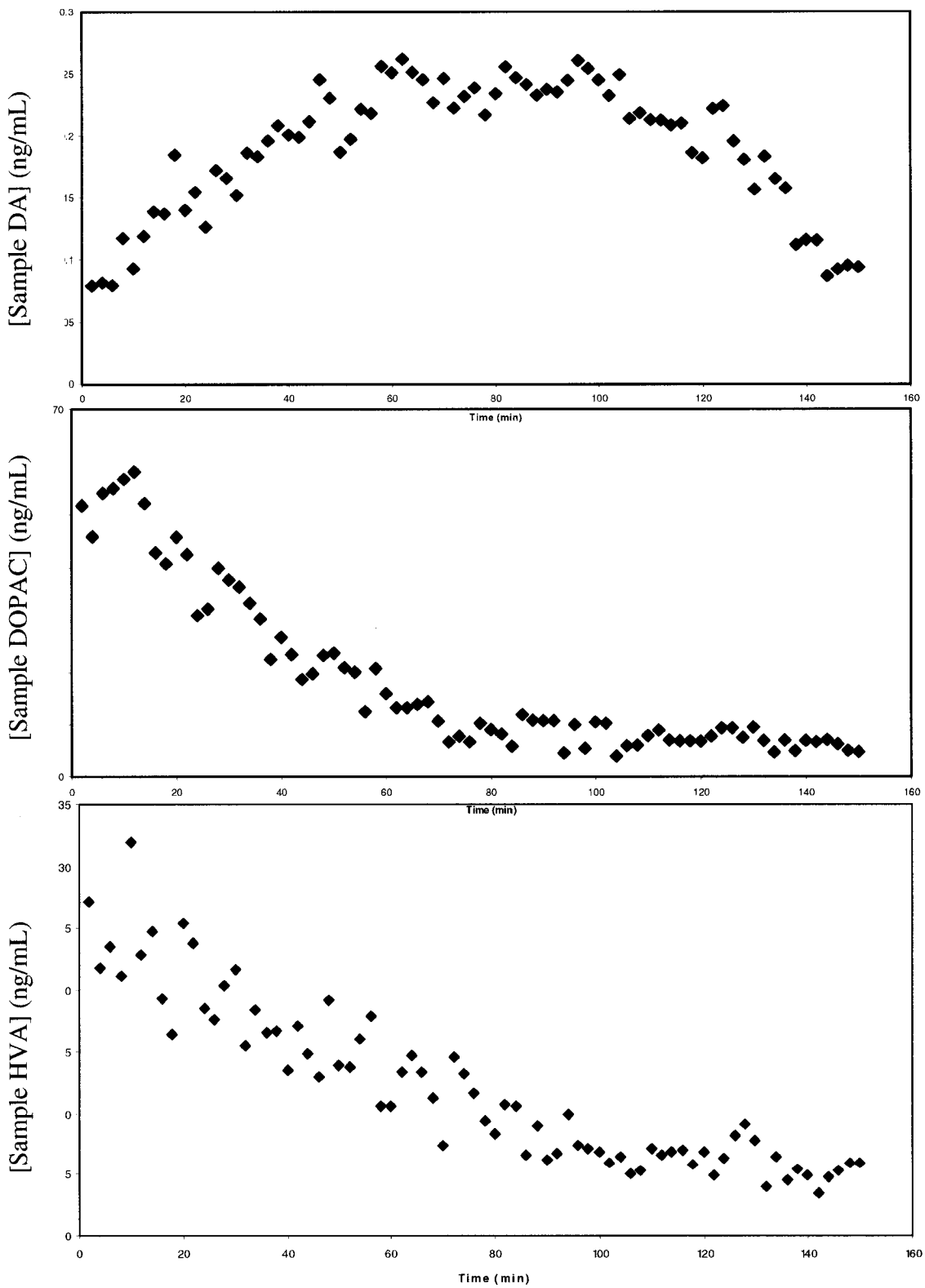

Figure 28 Concentration versus time profile of DA (A), DOPAC (B) and HVA (C) in the NAcc following administration of pargyline.

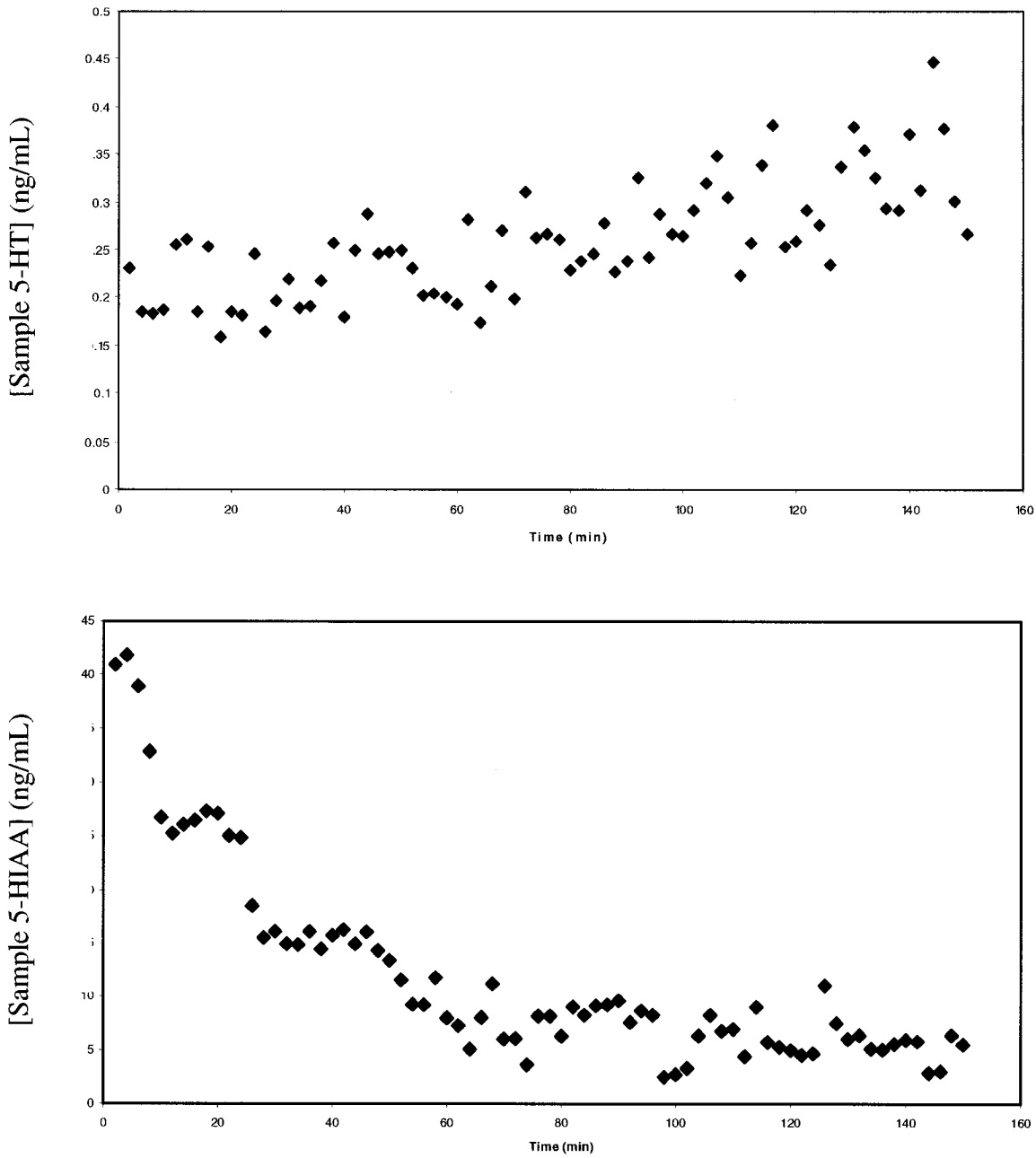

Figure 29 Concentration versus time profile of 5-HT (A) and 5-HIAA (B) in the NAcc following administration of pargyline.

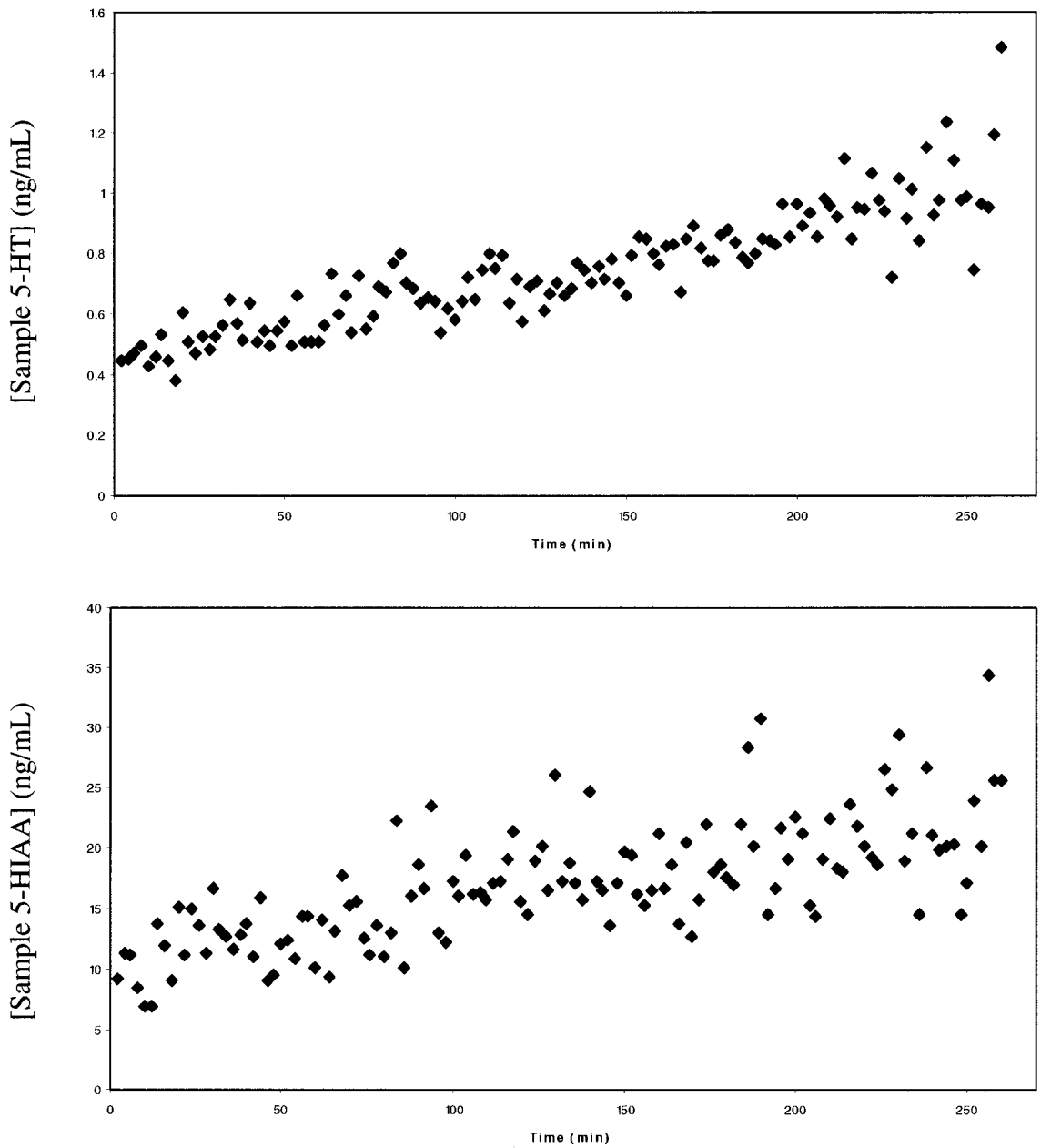

Figure 30 Concentration versus time profile of 5-HT (A) and 5-HIAA (B) in the NAcc following administration of fluoxetine.

This last experiment demonstrated that animal extracellular DA and 5-HT concentrations can be monitored using the technique developed. This provides an improved temporal resolution as compared to existing analytical methods that are coupled with microdialysis. As the goal of this study was not to verify the statistical significance of concentration measurements and specific responses to drugs, only a small population of animals was used to test each drug.

4. CONCLUSION

The main focus of this research consisted of developing and validating a new and simple method that would require minimal sample handling and preparation, offer high sensitivity, and rapid separations for a large number of analytes allowing for high throughput analysis, while requiring only 2 μL sample volumes for injection. High microdialysis temporal resolution was reached (2 min fractions) for the simultaneous monitoring of DA, 5-HT and their major metabolites, DOPAC, HVA and 5-HIAA, in the NAcc from a male rat using liquid chromatography with tandem mass spectrometry. Performance and reliability of the method was assessed by monitoring basal extracellular monoamine levels, and the quantitative responses of these neurotransmitters to three different drugs, namely amphetamine, pargyline and fluoxetine. Comparable pharmacokinetic profiles of the monoamines studied, induced by these drugs, to published data using alternative analytical methods were obtained. The high temporal resolution afforded by this assay resulted in an increased number of data points across the curve. Limits of quantitation of 100 fg on column for DA and 5-HT and 10 pg on column for DOPAC, HVA and 5-HIAA were attained.

Future Work

Future work should include repetition of the last experiment, with a larger animal population, in order to allow for statistical analysis and comparison to similar trials employing different analytical techniques. An interesting experiment, to be conducted in the near future, would be to determine how many more neurochemicals obtained from a microdialysis sample can be simultaneously analyzed using the technique developed. Additional studies should also focus on developing an automated system for online sampling and direct analysis of neurotransmitters. Automation would eliminate any errors caused by sampling and handling, thus resulting in more accurate measurements. Another way of improving this assay would be to direct some attention to the microdialysis sampling technique. The model of the probe and the semi-permeable membrane currently used offer very limited recovery percentages of the neurotransmitters available in the extracellular space. Improving the microdialysis technique, remodeling the probe or developing an alternative membrane would result in even higher temporal resolution.

5. REFERENCES

1 Pinel, JPJ Biopsychology. 5th edition. Allyn & Bacon. 2003. Chapter 4: Neural Conduction & Synaptic Transmission: 92-100.

2 Sloley, BD, Juorio, AV. Monoamine neurotransmitters in invertebrates and vertebrates: An examination of the diverse enzymatic pathways utilized to synthesize and inactivate biogenic amines. Int. Rev. Neurobiology. 1995. 38: 253-303.

3 Eisenhofer G, Huynh TT, Hiroi M, Pacak K. Understanding catecholamine metabolism as a guide to the biochemical diagnosis of pheochromocytoma. Rev Endocr Metab Disord. 2001. 2(3): 297-311.

4 Boulton AA, Eisenhofer G. Catecholamine metabolism. From molecular understanding to clinical diagnosis and treatment. Overview. Adv Pharmacol. 1998. 42: 273-92.

5 Elsworth, JD, Roth, RH. Dopamine Synthesis, Uptake, Metabolism, and Receptors: Relevance to Gene Therapy of Parkinson's Disease. Experimental Neurology. 1997. 144(1): 4-6.

6 Flatmark, T. Catecholamine biosynthesis and physiological regulation in neuroendocrine cells. Acta Physiol. Scand. 2000. 168: 1-17.

7 Weyler W, Hsu YP, Breakefield XO. Biochemistry and genetics of monoamine oxidase. Pharmacol Ther. 1990. 47(3): 391-417.

8 Lotta T, Vidgren J, Tilgmann C, Ulmanen I, Melen K, Julkunen I, Taskinen J. Kinetics of human soluble and membrane-bound catechol O-methyltransferase: a revised mechanism and description of the thermolabile variant of the enzyme. Biochemistry. 1995. 34(13): 4202-10.

9 Lehnert, H., Wurtman, R.J. Amino acid control of neurotransmitter synthesis and release: Physiological and clinical implications. Psychother. Psychosomat. 1993. 60: 18-32.

10 Wouters, J. Structural aspects of monoamine oxidase and its reversible inhibition. Curr. Med. Chem. 1998. 5: 137-162.

11 Youdim, M.B.H. (Ed.) Reversible and selective inhibitors of monoamine oxidase type A: New findings. Acta Psychiat. Scand. 1995. 91: 386.

12 Feldman, R.S. et al. Serotonin. Principles of Neuropsychopharmacology, , Sinauer Associates, MA. 1997. 345-389.

13 Beck O, Helander A, Carlsson S, Borg S. Changes in serotonin metabolism during treatment with the aldehyde dehydrogenase inhibitors disulfiram and cyanamide. Pharmacology Toxicology. 1995. 77(5): 323-6.

14 Duval F, Mokrani MC, Crocq MA, Bailey PE, Diep TS, Correa H, Macher JP. Dopaminergic function and the cortisol response to dexamethasone in psychotic depression. Prog Neuropsychopharmacol Biol Psychiatry. 2000. 24(2): 207-25.

15 Fink-Jensen A. Novel pharmacological approaches to the treatment of schizophrenia. Dan Med Bull. 2000. 47(3): 151-67.

16 Carboni E, Spielewoy C, Vacca C, Nosten-Bertrand M, Giros B, Di Chiara G. Cocaine and Amphetamine Increase Extracellular Dopamine in the Nucleus Accumbens of Mice Lacking the Dopamine Transporter Gene. Journal of Neuroscience. 2001. 21(9): RC141.

17 Freeman, ME, Kanyicska, B, Lerant, A and Nagy, G. Prolactin: structure, function and regulation of secretion. Physiological Reviews. 2000. 80: 1523-1631.

18 Lerant, A, DeMaria, AJE, and Freeman, ME. Decreased expression of Fos-related antigens (FRAS) in the hypothalamic dopaminergic neurons after immunoneutralization of endogenous prolactin. Endocrine. 2001. 16: 181-187.

19 Geddes JR, Freemantle N, Mason J, Eccles MP, Boynton J. SSRIs versus other antidepressants for depressive disorder. Cochrane Database Syst Rev. 2000. (2): CD001851.

20 Steiger H, Young SN, Kin NM, Koerner N, Israel M, Lageix P, Paris J. Implications of impulsive and affective symptoms for serotonin function in bulimia nervosa. Psychol Med. 2001. 31(1): 85-95.

21 Steiger H, Koerner N, Engelberg MJ, Israel M, Ng Ying Kin NM, Young SN. Self-destructiveness and serotonin function in bulimia nervosa. Psychiatry Res. 2001. 103(1): 15-26.

22 Hensler JG, Ferry RC, Labow DM, Kovachich GB, Frazer A. Quantitative autoradiography of the serotonin transporter to assess the distribution of serotonergic projections from the dorsal raphe nucleus. Synapse. 1994. 17(1): 1-15.

23 Zimbroff, DL, Kane, JM, Tamminga, CA, Daniel, DG, Mack, RJ, Wozniak, PJ; ,Sebree, TB, Wallin, BA, Kashkin, KB. Controlled, Dose-Response Study of Sertindole and Haloperidol in the Treatment of Schizophrenia. American Journal of Psychiatry. 1997. 154(6): 782-92.

24 Lucki I. The spectrum of behaviors influenced by serotonin. Biol Psychiatry. 1998. 44: 151-162.

25 Mahoney, MC, Connolly, BF, Smith, CM. Case Report - A Clozapine Overdose with Markedly Elevated Serum Levels. Journal of Clinical Pharmacology. 1999. 39(1): 97.

26 Mitchell JE, de Zwaan M, Roerig JL. Drug therapy for patients with eating disorders. Curr Drug Target CNS Neurol Disord. 2003. 2(1): 17-29.

27 Bacaltchuk J, Hay P, Trefiglio R. Antidepressants versus psychological treatments and their combination for bulimia nervosa. Cochrane Database Syst Rev. 2001. (4): CD003385.

28 Leshner AI, Koob GF. Drugs of abuse and the brain. Proc Assoc Am Physicians. 1999. 111(2): 99-108.

29 Berridge CW, O'Neil J, Wifler K. Amphetamine acts within the medial basal forebrain to initiate and maintain alert waking. Neuroscience. 1999. 93(3): 885-96.

30 Schwartz JR, Feldman NT, Fry JM, Harsh J. Efficacy and safety of modafinil for improving daytime wakefulness in patients treated previously with psychostimulants. Sleep Med. 2003. 4(1): 43-9.

31 Kollins SH. Comparing the abuse potential of methylphenidate versus other stimulants: a review of available evidence and relevance to the ADHD patient. Journal Clinical Psychiatry. 2003. 64(11): 14-8.

32 Jones S, Kornblum JL, Kauer JA. Amphetamine blocks long-term synaptic depression in the ventral tegmental area. Journal Neuroscience. 2000. 20(15): 5575-80.

33 Cryan JF, Hoyer D, Markou A. Withdrawal from chronic amphetamine induces Depressive-Like behavioral effects in rodents. Biol Psychiatry. 2003. 54(1): 49-58.

34 Schloss P, Williams DC. The serotonin transporter: a primary target for antidepressant drugs. Journal Psychopharmacology. 1998. 12(2): 115-21.

35 Hamilton ME, Redondo JL, Freeman AS. Overflow of dopamine and cholecystokinin in rat nucleus accumbens in response to acute drug administration. Synapse. 2000. 38(3): 238-42.

36 Fiorino DF, Phillips AG. Facilitation of sexual behavior and enhanced dopamine efflux in the nucleus accumbens of male rats after D-amphetamine-induced behavioral sensitization. Journal Neuroscience. 1999. 19(1): 456-63.

37 Brundege JM, Williams JT. Differential modulation of nucleus accumbens synapses. Journal Neurophysiology. 2002. 88(1): 142-51.

38 Velasco M, Luchsinger A. Dopamine: pharmacologic and therapeutic aspects. American Journal Therapeutics. 1998. 5(1): 37-43.

39 Heidbreder CA, Hedou G, Feldon J. Behavioral neurochemistry reveals a new functional dichotomy in the shell subregion of the nucleus accumbens. Prog Neuropsychopharmacol Biol Psychiatry. 1999. 23(1): 99-132.

40 Manter and Gatz's Essential of Clinical Neuroanatomy and Neurophysiology. Edition 8. F. A. Davis Co. Philadelphia.1992.

41 Reum T, Fink H, Marsden CA, Morgenstern R. Extracellular dopamine in the anterior nucleus accumbens is distinctly affected by ventral tegmental area administration of cholecystokinin and apomorphine: data from in vivo voltammetry. Neuropeptides. 1998. 32(2): 161-6.

42 Olive MF, Mehmert KK, Hodge CW. Microdialysis in the mouse nucleus accumbens: a method for detection of monoamine and amino acid neurotransmitters with simultaneous assessment of locomotor activity. Brain Research Protocols. 2000. 5(1): 16-24.

43 Elmquist WF, Sawchuk RJ. Use of microdialysis in drug delivery studies. Adv Drug Deliv Rev. 2000. 45(2-3): 123-4.

44 Lunte SM, Lunte CE. Microdialysis sampling for pharmacological studies: HPLC and CE analysis. Adv Chromatogr. 1996. 36: 383-432.

45 Davies MI, Cooper JD, Desmond SS, Lunte CE, Lunte SM. Analytical considerations for microdialysis sampling. Adv Drug Deliv Rev. 2000. 45(2-3): 169-88.

46 Westerink BH. Analysis of biogenic amines in microdialysates of the brain. Journal Chromatography B Biomedical Science Applications. 2000. 747(1-2): 21-32.

47 De Lange EC, de Boer AG, Breimer DD. Methodological issues in microdialysis sampling for pharmacokinetic studies. Adv Drug Deliv Rev. 2000. 45(2-3): 125-48.

48 Hillered L, Persson L. Theory and practice of microdialysis--prospect for future clinical use. Acta Neurochir Suppl (Wien). 1999. 75: 3-6.

49 Chen KC, Hoistad M, Kehr J, Fuxe K, Nicholson C. Theory relating in vitro and in vivo microdialysis with one or two probes. Journal Neurochemistry. 2002. 81(1): 108-21.

50 Zhu Y, Wong PS, Cregor M, Gitzen JF, Coury LA, Kissinger PT. *In vivo* microdialysis and reverse phase ion pair liquid chromatography/tandem mass spectrometry for the determination and identification of acetylcholine and related compounds in rat brain. Rapid Communications Mass Spectrometry. 2000. 14(18): 1695-700.

51 Hows ME, Organ AJ, Murray S, Dawson LA, Foxton R, Heidbreder C, Hughes ZA, Lacroix L, Shah AJ. High-performance liquid chromatography/tandem mass spectrometry assay for the rapid high sensitivity measurement of basal acetylcholine from microdialysates. Journal Neuroscience Methods. 2002. 121(1): 33-9.

52 Fuh MR, Tai YL, Pan WH. Determination of free-form of cocaine in rat brain by liquid chromatography-electrospray mass spectrometry with in vivo microdialysis. Journal Chromatography B Biomedical Science Applications. 2001. 752(1): 107-14.

53 Chen W, Liu L, Li X, Li J, Ji S, Zhang G, Chai Y. Separation and determination of strychnine and brucine in Strychnos nux-vomica L. and its preparation by capillary zone electrophoresis. Biomedical Chromatography. 2000. 14(8): 541-3.

54 Siren H, Karjalainen U. Study of catecholamines in patient urine samples by capillary electrophoresis. Journal Chromatography A. 1999. 853(1-2): 527-33.

55 Vuorensola K, Siren H. Determination of urinary catecholamines with capillary electrophoresis after solid-phase extraction. Journal Chromatography A. 2000. 895(1-2): 317-27.

56 Freed AL, Lunte SM. Separation of naphthalene-2,3-dicarboxaldehyde-derivatized-substance P and its metabolites by micellar electrokinetic chromatography. Electrophoresis. 2000. 21(10): 1992-6.

57 Wood AT, Hall MR. Reversed-phase high-performance liquid chromatography of catecholamines and indoleamines using a simple gradient solvent system and native fluorescence detection. Journal Chromatography B Biomedical Science Applications. 2000. 744(1): 221-5.

58 Gronier B, Perry KW, Rasmussen K. Activation of the mesocorticolimbic dopaminergic system by stimulation of muscarinic cholinergic receptors in the ventral tegmental area. Psychopharmacology (Berl). 2000. 147(4): 347-55.

59 Xu F, Gao M, Wang L, Jin L. Study on the effect of electromagnetic impulse on neurotransmitter metabolism in nerve cells by high-performance liquid chromatography-electrochemical detection coupled with microdialysis. Analytical Biochemistry. 2002. 307(1): 33-9.

60 Mayer BX, Namiranian K, Dehghanyar P, Stroh R, Mascher H, Muller M. Comparison of UV and tandem mass spectrometric detection for the high-performance liquid chromatographic determination of diclofenac in microdialysis samples. J Pharm Biomed Anal. 2003. 33(4): 745-54.

61 Andren PE, Caprioli RM. Determination of extracellular release of neurotensin in discrete rat brain regions utilizing in vivo microdialysis/electrospray mass spectrometry. Brain Research. 1999. 845(2): 123-9.

62 Parrot S, Bert L, Mouly-Badina L, Sauvinet V, Colussi-Mas J, Lambas-Senas L, Robert F, Bouilloux JP, Suaud-Chagny MF, Denoroy L, Renaud B. Microdialysis monitoring of catecholamines and excitatory amino acids in the rat and mouse brain: recent developments based on capillary electrophoresis with laser-induced fluorescence detection--a mini-review. Cell Mol Neurobiol. 2003. 23(4-5): 793-804.

63 Qian J, Wu Y, Yang H, Michael AC. An integrated decoupler for capillary electrophoresis with electrochemical detection: application to analysis of brain microdialysate. Analytical Chemistry. 1999. 71(20): 4486-92.

64 Park YH, Zhang X, Rubakhin SS, Sweedler JV. Independent optimization of capillary electrophoresis separation and native fluorescence detection conditions for indolamine and catecholamine measurements. Analytical Chemistry. 1999. 71(21): 4997-5002.

65 Fuller RR, Moroz LL, Gillette R, Sweedler JV. Single neuron analysis by capillary electrophoresis with fluorescence spectroscopy. Neuron. 1998. 20(2): 173-81.

66 Li YM, Qu Y, Vandenbussche E, Arckens L, Vandesande F. Analysis of extracellular gamma-aminobutyric acid, glutamate and aspartate in cat visual cortex by in vivo microdialysis and capillary electrophoresis-laser induced fluorescence detection. Journal Neuroscience Methods. 2001. 105(2): 211-5.

67 Takada Y, Yoshida M, Sakairi M, Koizumi H. Detection of gamma-aminobutyric acid in a living rat brain using in vivo microdialysis-capillary electrophoresis/mass spectrometry. Rapid Communications Mass Spectrometry. 1995. 9(10): 895-6.

68 Pfaus JG. Neurobiology of sexual behavior. Curr Opin Neurobiol. 1999. 9(6):751-8.

69 Pfaus JG, Kippin TE, Centeno S. Conditioning and sexual behavior: a review. Horm Behav. 2001. 40(2): 291-321.

70 Kebarle P. A brief overview of the present status of the mechanisms involved in electrospray mass spectrometry. Journal Mass Spectrometry. 2000. 35(7): 804-17.

71 Niessen WM. State-of-the-art in liquid chromatography-mass spectrometry. Journal Chromatography A. 1999. 856(1-2): 179-97.

72 Gaskell, SJ. Electrospray: Principles and Practice. Journal of Mass Spectrometry. 1997. 32: 677-688.

73 Bruins, AP. Mechanistic Aspects of Electrospray Ionization. Journal of Chromatography A. 1998. 794: 345-357.

74 Perkin Elmer Sciex Software Image.

75 March, R. E. An Introduction to Quadrupole Ion Trap Mass Spectrometry. Journal of Mass Spectrometry. 1997. 32: 351-369.

76 De Hoffmann, E. Tandem Mass Spectrometry: a Primer. Journal of Mass Spectrometry. 1996. 31: 129-137.

77 Haskins WE, Wang Z, Watson CJ, Rostand RR, Witowski SR, Powell DH, Kennedy RT., Capillary LC-MS2 at the attomole level for monitoring and discovering endogenous peptides in microdialysis samples collected *in vivo*. Analytical Chemistry. 2001. 73(21): 5005-13.

78 Iyer RN, Davis MD, Juneau PL, Giordani AB. Brain extracellular levels of the putative antipsychotic CI-1007 and its effects on striatal and nucleus accumbens dopamine overflow in the awake rat. J Pharm Pharmacol. 1998. 50(10): 1147-53.

79 Brautigam L, Vetter G, Tegeder I, Heinkele G, Geisslinger G. Determination of celecoxib in human plasma and rat microdialysis samples by liquid chromatography tandem mass spectrometry. Journal Chromatography B Biomedical Science Applications. 2001. 761(2): 203-12.

80 Oertel R, Richter K, Ebert U, Kirch W. Determination of scopolamine in human serum and microdialysis samples by liquid chromatography-tandem mass spectrometry. Journal Chromatography B Biomedical Science Applications. 2001. 750(1): 121-8.

81 Shen H, Witowski SR, Boyd BW, Kennedy RT. Detection of peptides by precolumn derivatization with biuret reagent and preconcentration on capillary liquid chromatography columns with electrochemical detection. Analytical Chemistry. 1999. 71(5): 987-94.

82 Eldrup E, Richter EA. DOPA, dopamine, and DOPAC concentrations in the rat gastrointestinal tract decrease during fasting. Am J Physiol Endocrinol Metab. 2000. 279(4): E815-22.

83 Dhondt JL, Forzy G. Usual values for 5-hydroxy-indol acetic acid and homovanillic acid in cerebrospinal fluid. Ann Biol Clin (Paris). 2003. 61(1): 69-75.

84 Heidbreder CA, Lacroix L, Atkins AR, Organ AJ, Murray S, West A, Shah AJ. Development and application of a sensitive high performance ion-exchange chromatography method for the simultaneous measurement of dopamine, 5-hydroxytryptamine and norepinephrine in microdialysates from the rat brain. Journal Neuroscience Methods. 2001. 112(2): 135-44.

85 Rumbold K, Okatch H, Torto N, Siika-Aho M, Gubitz G, Robra KH, Prior B. Monitoring on-line desalted lignocellulosic hydrolysates by microdialysis sampling micro-high performance anion exchange chromatography with integrated pulsed electrochemical detection/mass spectrometry. Biotechnol Bioeng. 2002. 78(7): 822-8.

86 Cadoni C, Solinas M, Di Chiara G. Psychostimulant sensitization: differential changes in accumbal shell and core dopamine. European Journal of Pharmacology. 2000. 388: 69-76.

87 Vezina P, Lorrain DS, Arnold GM, Austin JD, Suto N. Sensitization of midbrain dopamine neuron reactivity promotes the pursuit of amphetamine. Journal of Neuroscience. 2002. 22(11): 4654-4662.

88 Lamensdorf I., Porat S., Simantov R., Finberg J. P. M. Effect of low-dose treatment with selegilne on dopamine thransporter (DAT) expression and amphetamine-induced dopamine release *in vivo*. British Journal of Pharmacology. 1999. 126: 997-1002.

89 Nakamura M., Ishii A., Nakahara D. Characetrization of ß-phenylethylamine-induced monoamine release in rat nucleus accumbens: a microdialysis study. European Journal of Pharmacology. 1998. 349: 163-169.

90 Frantz K.J., Hansson K.J., Stouffer D.G., Parsons L.H. 5-HT_6 receptor antagonism potentiates the behavioural and neurochemical effects of amphetamine but not cocaine. Neuropharmacology. 2002. 42: 170-180.

91 Zetterstrom T., Sharp T., Collin A.K., Ungerstedt U. In vivo measurement of extracellular dopamine and DOPAC in rat striatum after various dopamine-

releasing drugs; implications for the origin of extracellular DOPAC. European Journal of Pharmacology. 1998. 148(3): 327-34.

92 Blaha C.D., Cory A., Phillips A.G. Does monoamine oxidase inhibition by pargyline increase extracellular dopamine concentrations in the striatum? Neuroscience. 1996. 75(2): 543-50.